The **C**ryogenic **S**torage **R**ing **CSR**

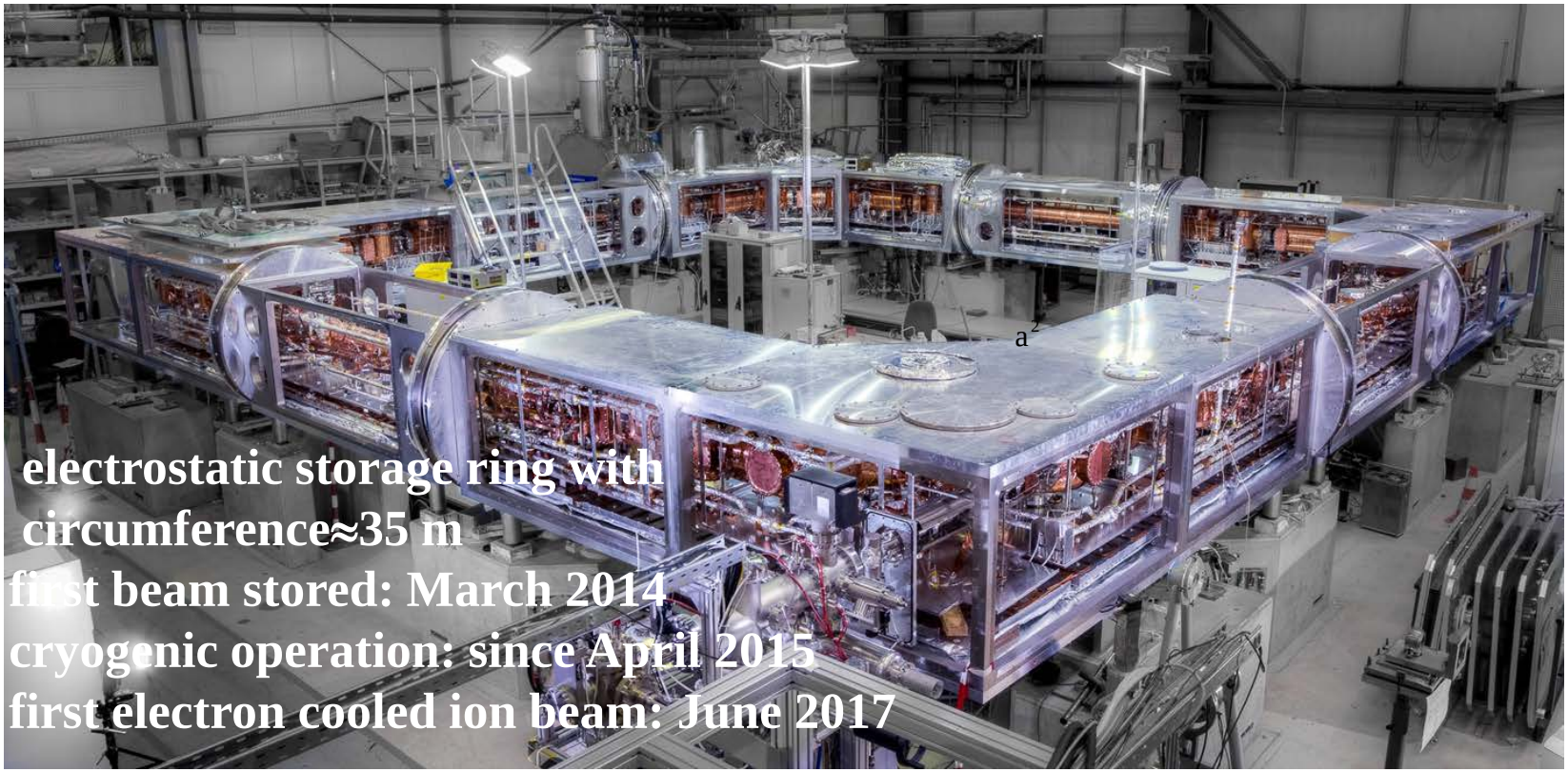

Manfred Grieser

Max Planck Institute for Nuclear Physics

GSI , February 15th, 2018

Purpose of the CSR

main research field: molecular ion physics

goal: all molecular ions to have in the same **ν=0**, **J=0** quantum state

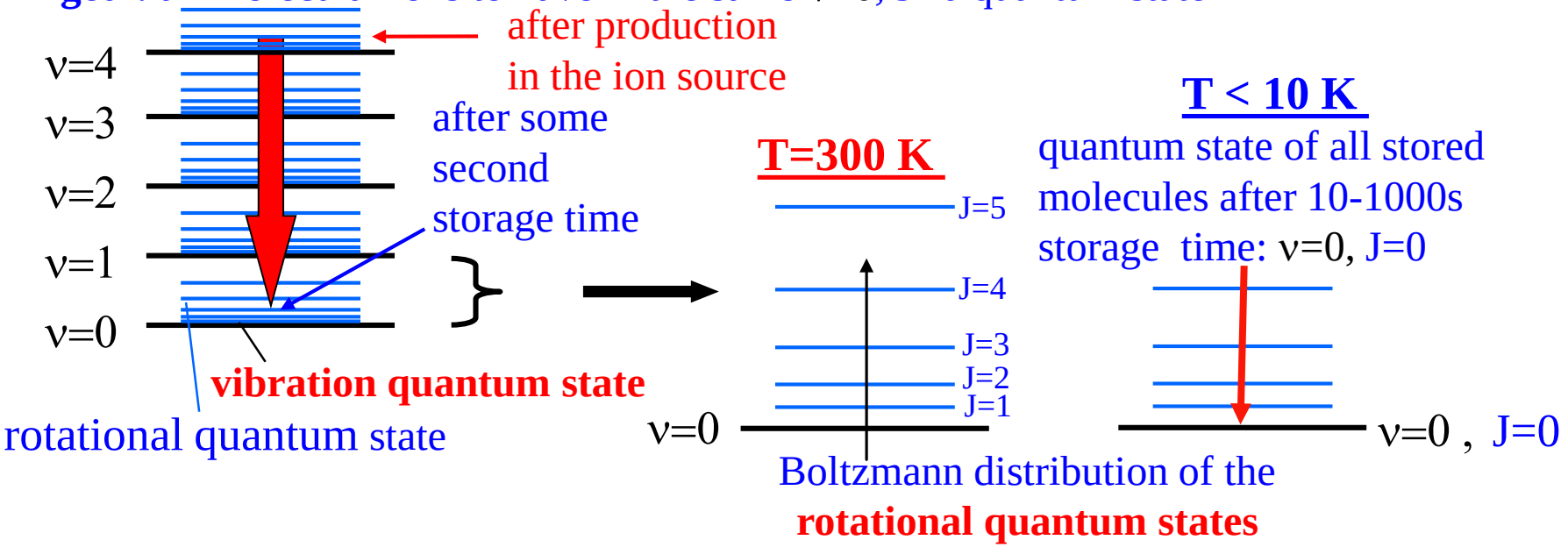

to get all molecular ions in the same molecular quantum state (ν=0, J=0) the molecular ions have to be stored at **T<10 K**

⇒ a new **C**ryogenic **S**torage **R**ing (**CSR**) at MPIK Heidelberg

in opposite to other storage rings it is an **electrostatic storage ring**

Overview of the CSR

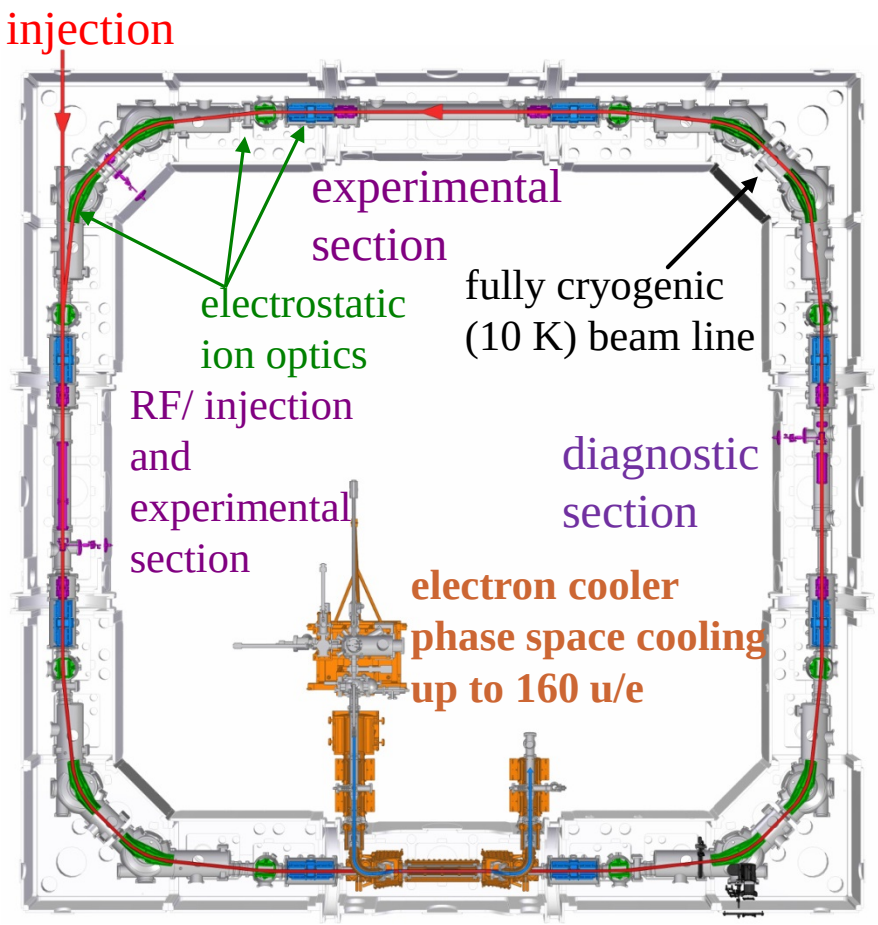

circumference: ≈ 35 m
beam energy: (20-300)·q keV
temperature: 10-300 K
residual gas densities:
(at $\overline{T} \approx 10$ K): <20 molecules/cm^3

with electron cooling
m/q range: 1 -160
(at E/Q=300 kV)
lowest rigidity: p^+, H^- at E/Q= 20 kV
Bρ=0.02 Tm

Electrostatic beam optics Elements

- 4-fold symmetric storage ring
  all CSR corner sections identical
- 8 pairs of **quadrupoles** (±10 kV, ∅ =100mm)
- 8 **6°- electrostatic deflector** (±30 kV, g=120mm)
- 8 **39°-electrostatic deflector** (±30 kV, g=60mm)
- 8 vertical electrostatic deflectors

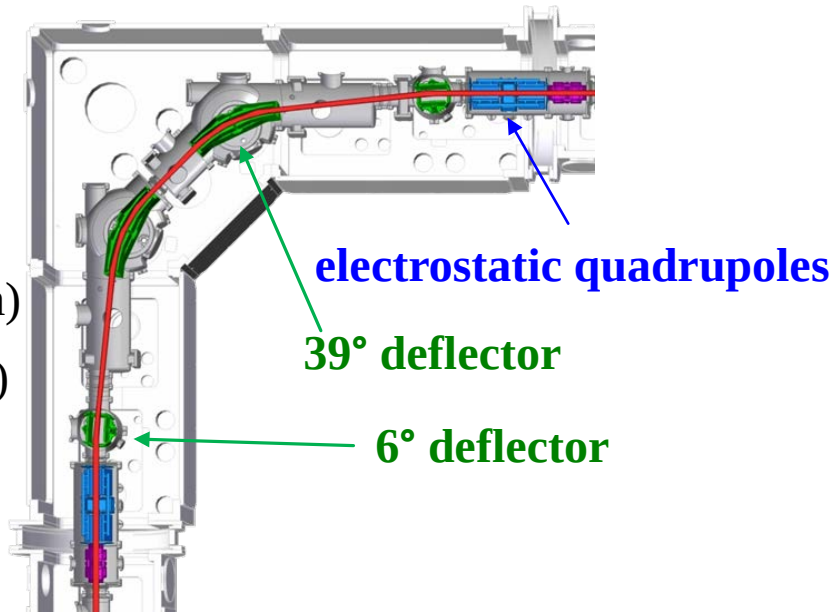

39^0 cylindrical deflector

electrostatic quadrupoles with vertical steerer

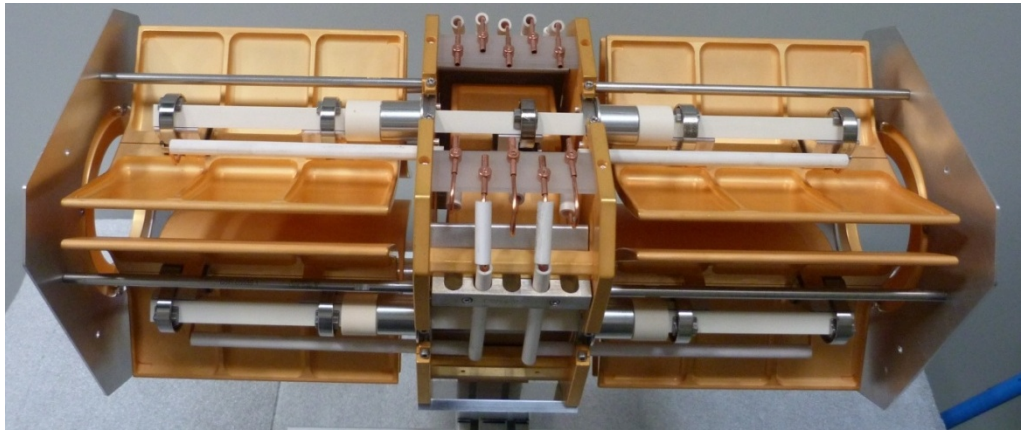

Electrostatic Quadrupole of the CSR

quadrupole electrode

inner vacuum chamber

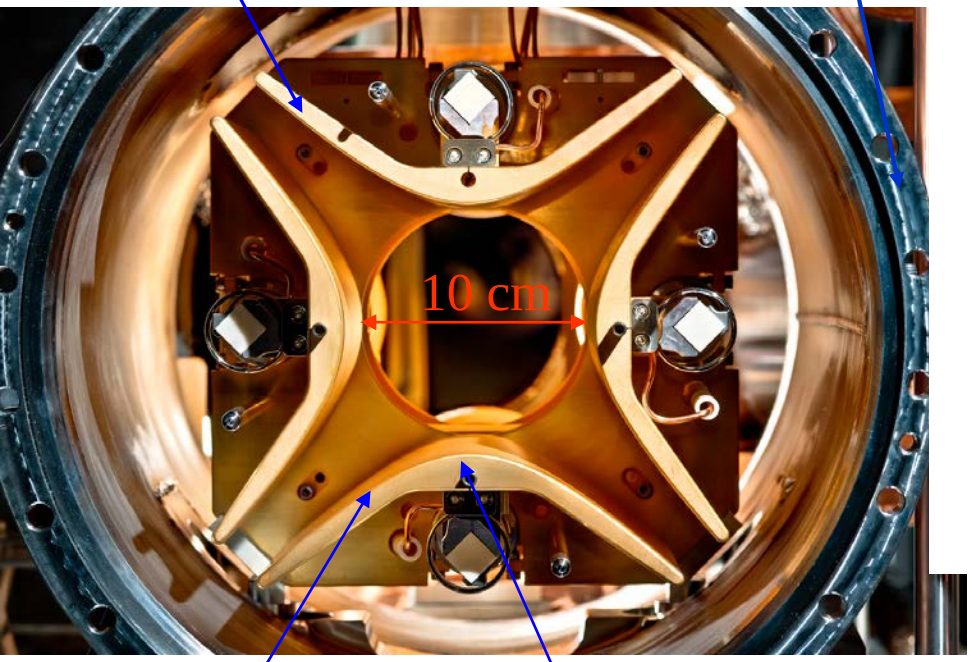

quadrupole electrode

hyperbolic profile

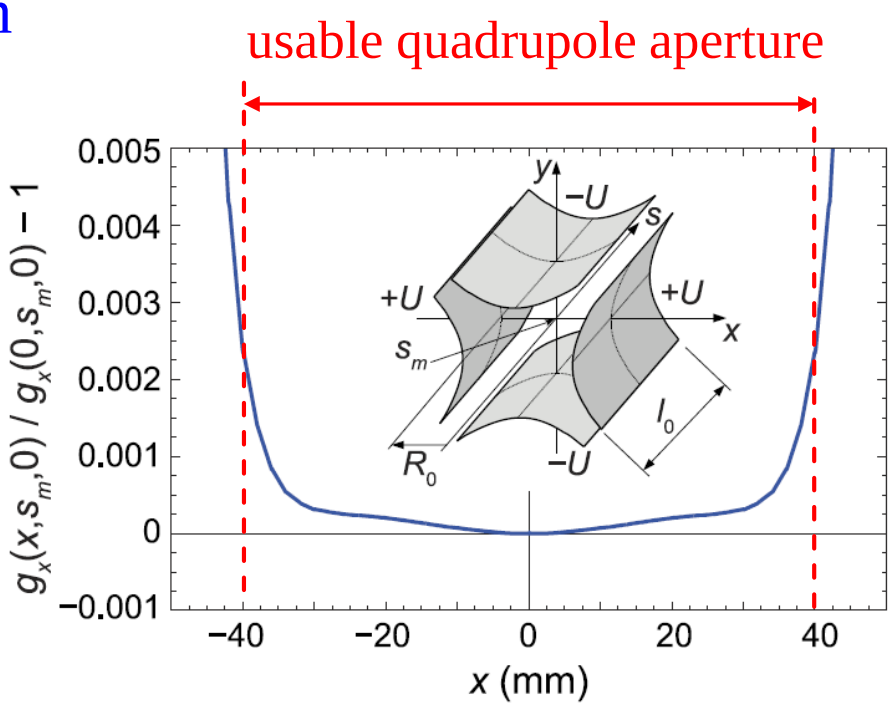

Relative deviation of the field gradient in the CSR focusing quadrupole. The longitudinal coordinate lies in the middle of a quadrupole unit.

l_0=200 mm

maximum electrode voltage: U_{max}=±10kV

Lattice of the CSR

CSR corner

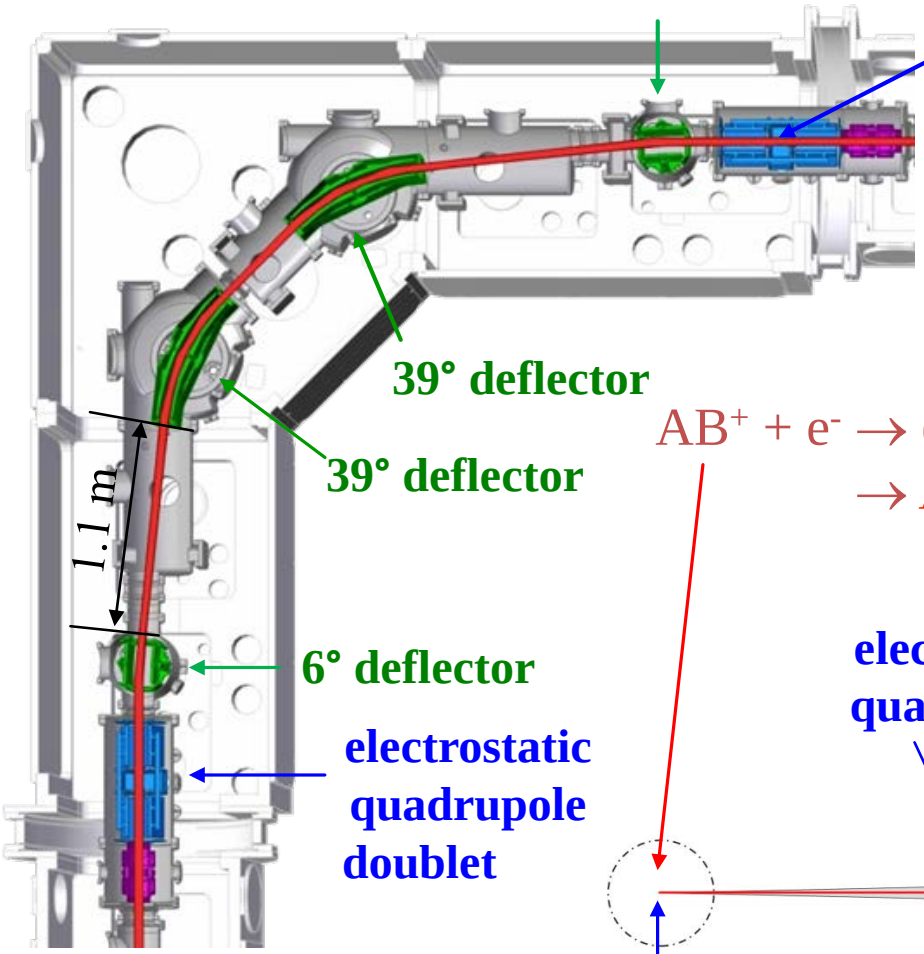

Dissociative Recombination

$AB^+ + e^- \rightarrow (AB)^*$

$\rightarrow A+B$

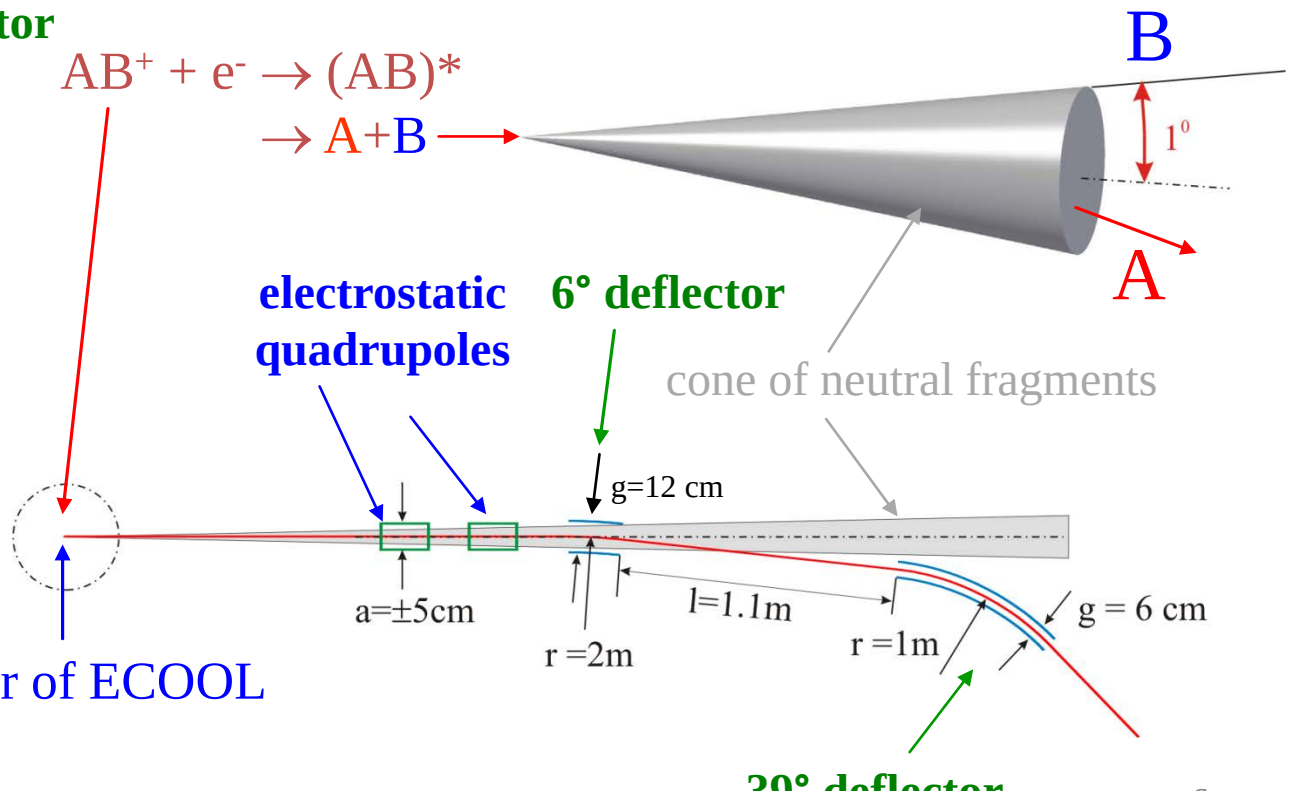

Lattice calculation with MAD8

MAD8 provides the opportunity to define transport matrixes by the user.
To get the 6x6 transport matrixes for the electrostatic elements the equation of motion was investigated analytical by solving the differential equation:
a.) non relativistic case:

$$m\frac{d^2\vec{r}}{dt^2}=Q\vec{E}(\vec{r}(t))$$

electrical field in the electrostatic elements

b.) relativistic case:
calculated from the relativistic Hamiltonian published in

PHYSICAL REVIEW SPECIAL TOPICS - ACCELERATORS AND BEAMS **7**, 120101 (2004)

Heavy ion storage ring without linear dispersion

Masahiro Ikegami, Akira Noda, and Mikio Tanabe
Institute for Chemical Research, Kyoto University, Gokanosho, Uji, 611-0011, Kyoto, Japan
Manfred Grieser
Max-Planck-Institut für Kernphysik, Postfach 103980, 69029 Heidelberg, Germany
Hiromi Okamoto
Graduate School of Advanced Sciences of Matter, Hiroshima University, 1-3-1 Kagamiyama, Higashi-Hiroshima, 739-8530, Hiroshima, Japan

for $\vec{B}=0$

Cylinder deflector matrix in MAD8:

phase space coordinates:

$$(x,\tilde{p}_x=\frac{p_x}{p_0},y,\tilde{p}_y=\frac{p_y}{p_0},-c\Delta t,\frac{\Delta E}{p_0 c})$$

energy deviation to central particle where:

$$\frac{d}{ds}\frac{\Delta E}{p_0 c}=0 \quad !$$

$$E=E_k+Q\phi(\vec{r})$$

p_0=constant (ϕ=0)

relativistic case

with $r_k=\frac{1}{\rho_0}\sqrt{1+\frac{1}{\gamma^2}}$

$$M=\begin{pmatrix} \cos(Lr_k) & \frac{\sin(Lr_k)}{r_k} & 0 & 0 & 0 & \frac{\rho_0-\cos(Lr_k)\rho_0}{\beta} \\ -\sin(Lr_k)r_k & \cos(Lr_k) & 0 & 0 & 0 & \frac{\sin(Lr_k)r_k\rho_0}{\beta} \\ 0 & 0 & 1 & L & 0 & 0 \\ 0 & 0 & 0 & 1 & 0 & 0 \\ -\frac{\sin(Lr_k)r_k\rho_0}{\beta} & \frac{(\cos(Lr_k)-1)\rho_0}{\beta} & 0 & 0 & 1 & \frac{\sin(Lr_k)r_k\rho_0^2-L}{\beta^2} \\ 0 & 0 & 0 & 0 & 0 & 1 \end{pmatrix}$$

transit time effects: η, f_s ….

Lattice calculation with MAD8

Example of MAD8 calculation

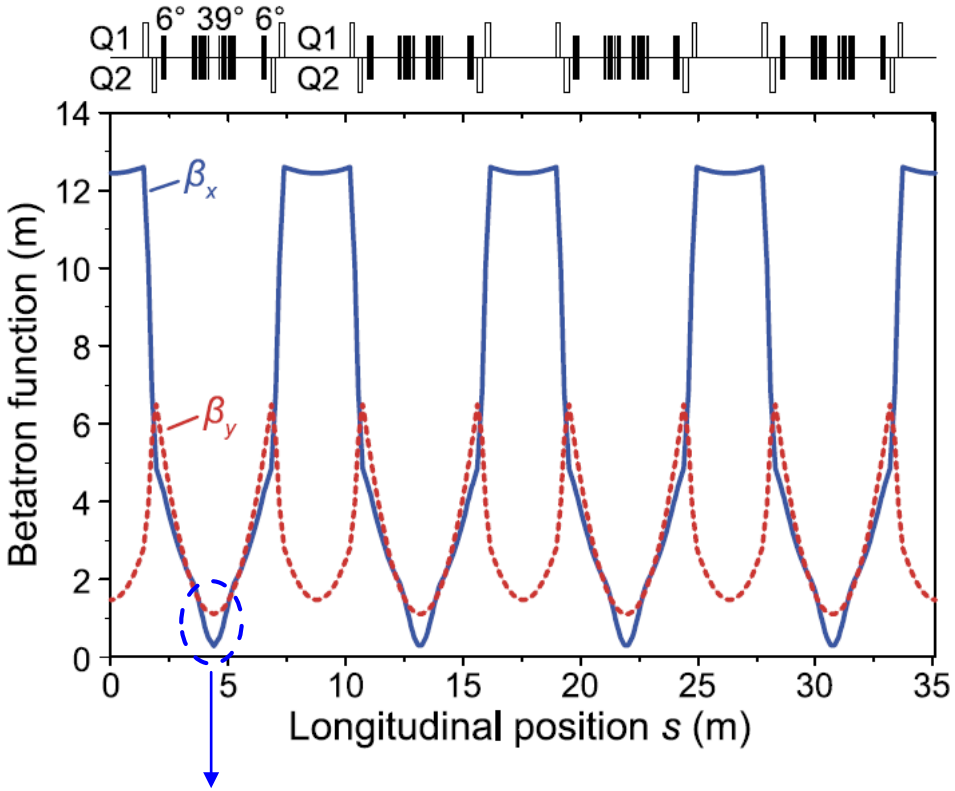

small horizontal beam size in the deflectors

Horizontal and vertical betatron functions ß$_x$ and ß$_y$ calculated by the MAD8 code for the standard settings of the CSR (Q_x=Q_y=2.59)

coupling of the horizontal and vertical motion.

Coupling effects were been investigated experimentally and by simulation (later in the talk)

Tracking through real electrostatic fields with G4beamline

G4beamline screen output

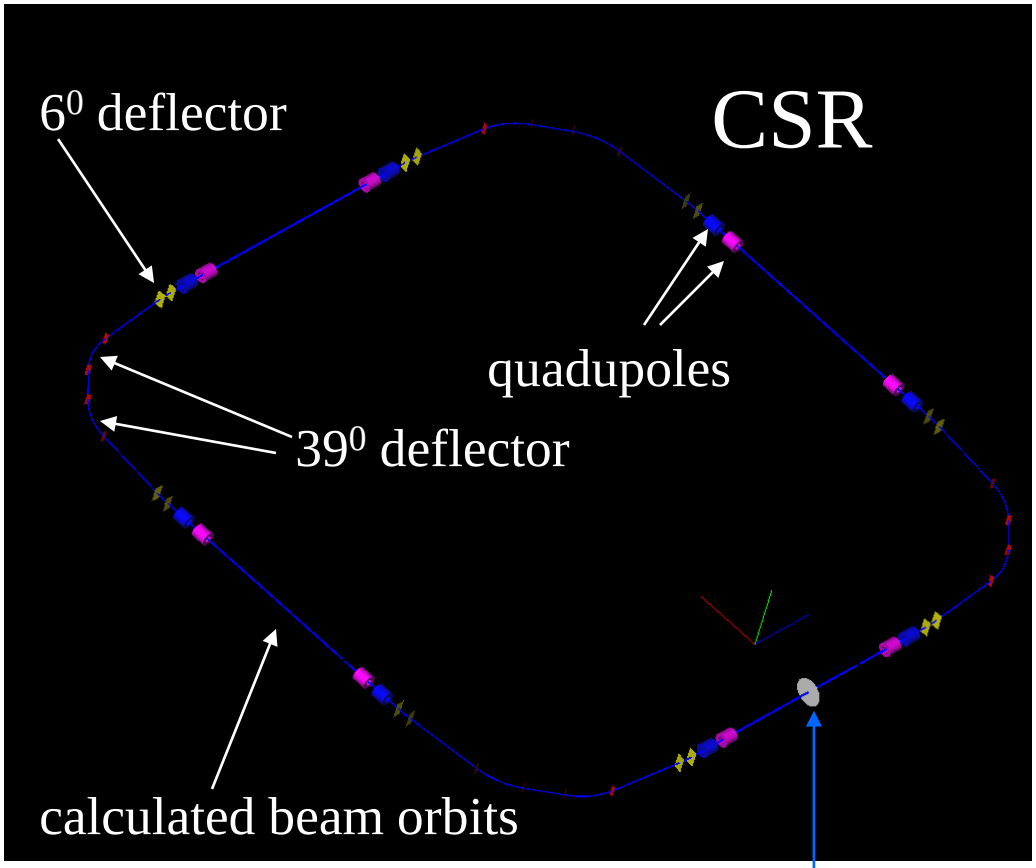

horizontal phase space coordinates of a single particle at observation point obtained for several turns

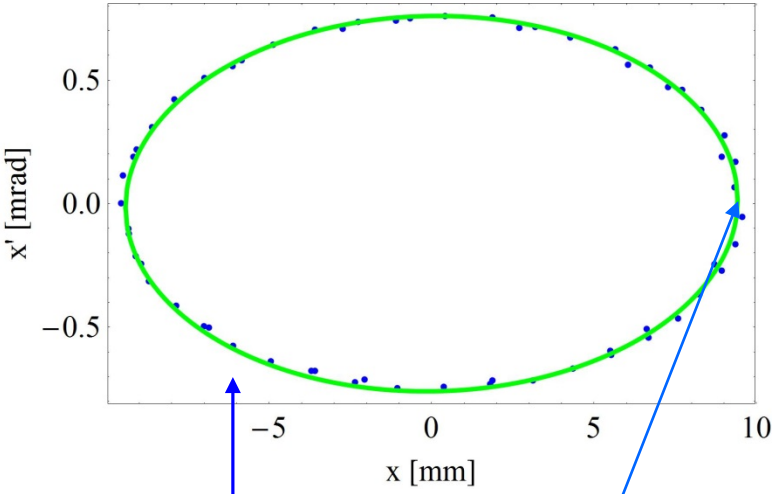

start coordinate x=10 mm

each element is described by the field table obtained with TOSCA

start and observation point of the **phase space coordinates**

Calculation of the field maps with TOSCA

example: 39^0 deflector

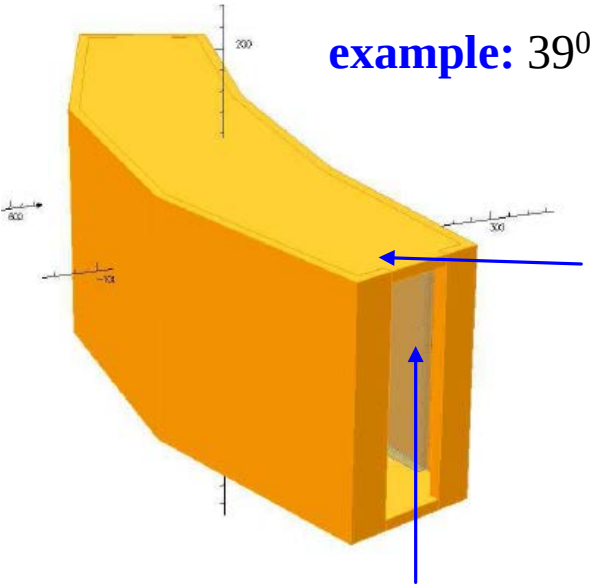

electrode cage of 39^0 deflector

electrodes

small mesh size close to central orbit

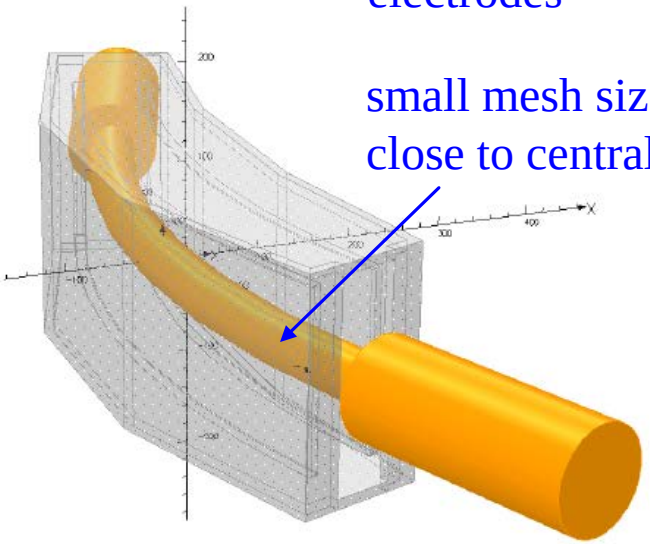

absolute value of electric field in the plane of the central orbit

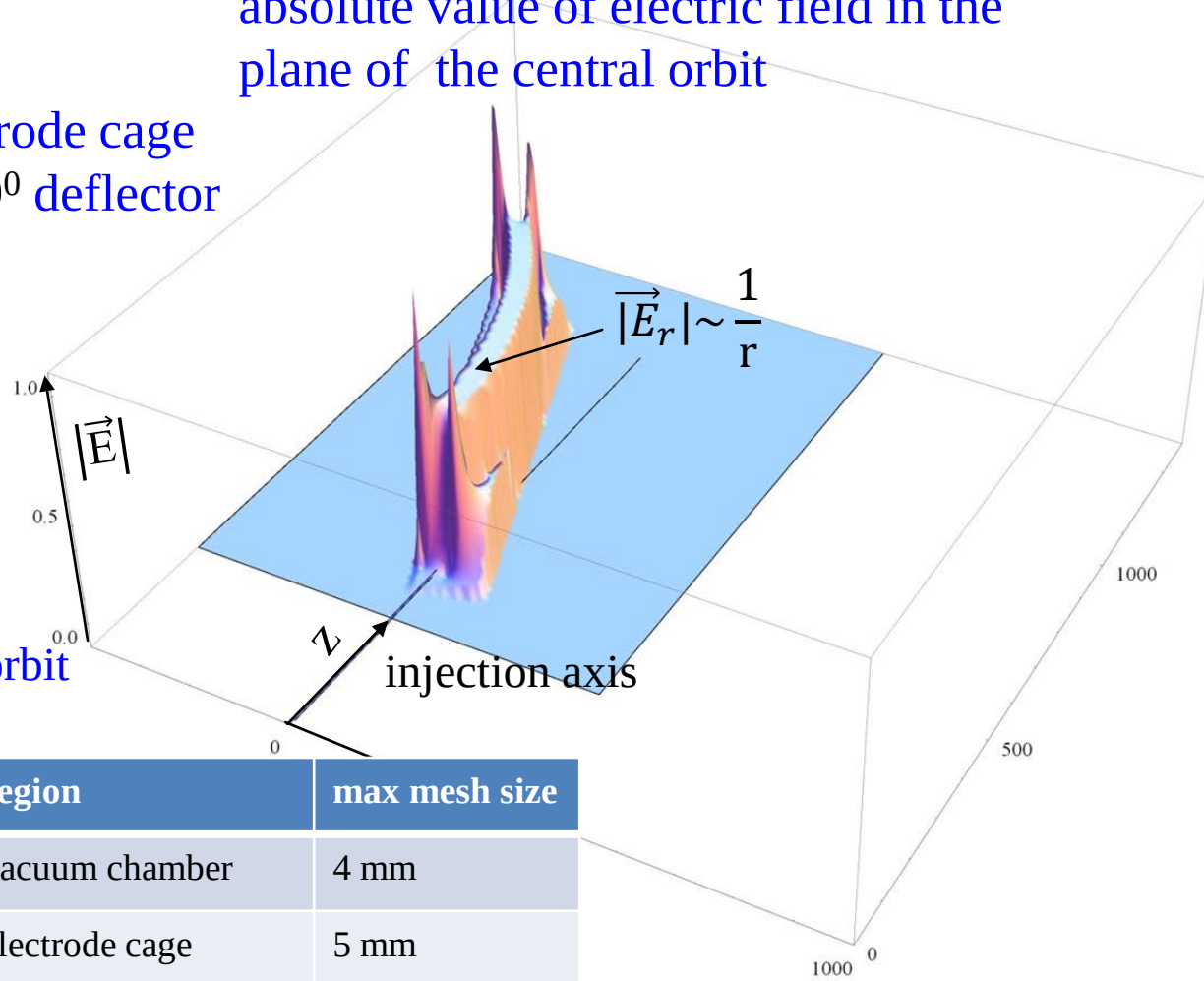

region	max mesh size
vacuum chamber	4 mm
electrode cage	5 mm
electrodes	4 mm
around central orbit	2 mm

Determine of the deflection angle of the 39^0 deflector

Length of the electrodes changed in two 2-3 iterations until a total deflection angle of 39^0 in tracking calculations with a protons were realized.

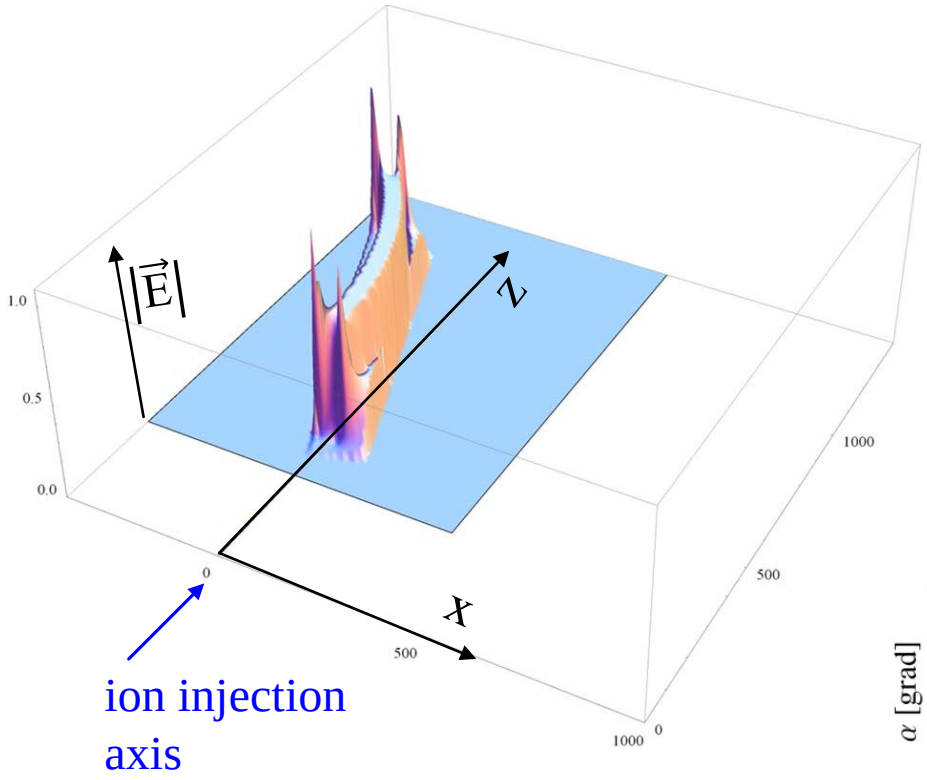

ion injection axis

deflection angle

$$\alpha = \left| \arctan\left(\frac{v_x}{v_z} \right) \right|$$

v_x – x coordinate of the velocity

v_z – z coordinate of the velocity

deflection angle was calculated from v_x,v_y determined with G4beamline in a single ion tracking calculation

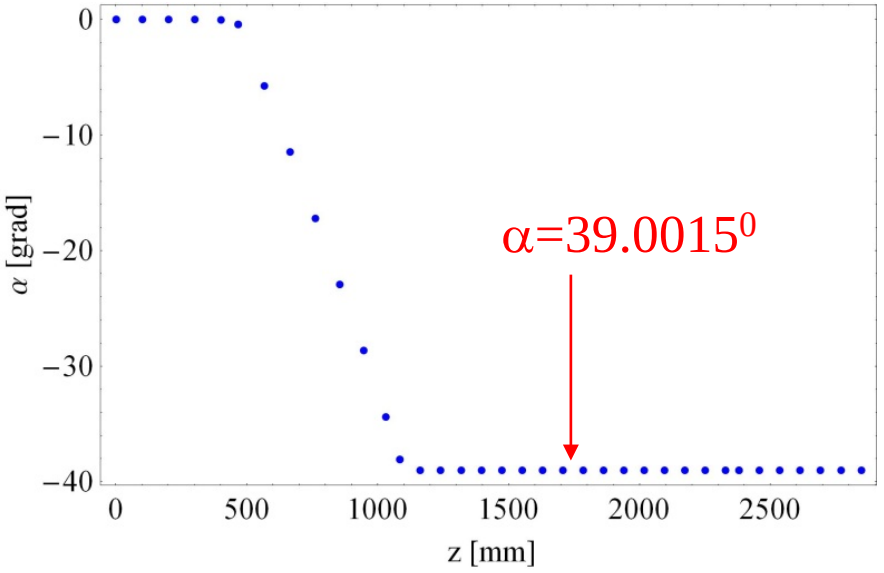

Nominal and actual orbit calculated with g4beamline

proton orbit with reference momentum,
tracked through the 39^0 deflector

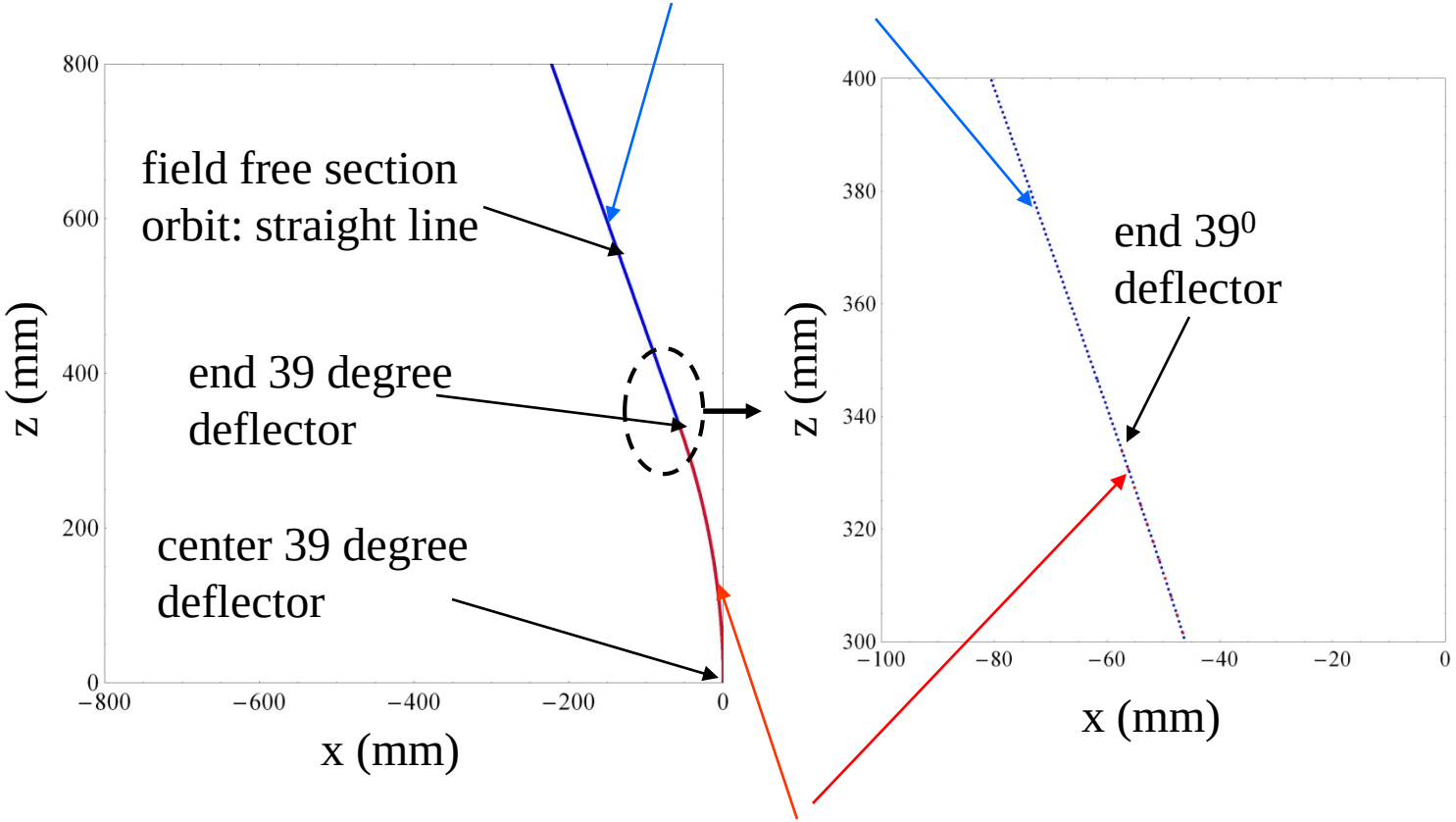

nominal orbit (central orbit): circle with r=1000 mm

tracked reference particle is exactly on the nominal (central orbit)

Construction of CSR ring in G4beamline

Determination of the closed orbit shift

G4beamline screen output

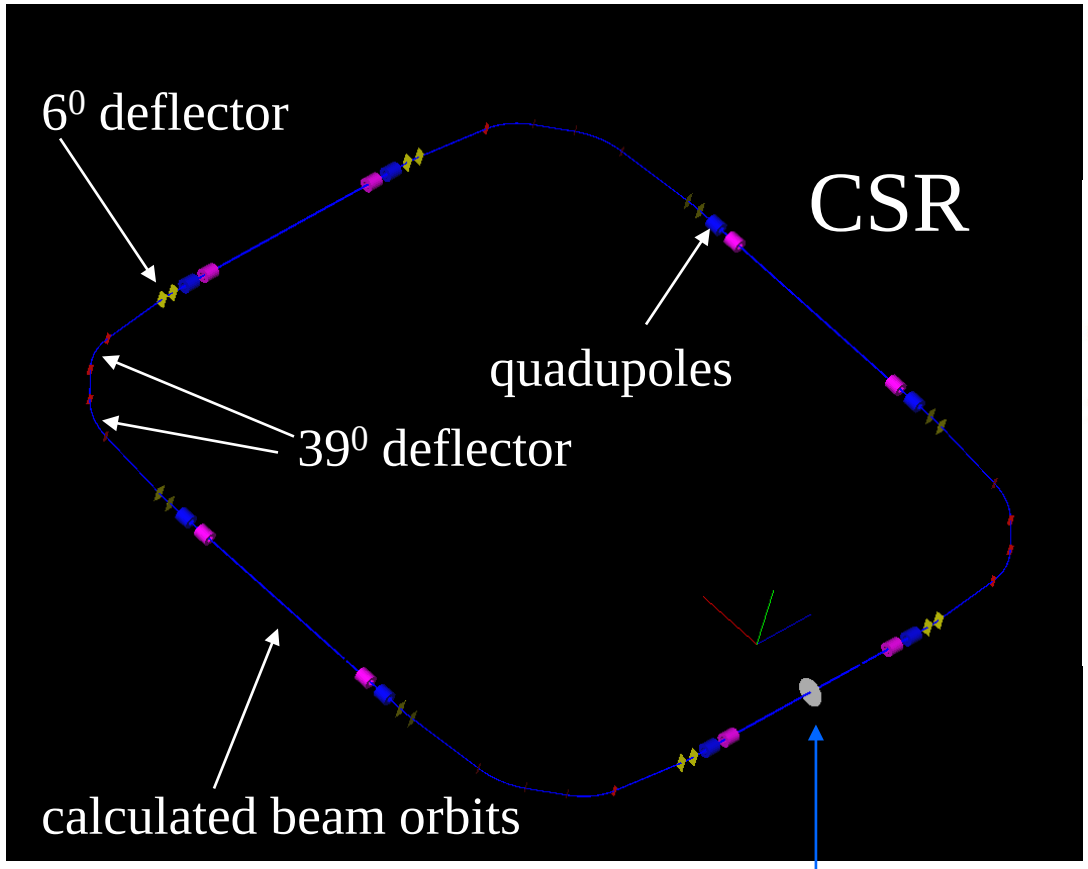

start and observation point x=10 mm

horizontal phase space coordinates of a single particle at observation point with reference momentum

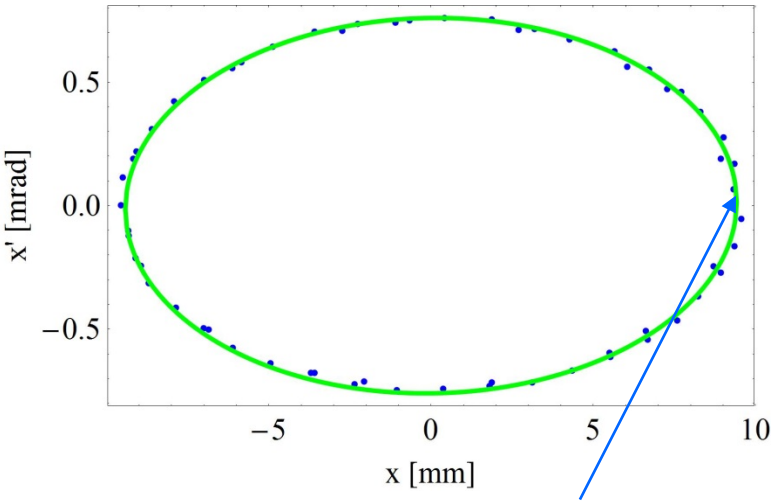

start coordinate x=10 mm

Δx=0.405 mm
Δx'=-0.047 mrad

Twiss parameter at the center of a straight section

horizontal

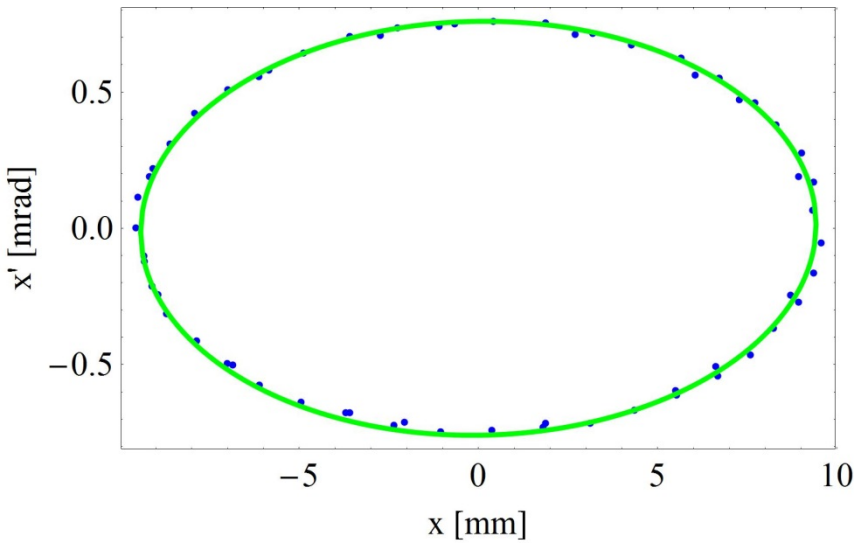

α=–0.01856
β=12.41 m
γ=0.08061
ε=7.15 mm·mrad

vertical

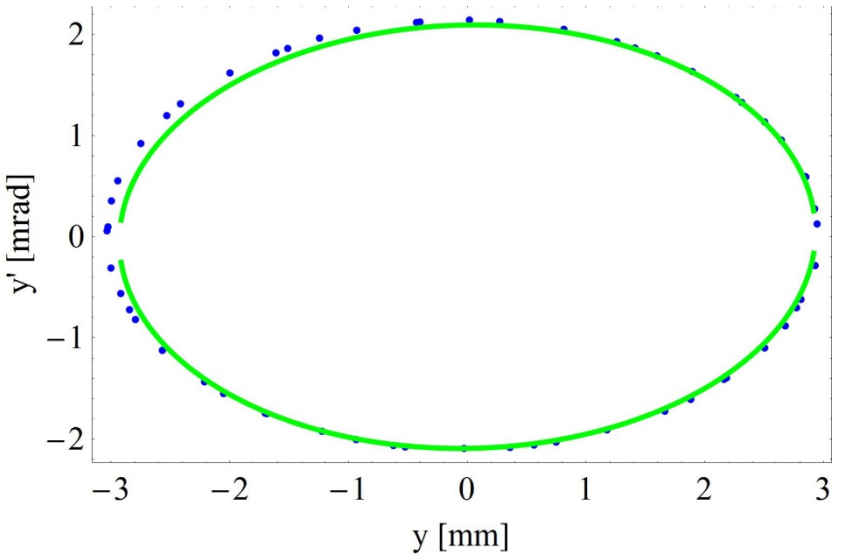

α=–0.0217
β=1.40 m
γ=0.7143
ε=6.13 mm·mrad

quadrupole setting for 300 keV protons:

family1: U=4.015 kV
family2: U=-5.030 kV

Calculated β functions with MAD8

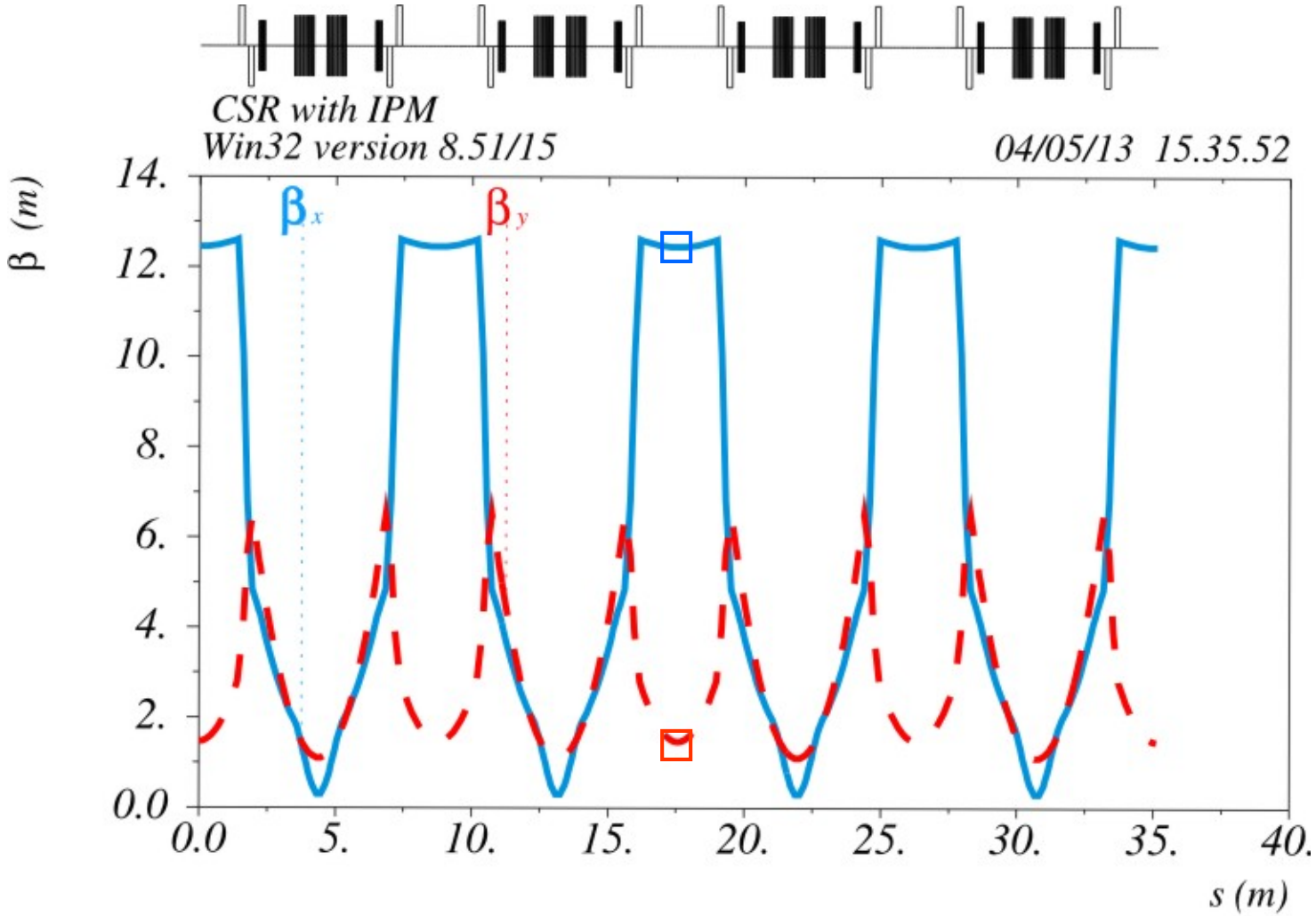

$\delta_E / p_0 c = 0.$

Table name = TWISS

MAD8

$ß_x$=12.44 m

$ß_y$=1.47 m

G4beamline (G4bl)

$ß_x$=12.41 m

$ß_y$=1.40 m

Dispersion comparison between G4bl and MAD8

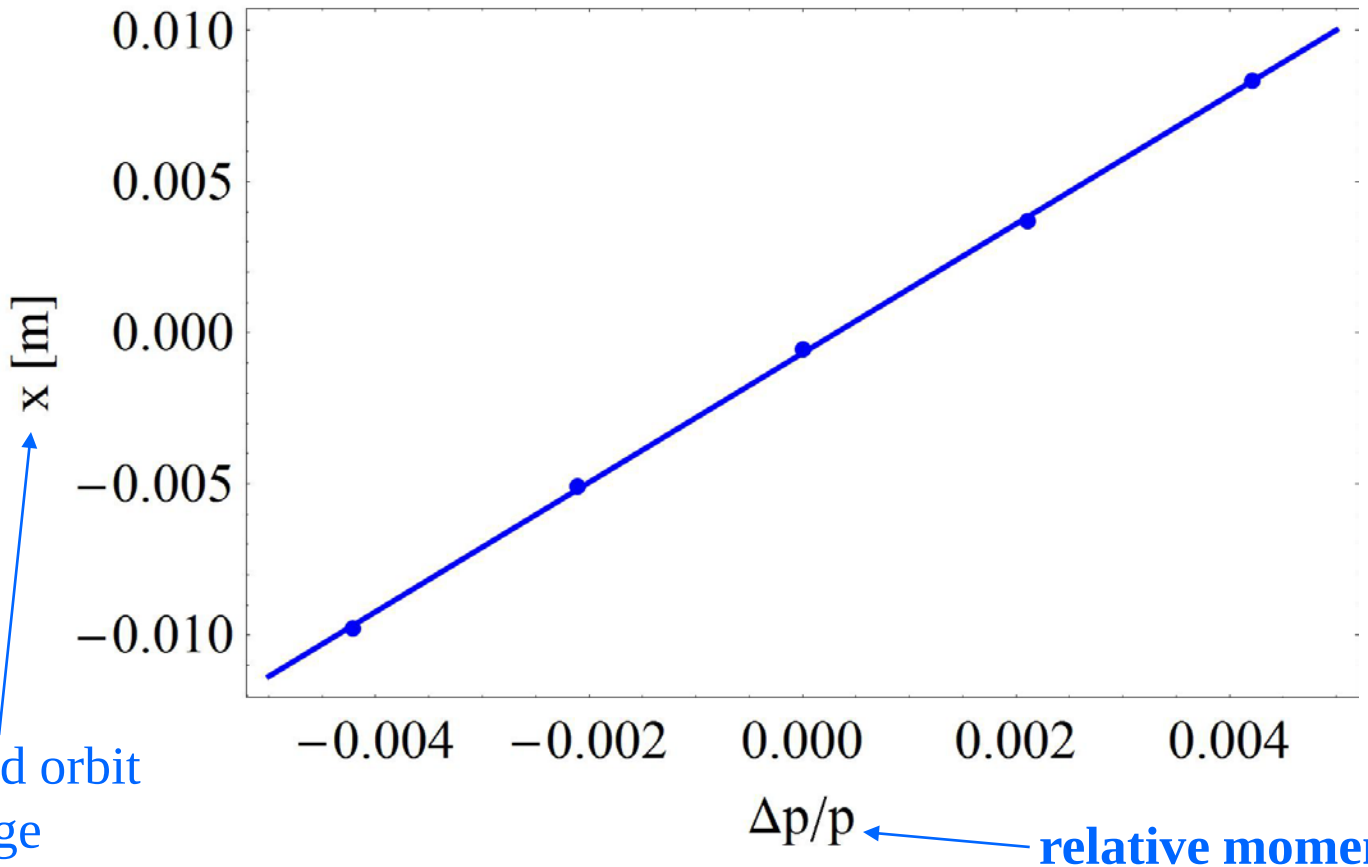

⇒ dispersion D_x=2.1 m (G4beamline)

MAD8: D_x=2.06 m **center straight section**

Horizontal envelope in the CSR

Comparison of MAD8 with TOSCA

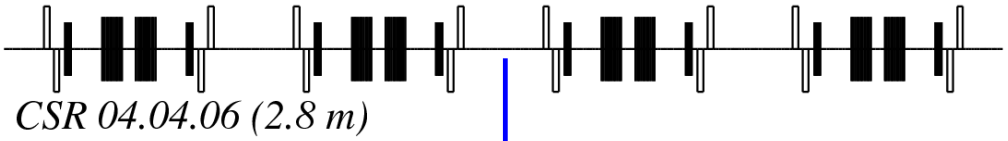

CSR 04.04.06 (2.8 m)

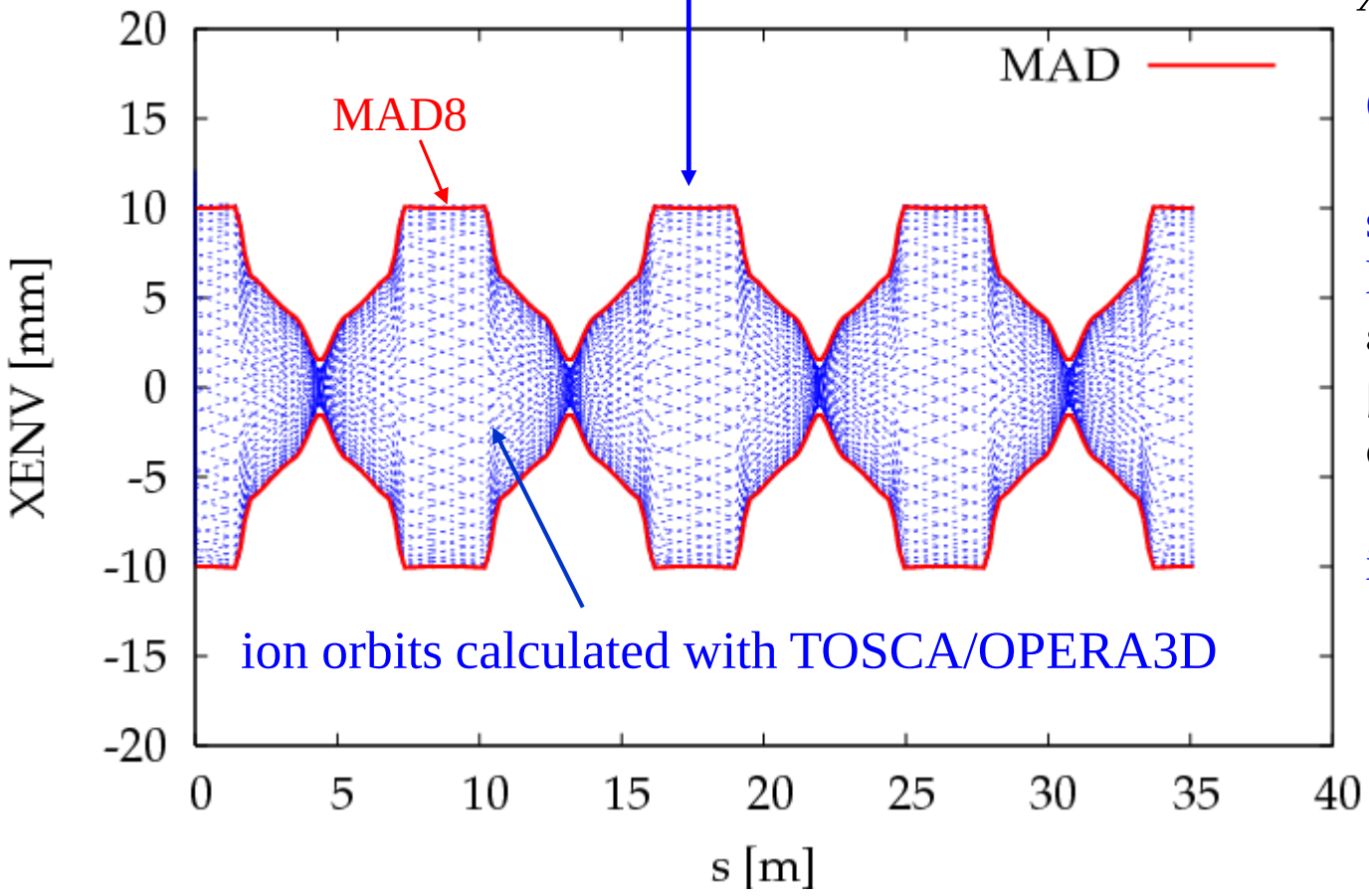

$$x_{env}(s)=\sqrt{\varepsilon_x \cdot \beta_x(s)}$$

Opera 3D calculations

start coordinate:
lying on ellipse with
ε_x=8 mm·mrad
β_x= 12.1 m
α_x=0

ion: 20 keV proton

Vertical envelope in the CSR

Comparison of MAD8 with TOSCA

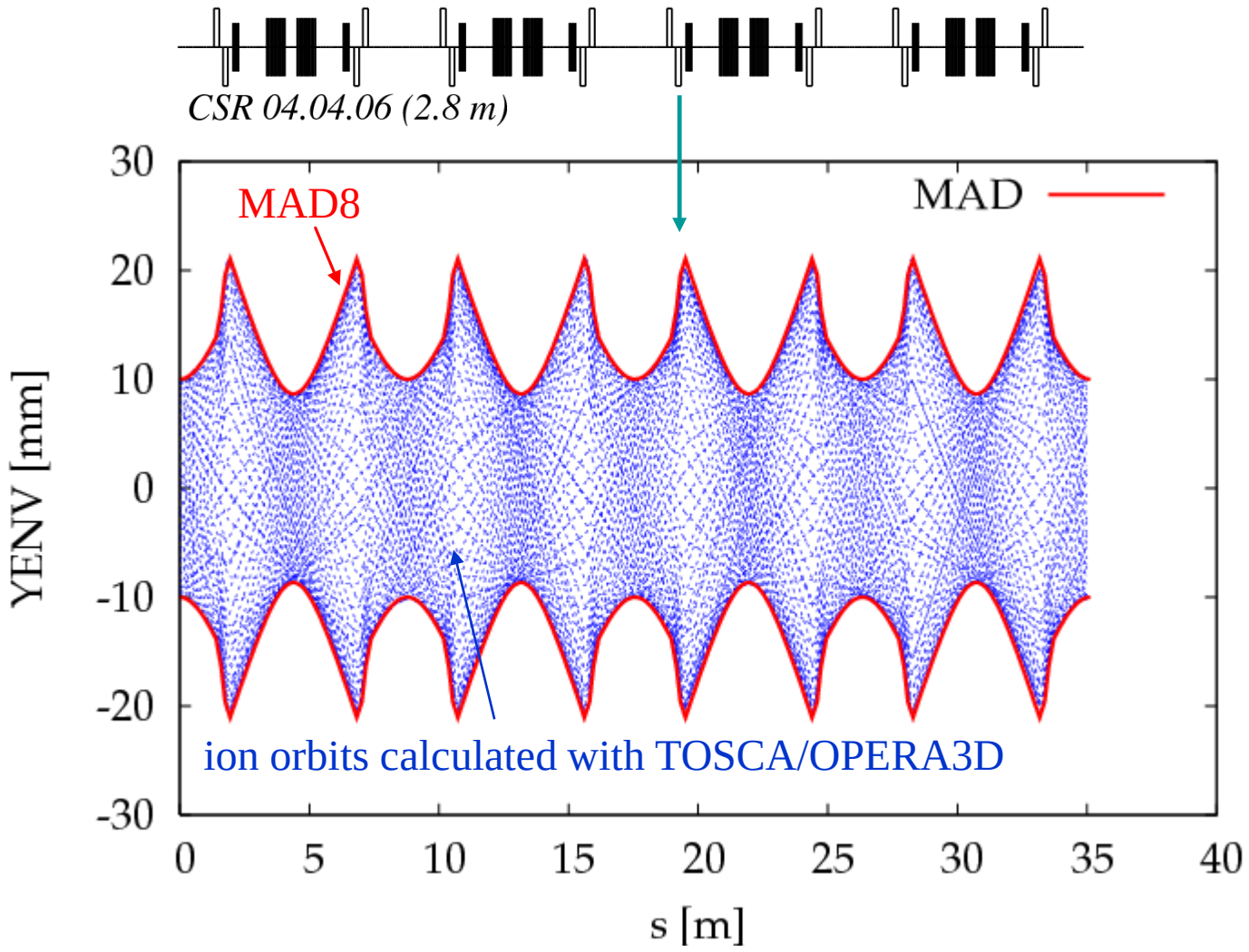

$$y_{env}(s)=\sqrt{\varepsilon_y \cdot \beta_y(s)}$$

Opera 3D calculations

start coordinate:
lying on ellipse with
ε_y=68.1 mm·mrad
β_y= 1.3 m
α_y=0

ion: 20 keV proton

Comparison of MAD8, g4beamline and Tosca simulations

TABLE I. Betatron functions (β_x, β_y) and dispersion (D_x) in the center of the CSR straight sections, together with betatron tunes Q_x, Q_y of the CSR. Results from matrix calculations (MAD8[29]) are compared to those from all-ring tracking calculations using TOSCA[32] and G4beamline.[33] The tracking calculations also yield the approximate ring acceptances A_x, A_y, which are given for zero-emittance ion beams.

Parameter	MAD8	TOSCA	G4beamline	Unit
β_x	12.44	12.1	12.41	m
β_y	1.47	1.3	1.4	m
D_x	2.06	2.1	2.1	m
Q_x	2.59	2.60	2.60	
Q_y	2.59	2.61	2.62	
A_x		120	120	mm mrad
A_y		180	170	mm mrad

A_x –horizontal acceptance for $\varepsilon_y \to 0$

A_y- vertical acceptance for $\varepsilon_x \to 0$

(without consideration of magnetic field of the earth and ECOOL)

Cryostat of the CSR

isolation vacuum
ca. 10^{-6} mbar

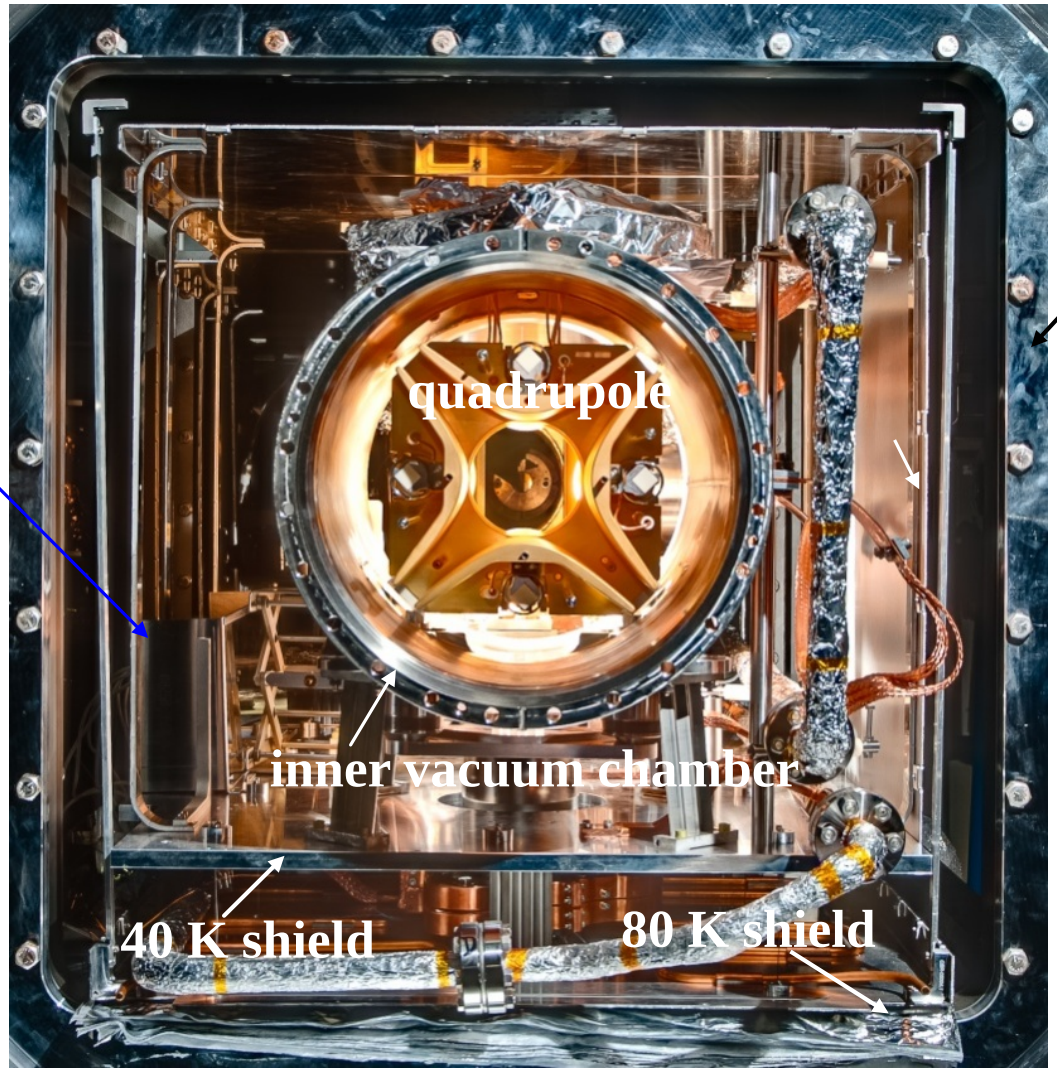

isolation
vacuum chamber

The support of the optical elements

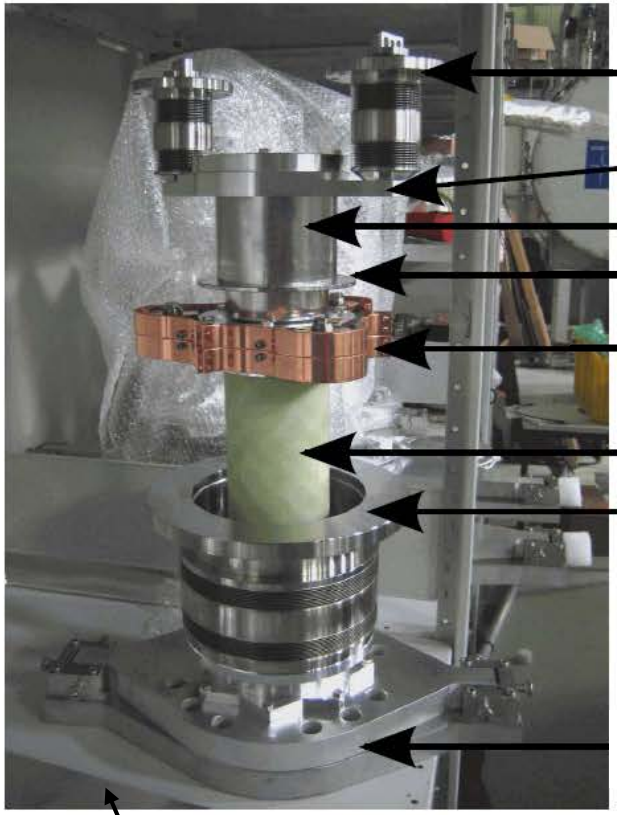

experimental vacuum chamber

thermal anchor at 10 K

stainless steel meander

thermal anchor at 40 K

thermal anchor at 80 K

GFK tube

beginning of isolation vacuum

concrete block

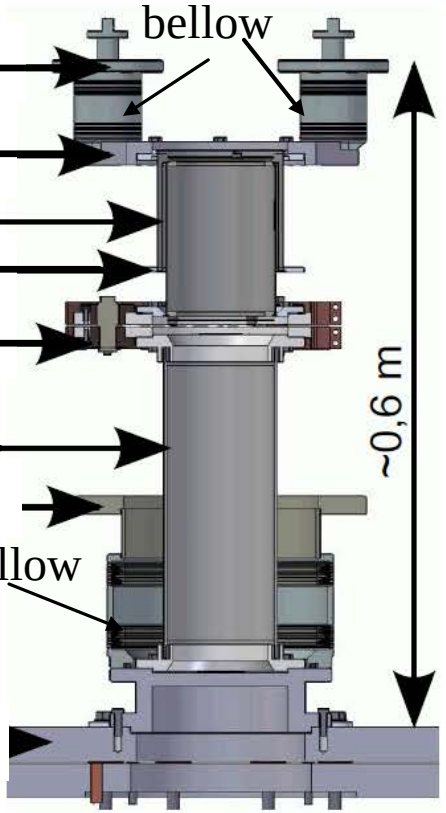

bellow

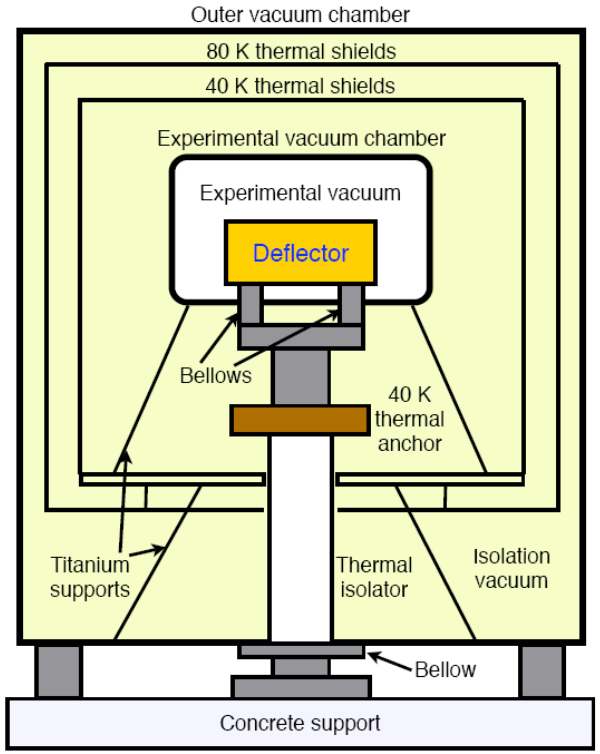

Pumping at cryogenic temperatures

cold unit

In < 10-K-operation:
cryo adsorption at 10-K-walls,
2-K cryo condensation pumps

He gas

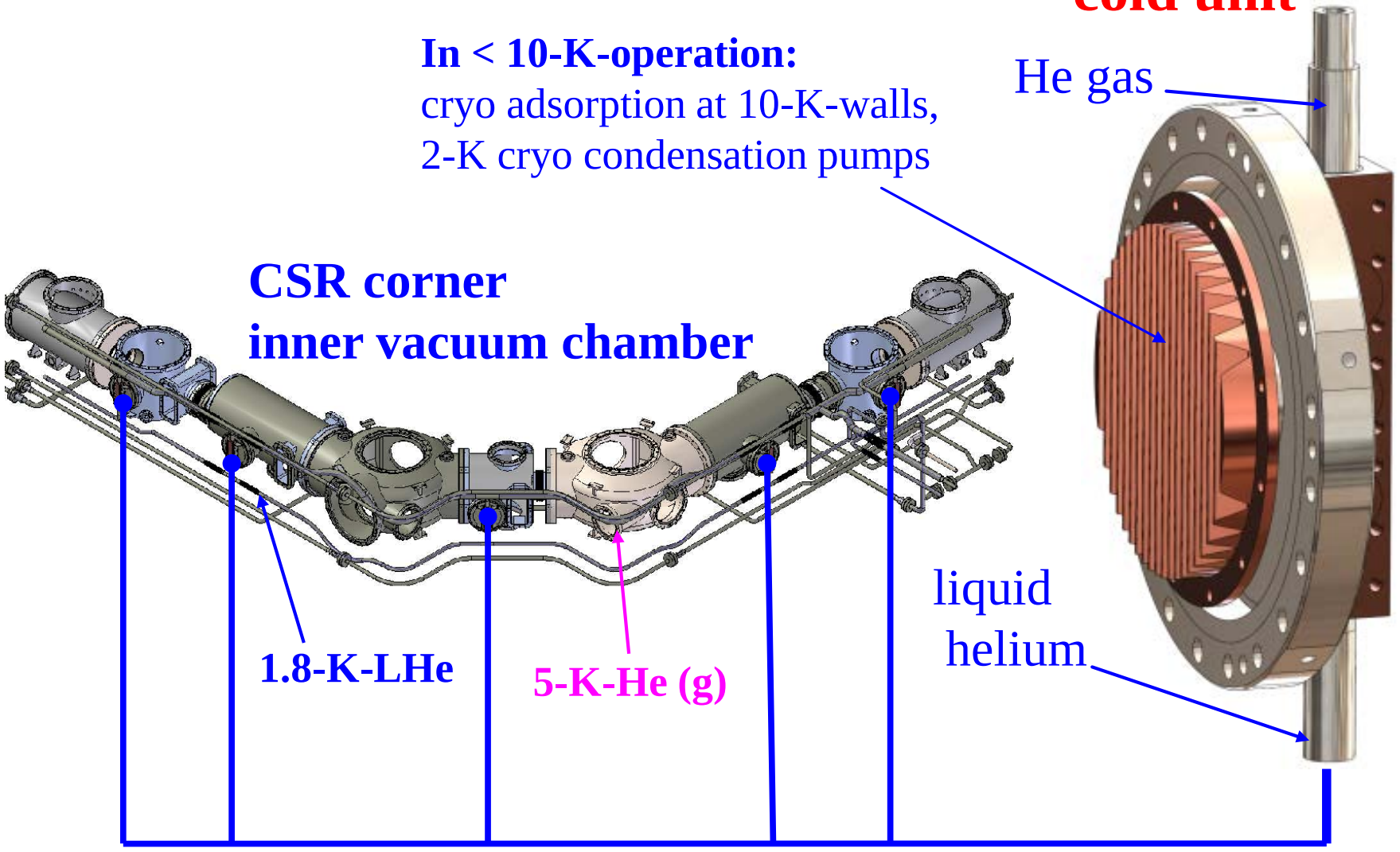

Pumping in the 300 K operation

In 300-K-operation:
250°C bake-out,
Ion-getter pumps,
NEG pump (strips),
bake-able charcoal **cryo-pumps**

NEC pump

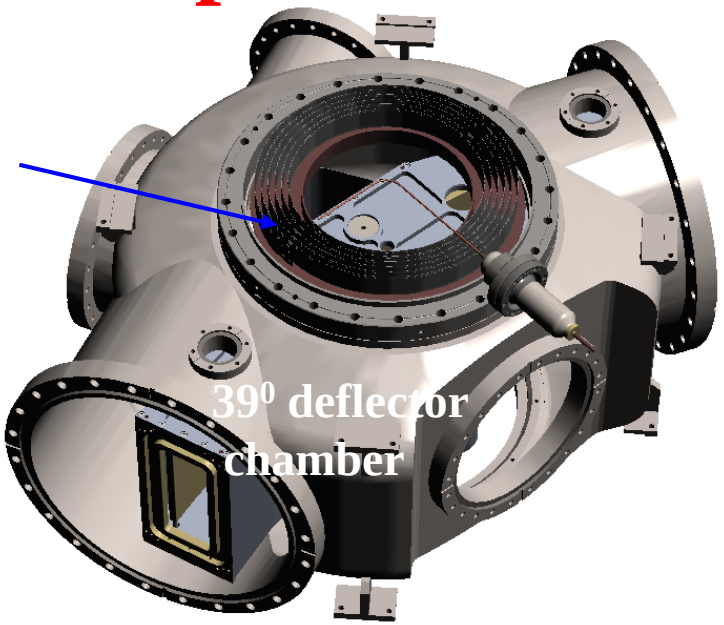

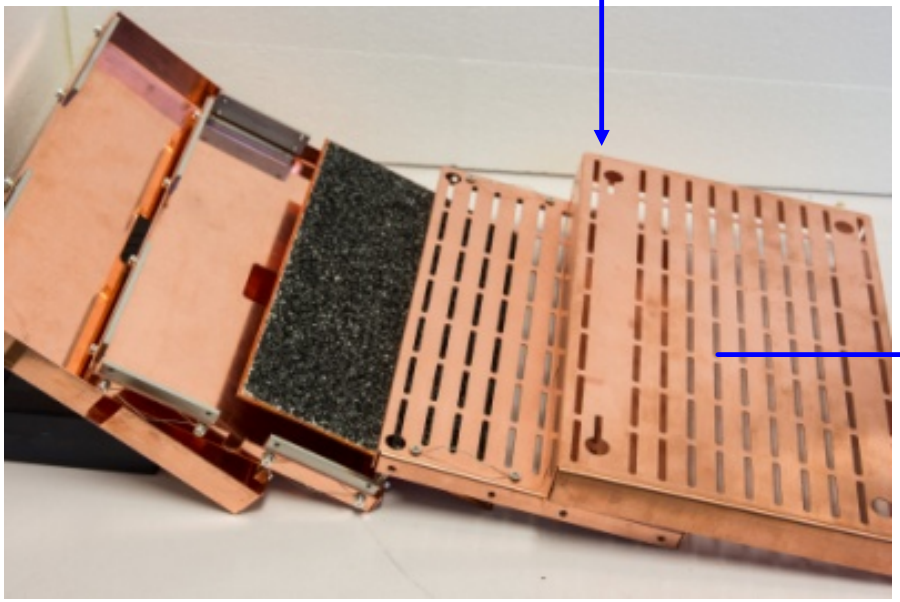

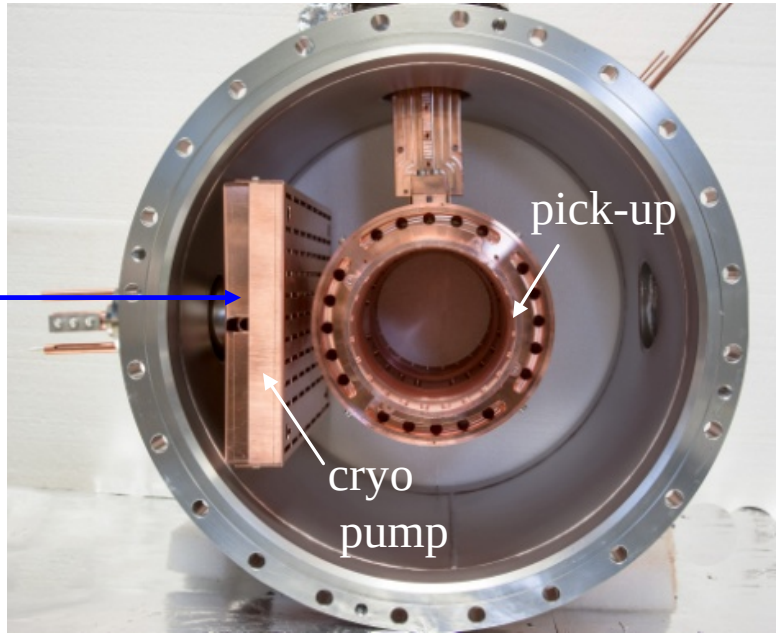

High Voltage platforms

CSR main injector:
ion sources on a high
voltage plat form of **±300 kV**

± 40 keV platform with positive and negative ion sources

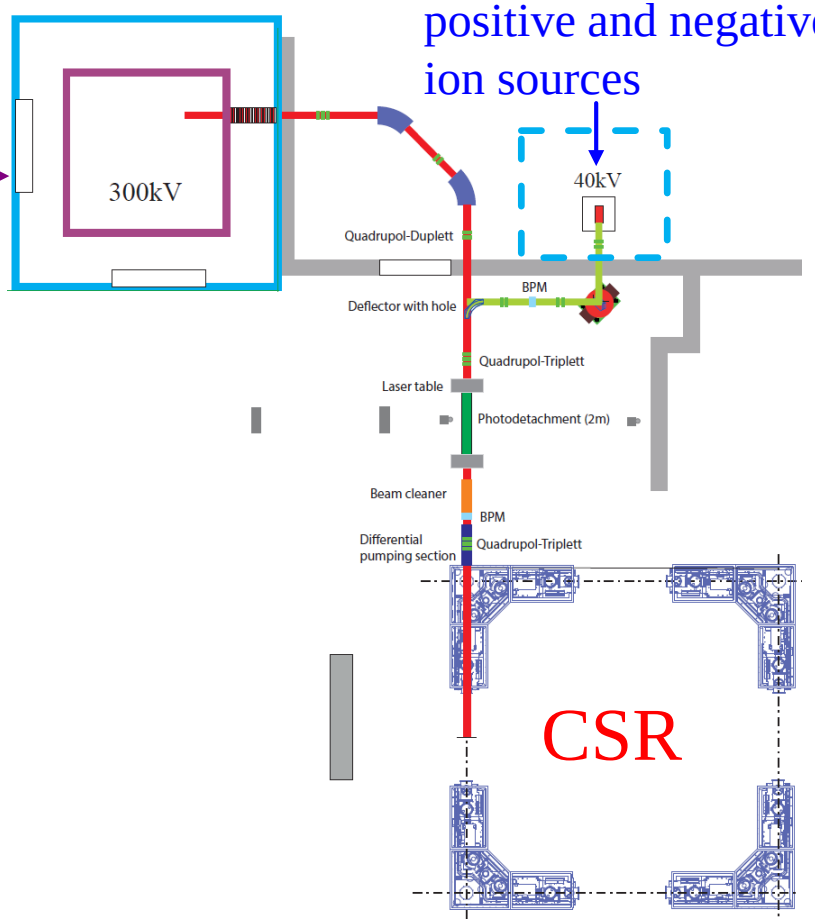

Ion sources

± 40 keV platform with positive and negative ion sources

CSR main injector: ±300 kV

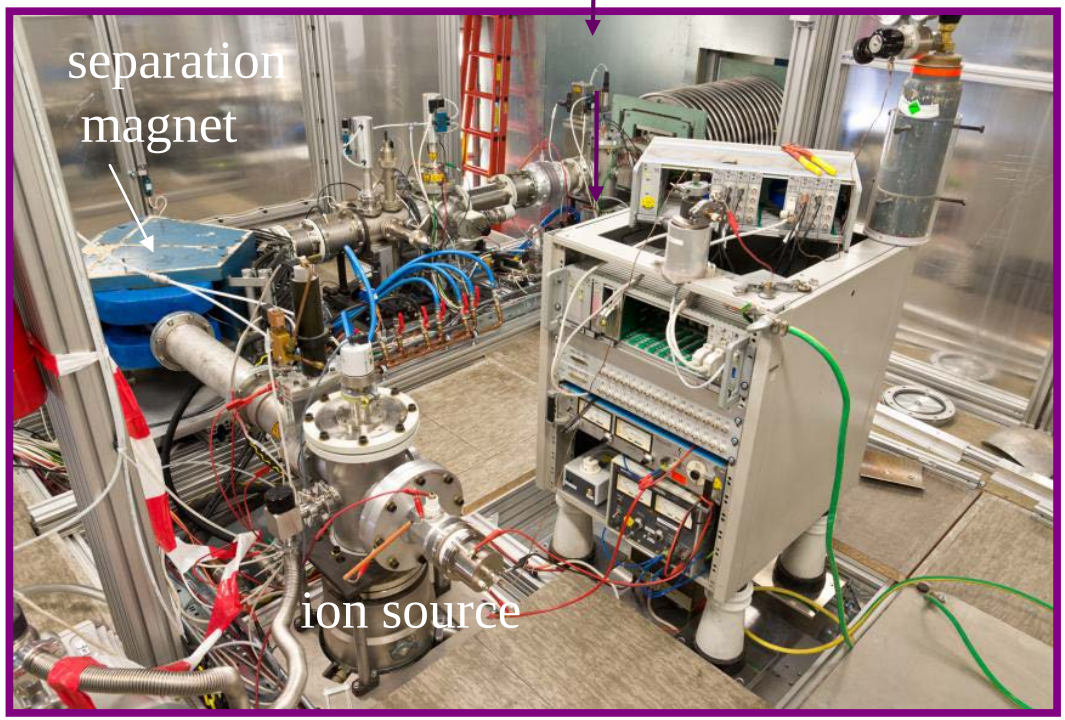

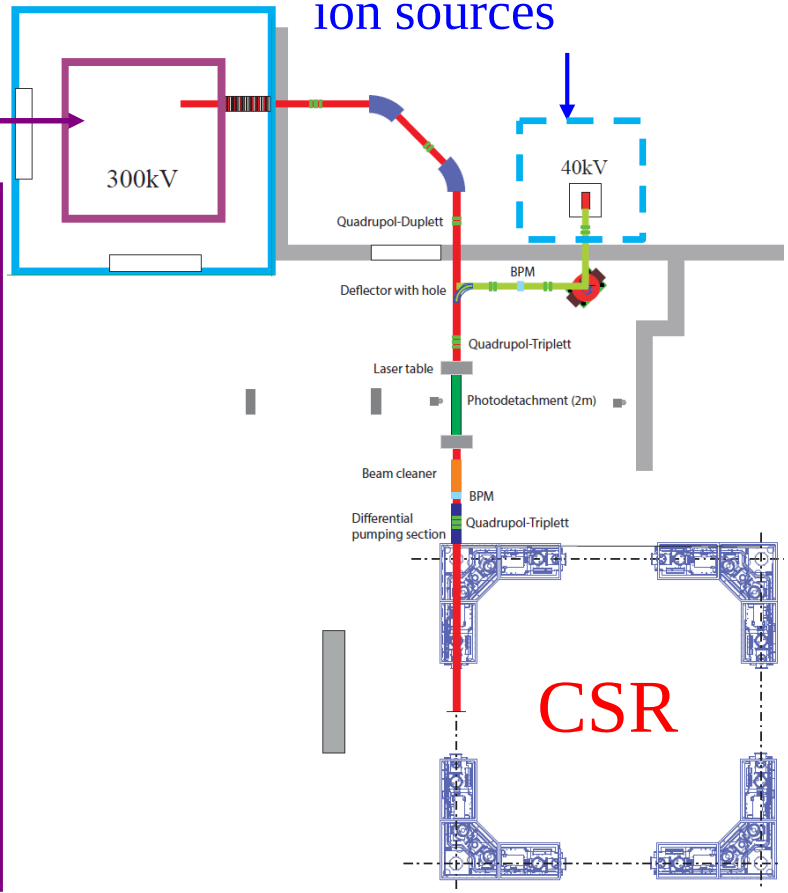

Transferline between ion source and CSR

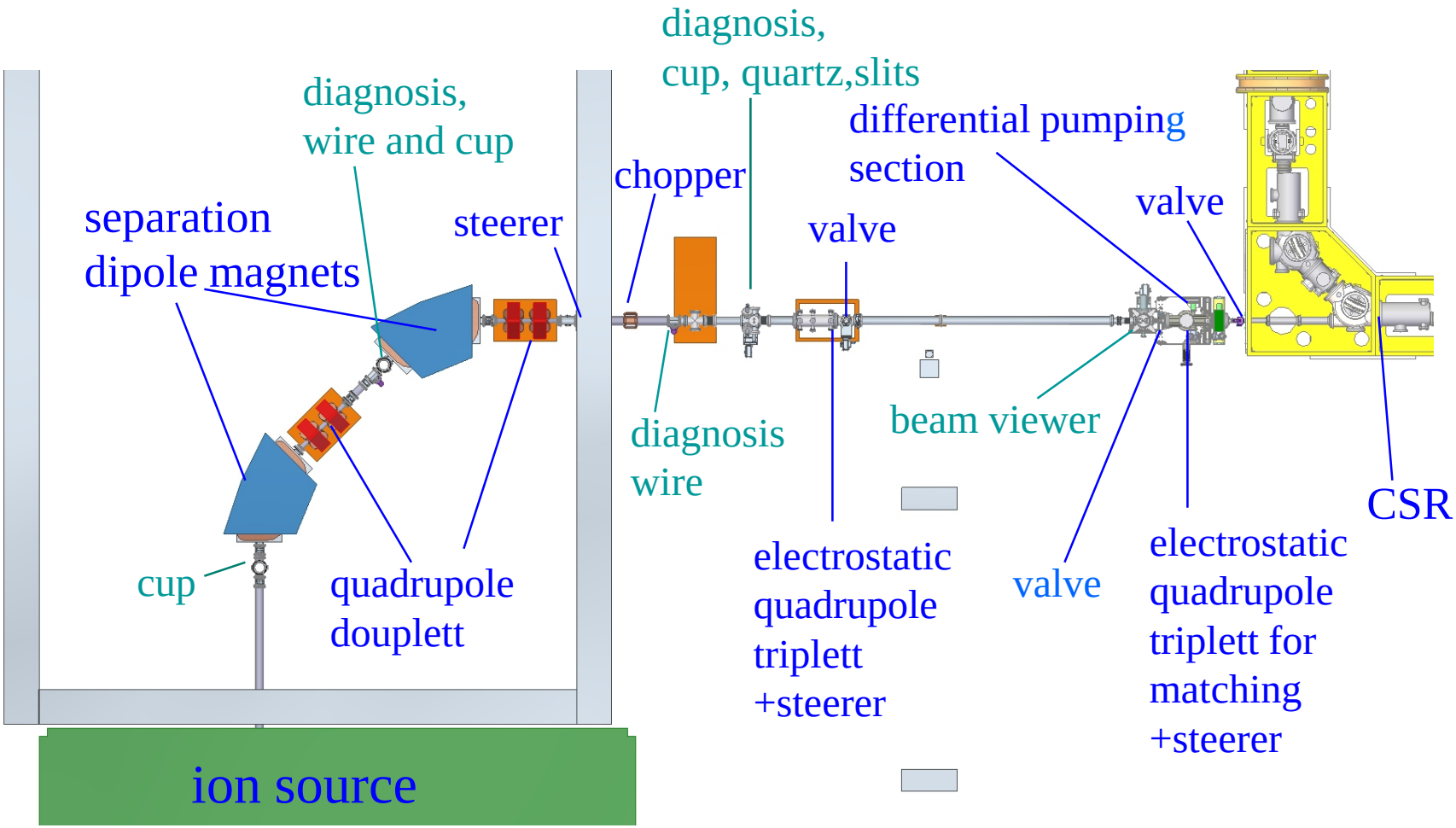

Single Turn injection

injector
beam

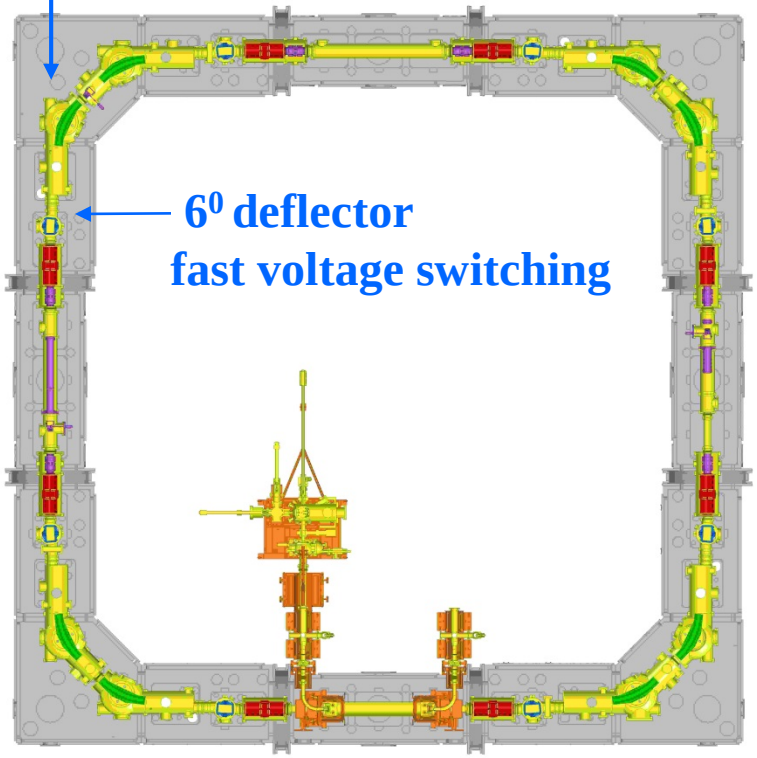

T_0-revolution time
T_i-injector beam pulse length

$$T_i \approx \frac{T_0}{2}$$ (example)

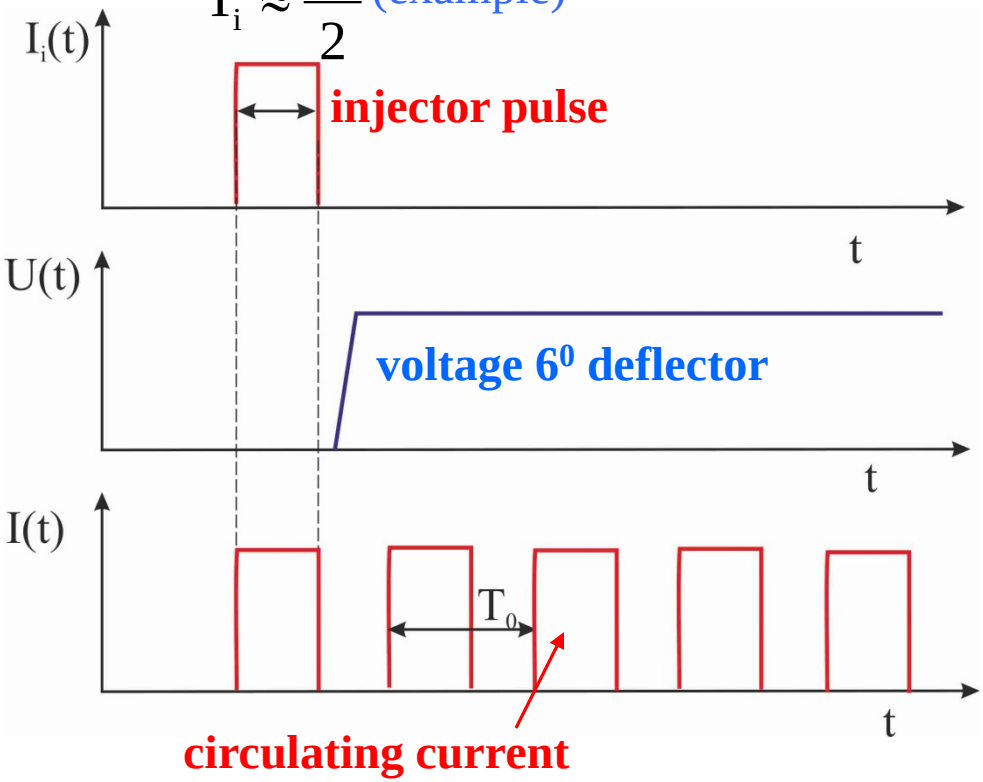

First Cryogenic operation

Cool down of the CSR

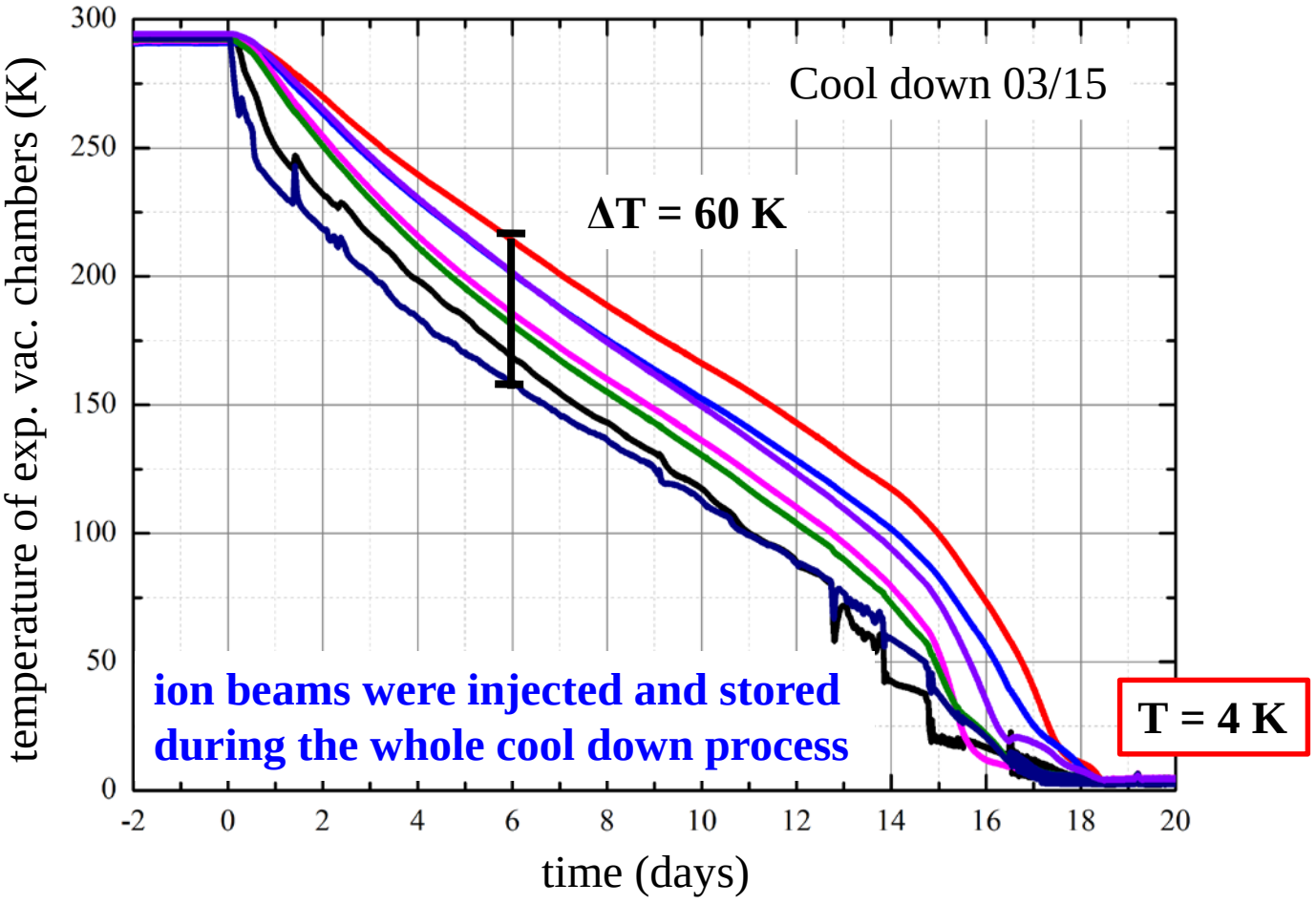

Beam profiler for first turn diagnosis

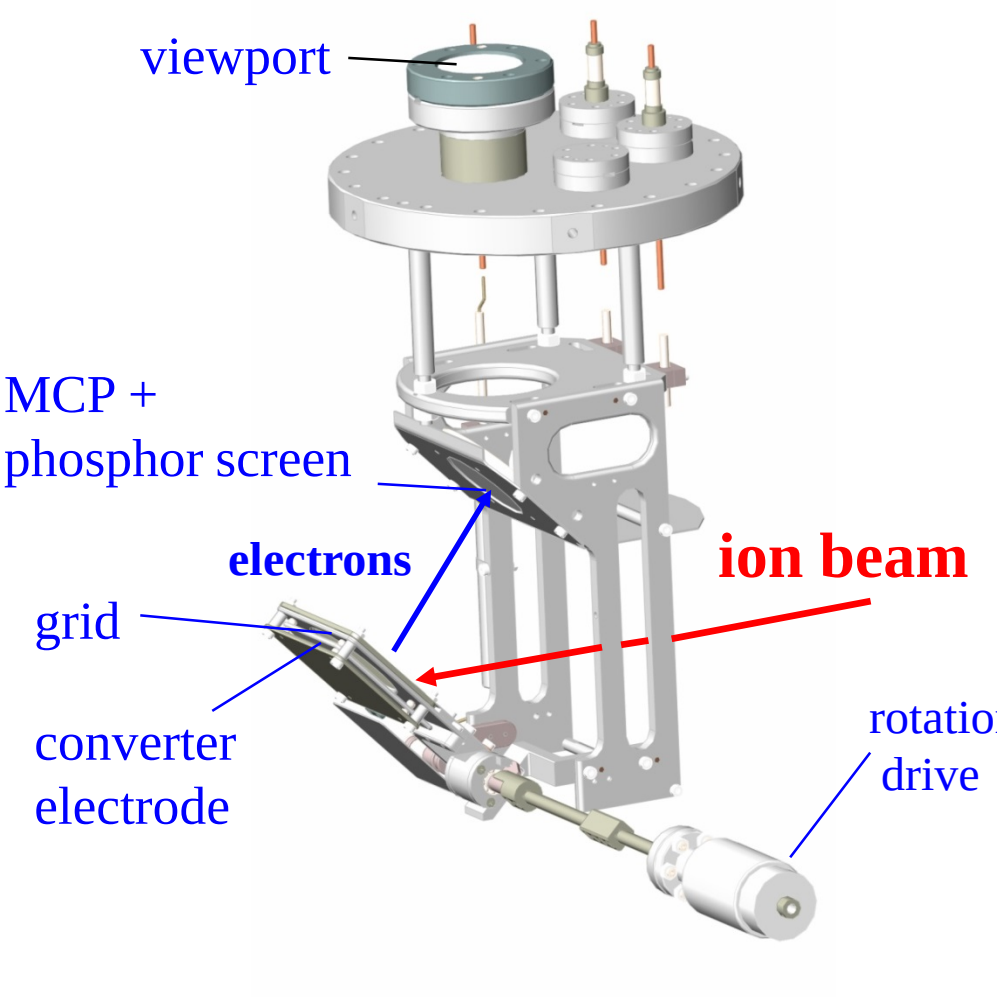

scheme

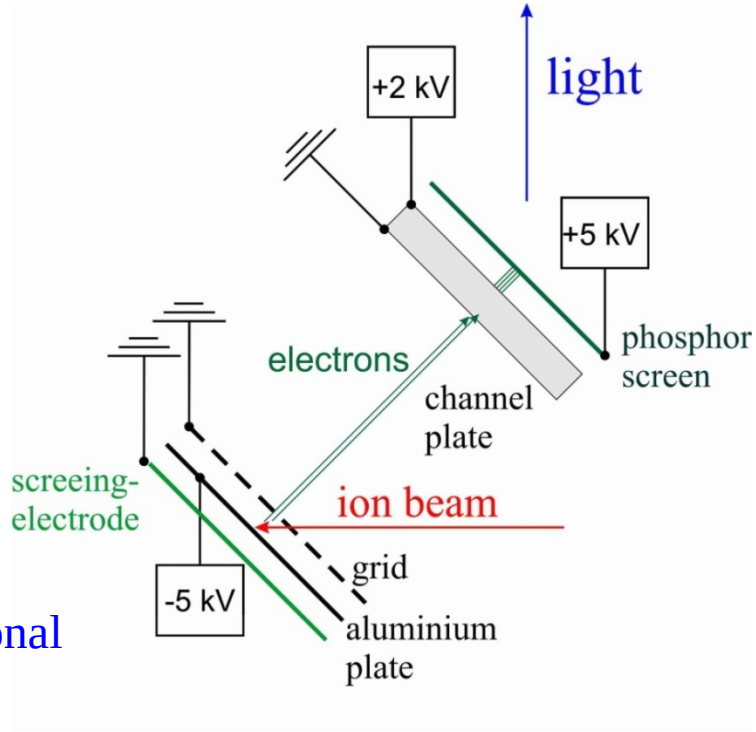

Diagnostics for ion beam injection

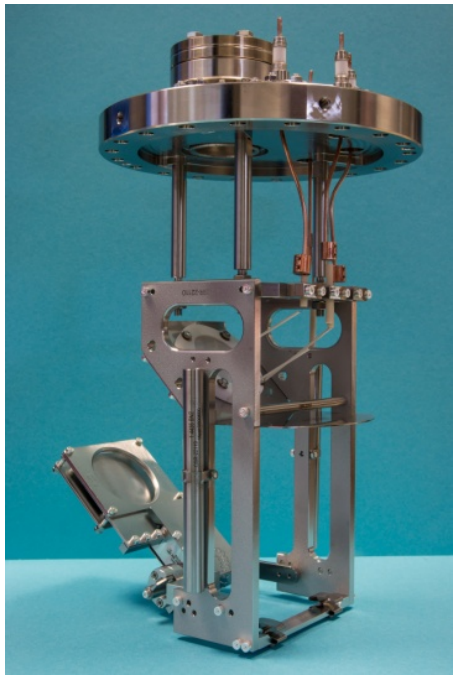

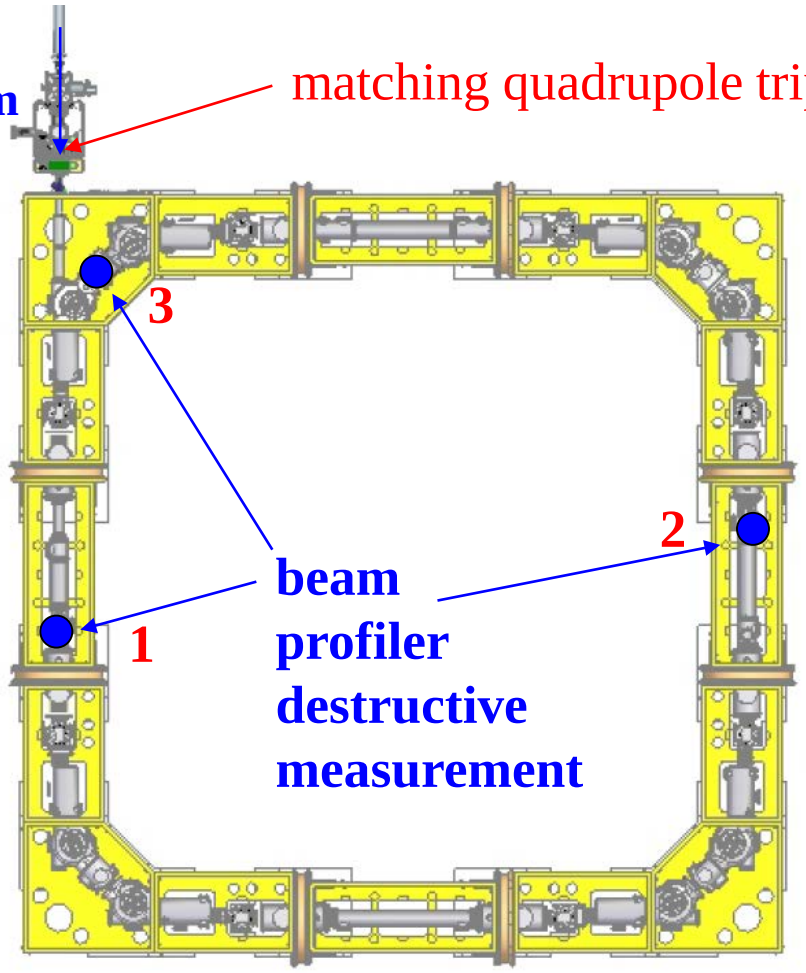

beam image

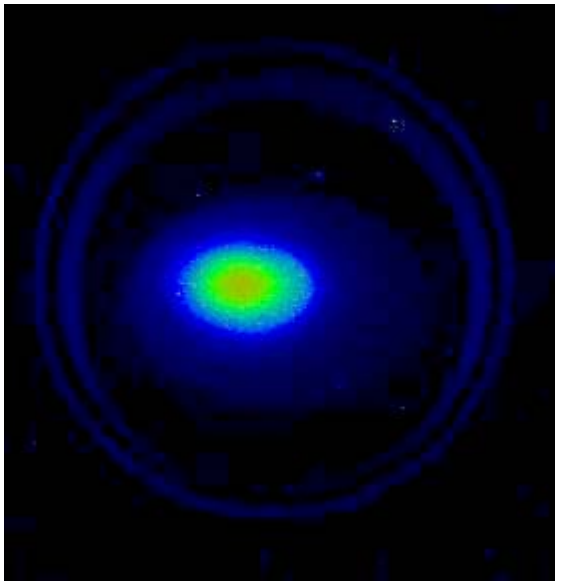

The diagnosis section

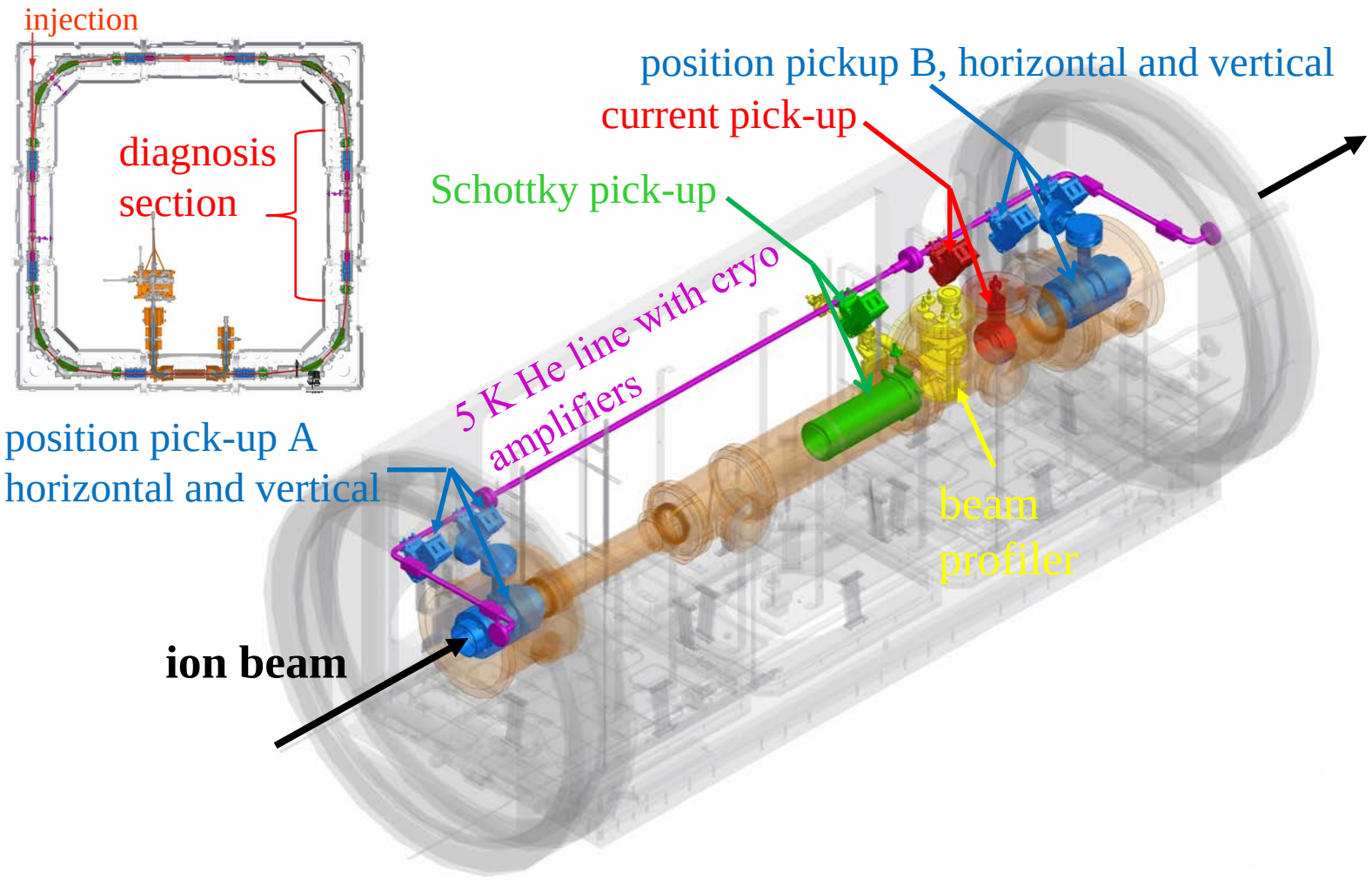

The current and Schottky pick-up

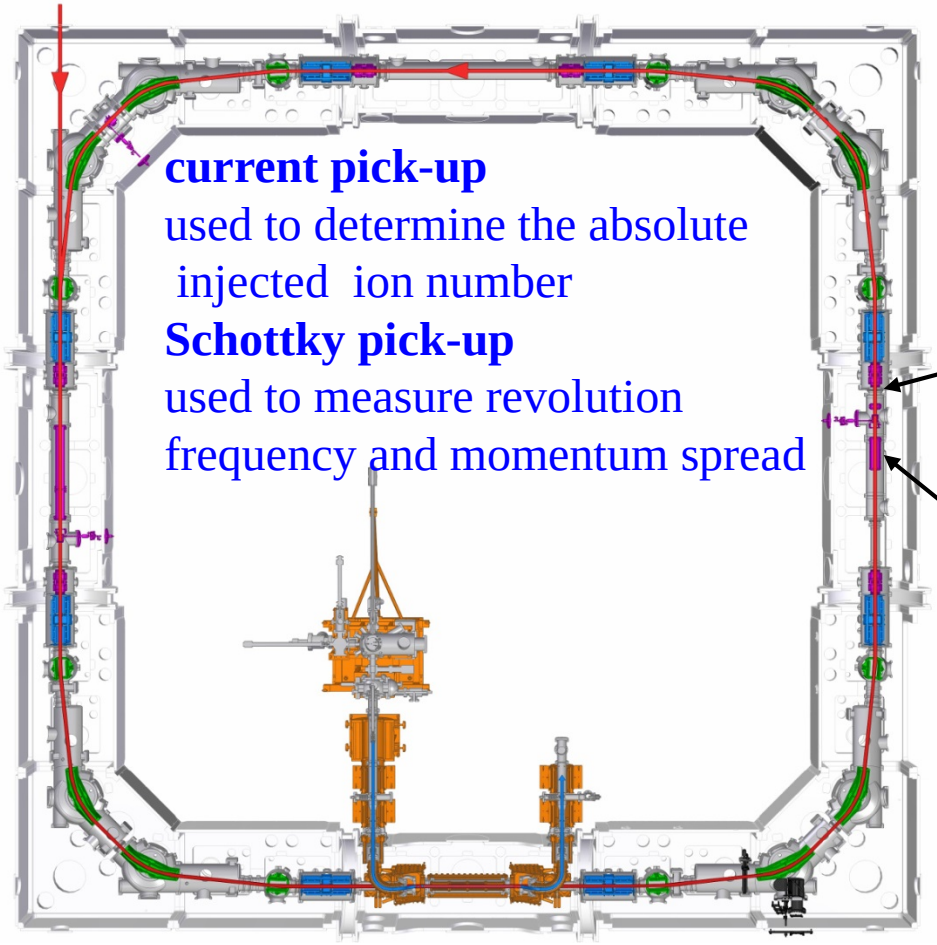

current pick-up
used to determine the absolute injected ion number

Schottky pick-up
used to measure revolution frequency and momentum spread

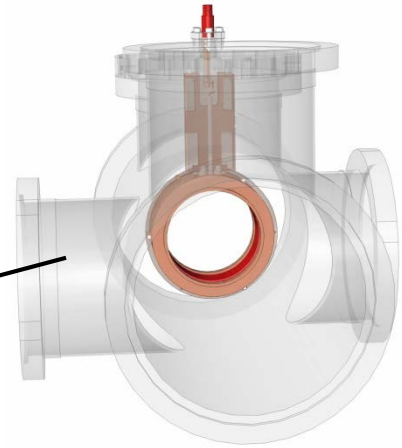

current pick-up

tube:
L= 3.5 cm
ϕ =10 cm

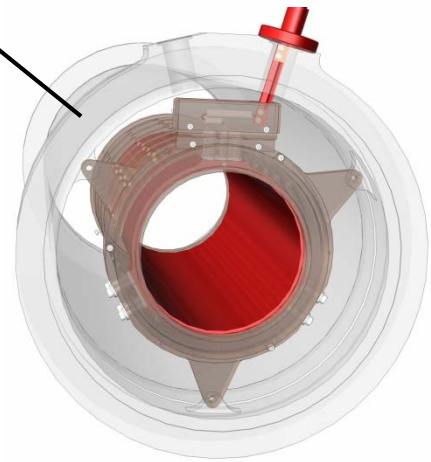

Schottky pick-up

tube:
L= 34 cm
ϕ =10 cm

Current pick-up

-used to measure the **absolute number** of the injected ion number (pulsed beam)

-sensitivity 10^6 singly charged ions

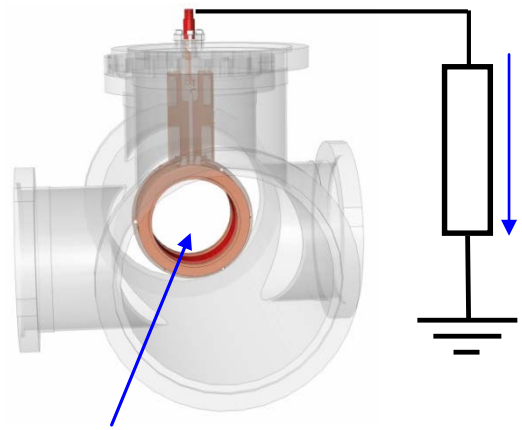

$$U(t) = \frac{X_u}{C}\frac{L}{v}I(t)$$

X_u- signal amplification

L- pick-up length

v-velocity

C- capacity

tube: ψ=10 cm, L=3.5 cm

measured current signal of an $^{40}Ar^+$ ions (E= 60 keV)

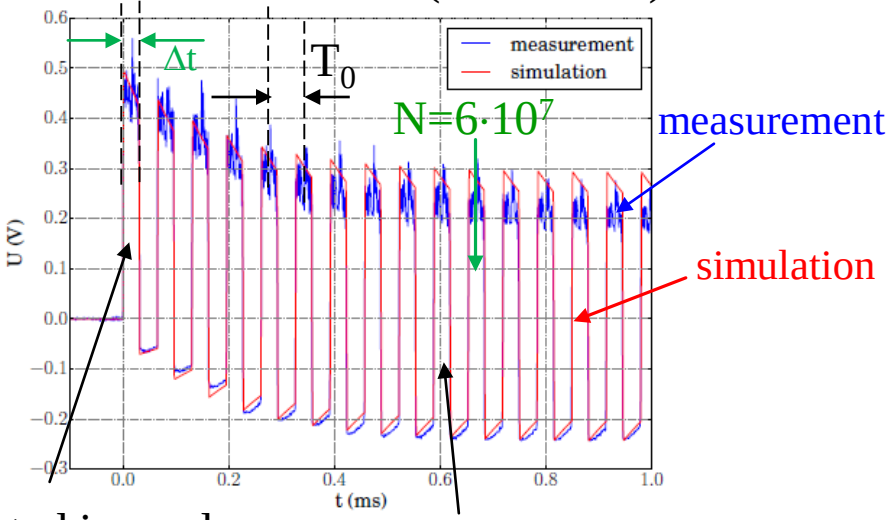

integration over one pulse

$$N = \frac{1}{qe}\int_{t_1}^{t_2} I(t)dt = \frac{1}{qe}\frac{Cv}{L}\int_{t_1}^{t_2}\frac{U(t)}{X_u}dt$$

T_0- revolution time

pulse length Δt is set up with an chopper located in the transfer line to the CSR

Schottky noise spectrum

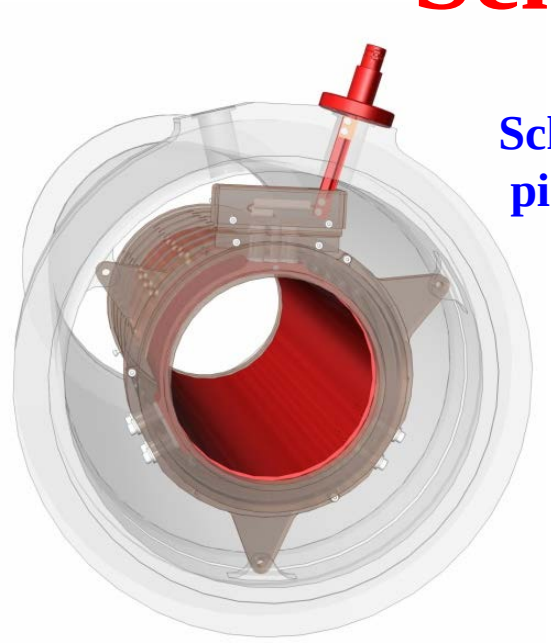

Schottky pick-up

Time development of the Schottky noise spectrum (60 keV CO_2^- ions)

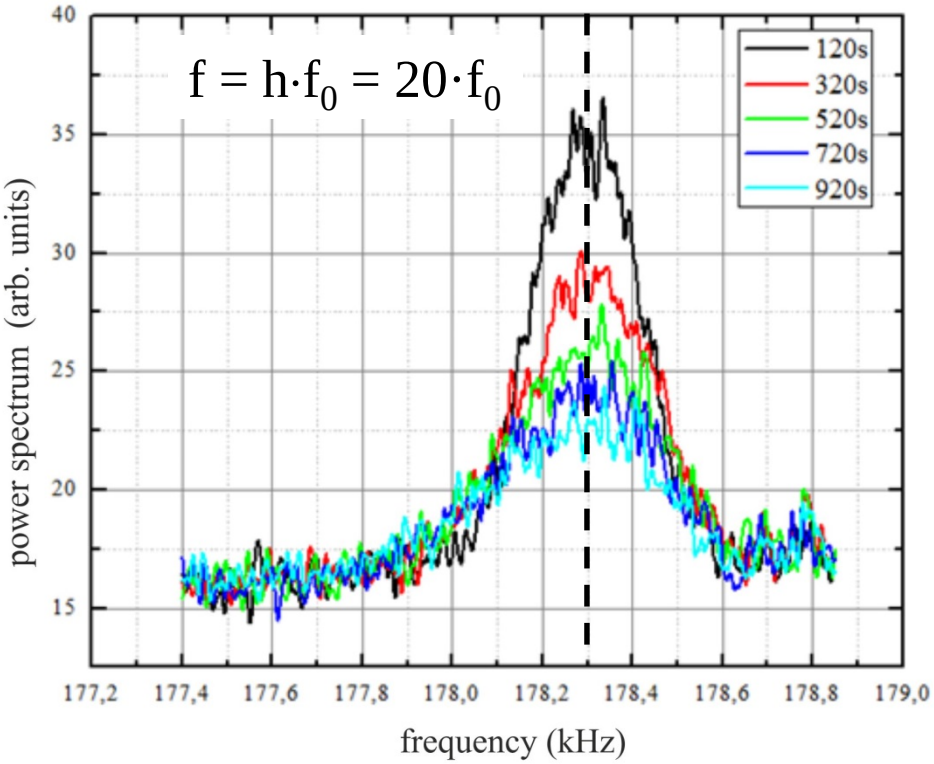

slip factor

$$\eta = \frac{\Delta f / f}{\Delta p / p} = 1 - \frac{1}{\gamma_{th}^2} = 0.7$$

standard mode

(non relativistic approach)

Lifetime Measurements of a stored Co_2^- beam with Schottky noise analysis

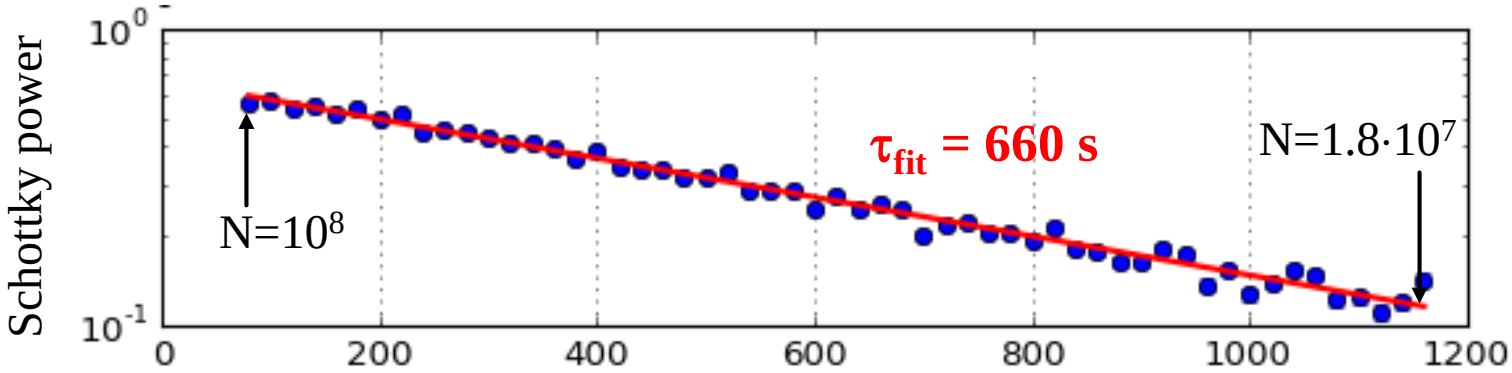

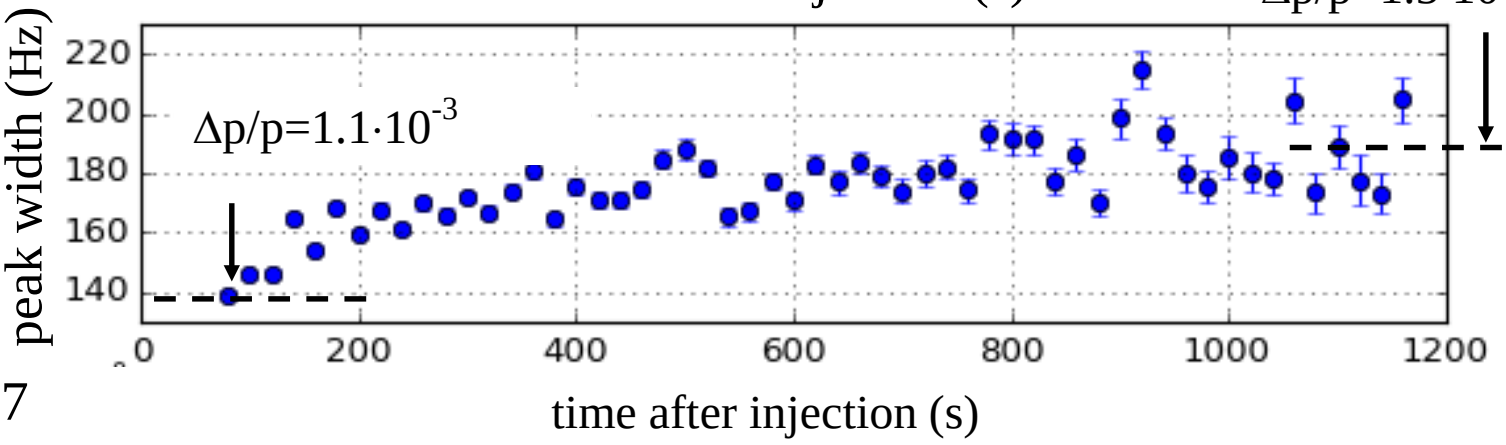

due to noise on the electrodes increasing of $\Delta p/p$

$$\eta = \frac{\Delta f / f}{\Delta p / p} = 1 - \frac{1}{\gamma_{th}^2} = 0.7$$

observation frequency: $f = h \cdot f_0 = 20 \cdot f_0$

Lifetime Measurement of stored Ag_2^- ions (E=60 keV)

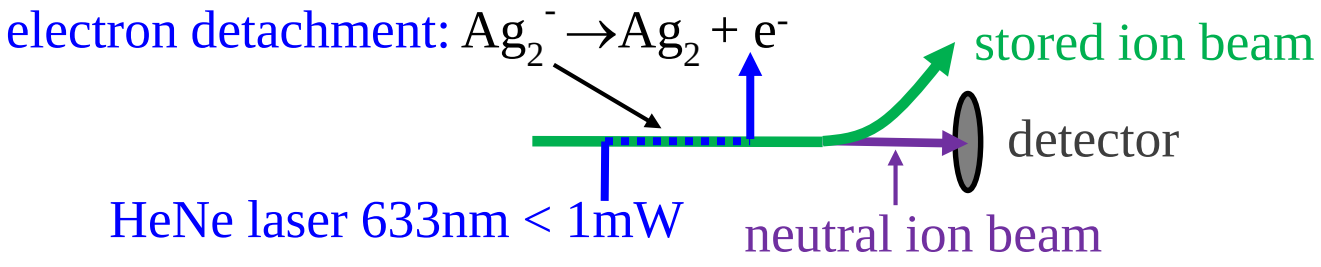

neutral rate on the detector

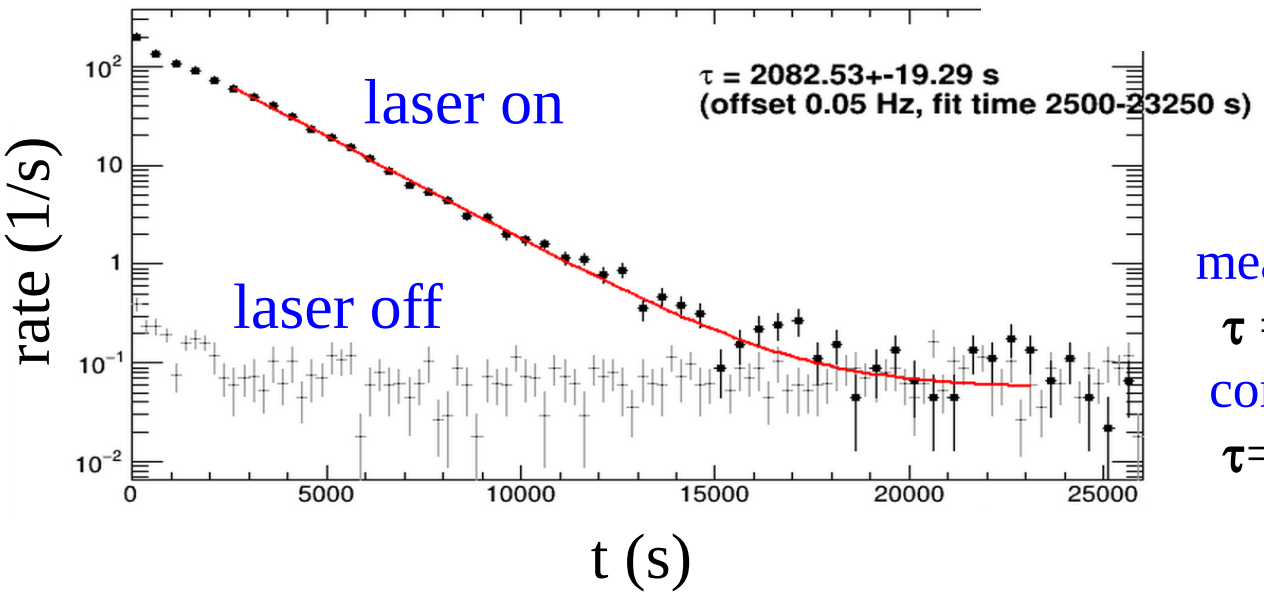

measured life time:

τ =2082 s

corrected for laser depletion:

τ=2500 s

Measurement of the residual gas density

simulation of the neutralization process **with g4beamline**

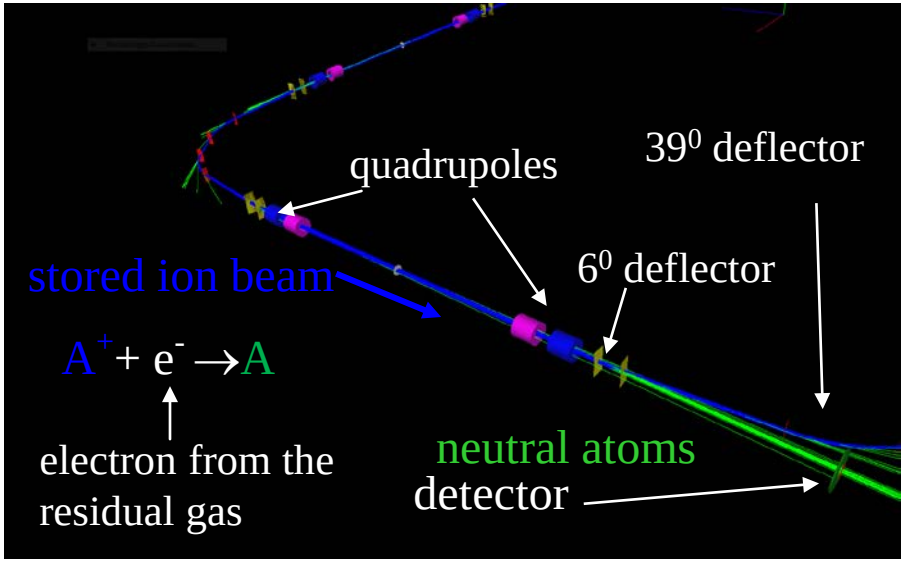

simulation results

fraction of ions η_f hitting the detector

$\varepsilon_{x,90\%}$ (mm mrad)	η_f
0.5	0.126
9.1	0.119
23.0	0.118

average value $\eta_f = 0.121$

$$R(t) = \eta_f \cdot \frac{N(t)}{\tau_c} \qquad \tau_c = \frac{1}{n \cdot v \cdot \sigma}$$

σ- cross section for neutralization

singly charged 50-60 keV ions (for H_2):

Ar^+: $\sigma = 5.3 \cdot 10^{-16}$ cm^2 **O^-:** $\sigma = 3.4 \cdot 10^{-16}$ cm^2

v- velocity

n- residual rest gas density

R(t)- detector rate

N(t)- number of stored particles

measurement:

$^{40}Ar^+$ (E=60 keV) and $N = 2 \cdot 10^8$:

$R < 10$ 1/s $\Rightarrow$ **n< 20 H_2 molecules/cm^3** !!!

$\Rightarrow$ vacuum life time: $\tau_v > 10^6$ s $\approx$ 280 h $\Rightarrow$ lifetime is not residual gas dependent !!!

Beam Position Monitor (BPM)

CSR has 6 horizontal and
6 vertical position pick ups (BPM)

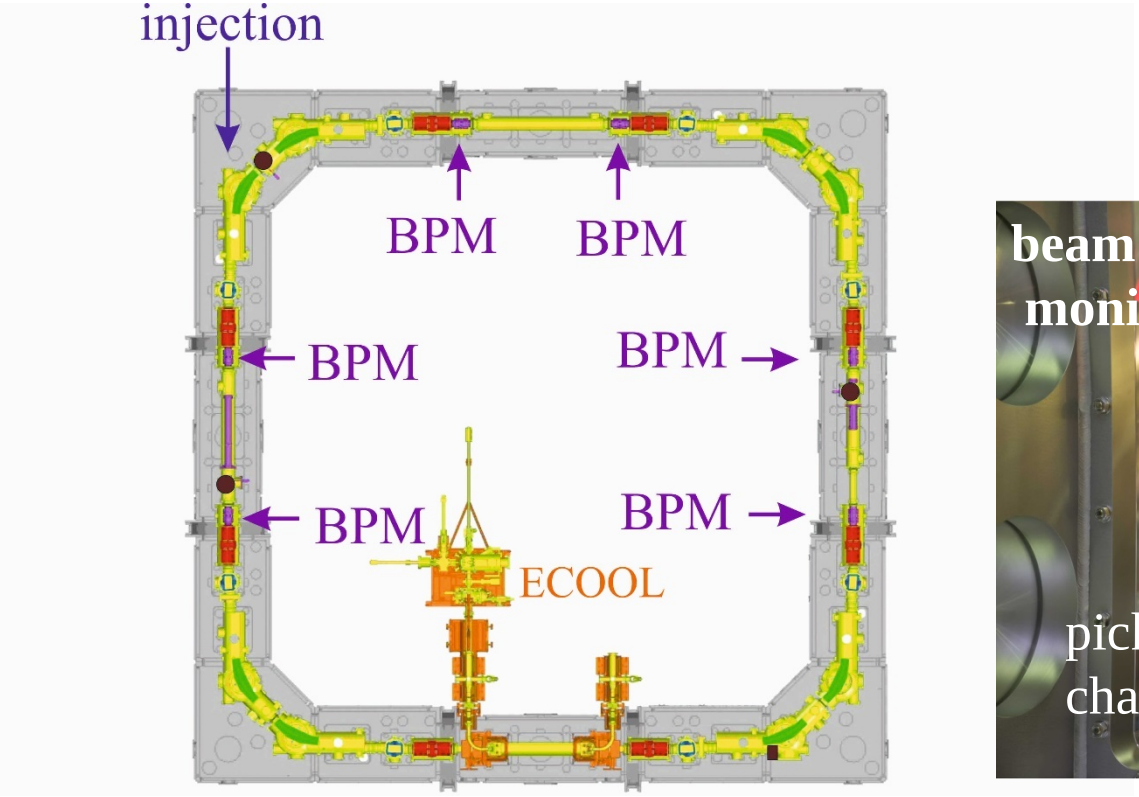

tube divided in
two parts

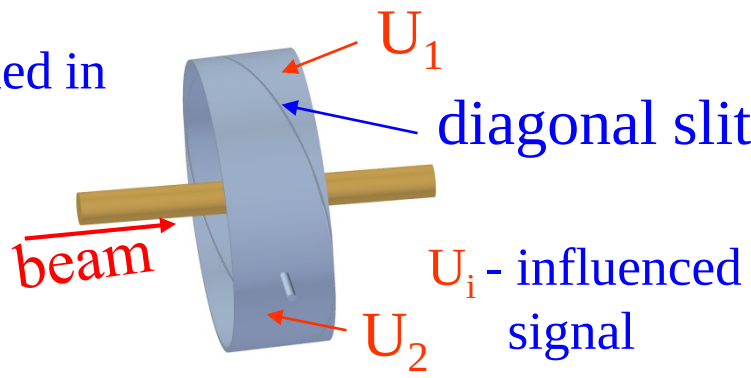

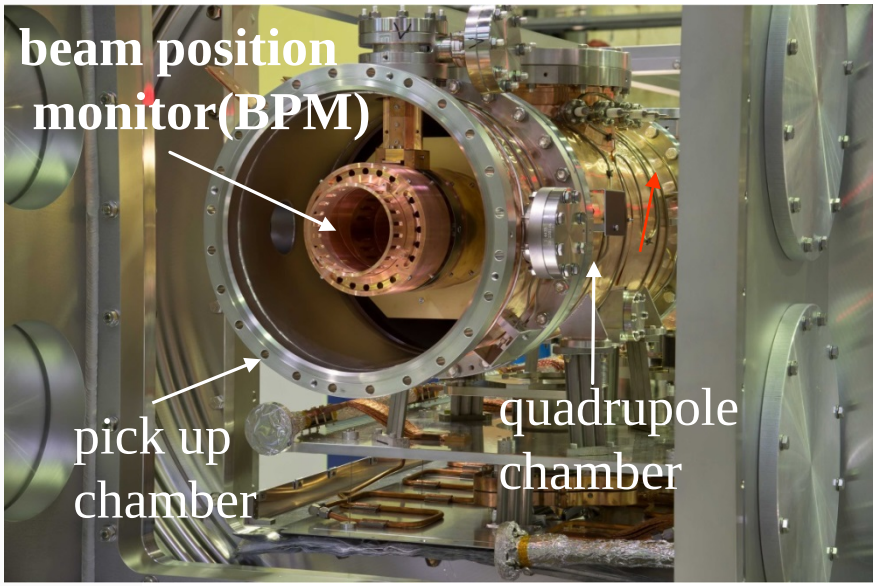

Dispersion in the straight section

pick-up measurements

closed orbit change x via variation of all potentials by $\Delta\phi/\phi$

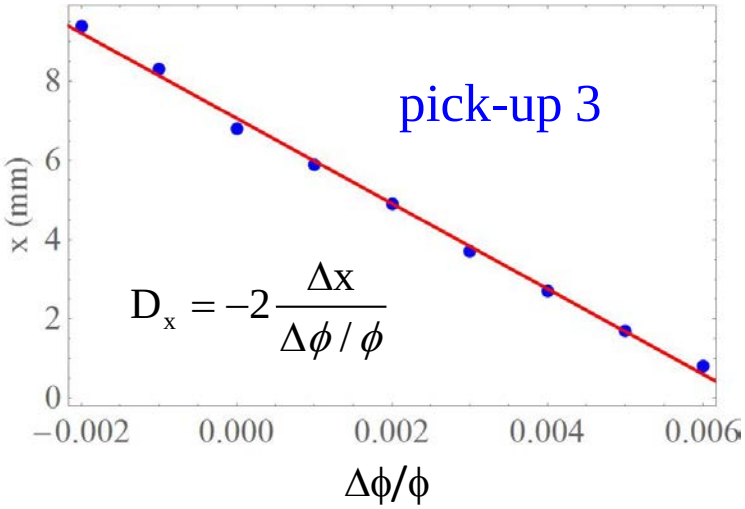

average value

$\overline{D}_x = 2.17$ m

pick-up	D_x (m)
1	2.19
2	2.23
3	2.15
4	2.17
5	2.16
6	2.09

$\overline{D}_x = 2.17$ m

g4beamline simulation

tracking of particles with different momenta and plotting the closed orbit position x as a function of $\Delta p/p$

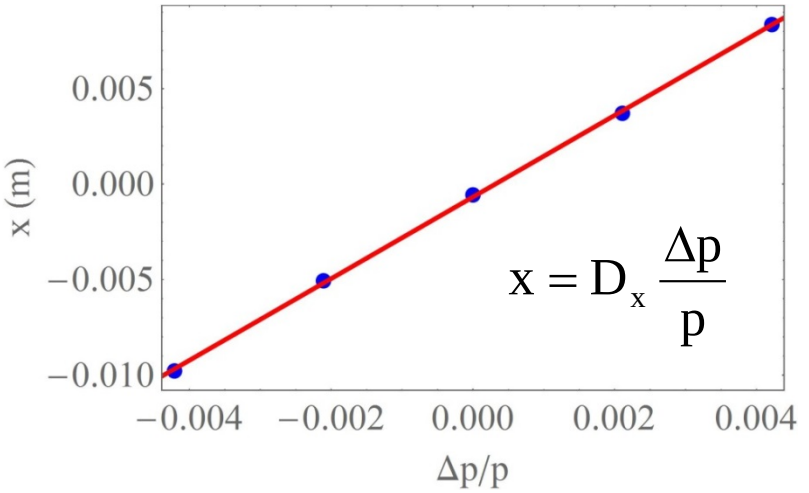

D_x=2.14 m

Application of pick-up measurements

determination of the horizontal and vertical tune

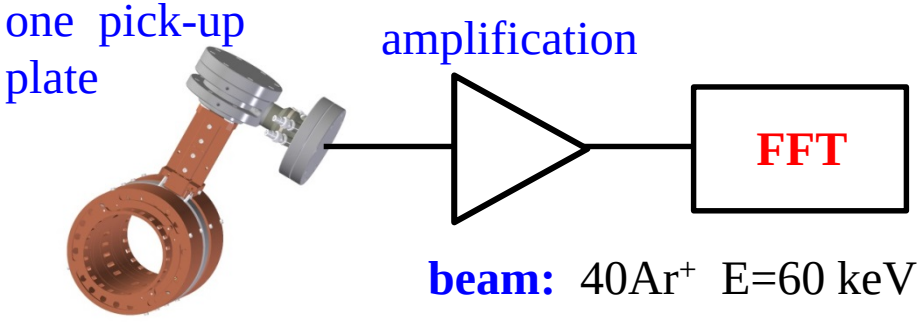

excitation of the betatron oscillation by off axis injection of the beam

spectrum of a pick-up signal induced on a horizontal plate

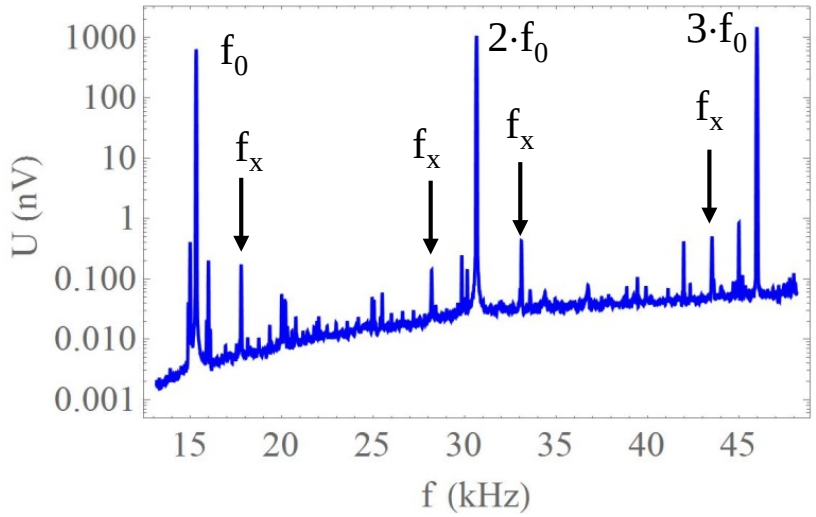

f_0- revolution frequency

f_x - betatron side band

$$f_x = f_0(n \pm q_x)$$

n- integer number

q_x- non integer part of the tune

effective quadrupole length

The effective quadrupole length are determine by matching the measured tunes with the calculated tunes.

result:

calculated with **TOSCA**: l_{eff}=0.211 m

measurement:

quadrupole family 1: l_{eff}=0.208 m

quadrupole family 2: l_{eff}=0.209 m

Determination of horizontal ß$_x$ and vertical ß$_y$ functions

$$\Delta Q_x = \frac{1}{4\pi}\int \beta_x(s)\Delta k(s)\,ds$$

$$\bar{\beta}_x = \frac{\pi}{2}\frac{U}{k}\frac{\Delta Q_x}{\Delta U}\frac{1}{L_m}$$

horizontal tune as a function of voltage of quadrupole family 2

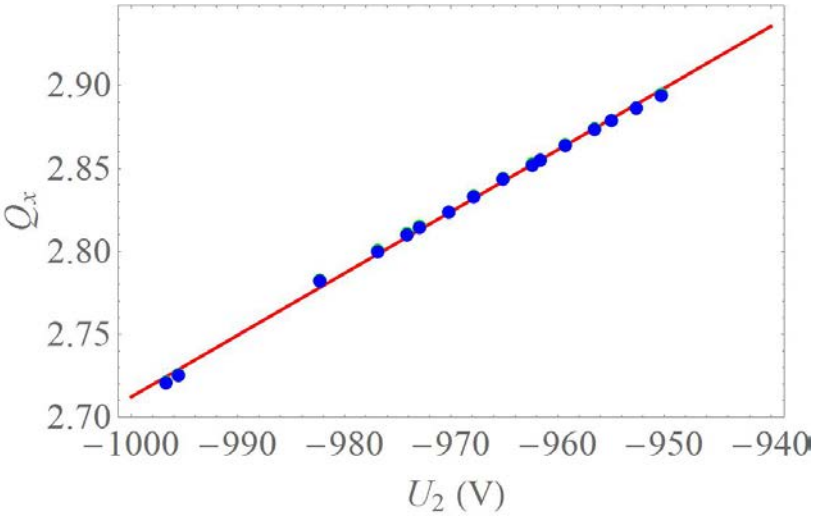

Q_x- horizontal tune

U_2 -voltage of quadrupole family 2

MAD calculation of horizontal and vertical β function (standard mode)

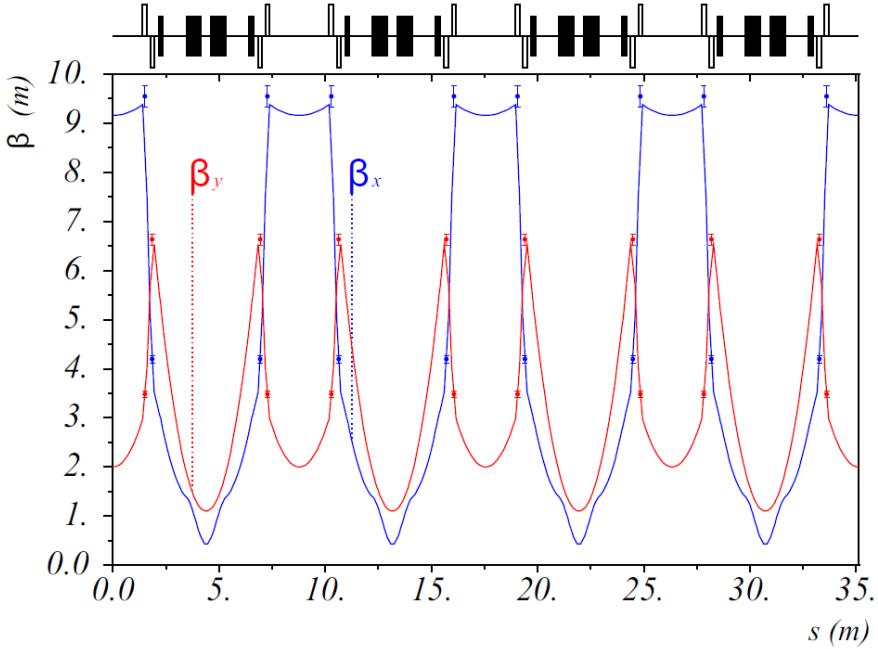

- measured vertical ß$_x$ function
- measured vertical ß$_y$ function

Comparison of measured and calculated ß function for working point II

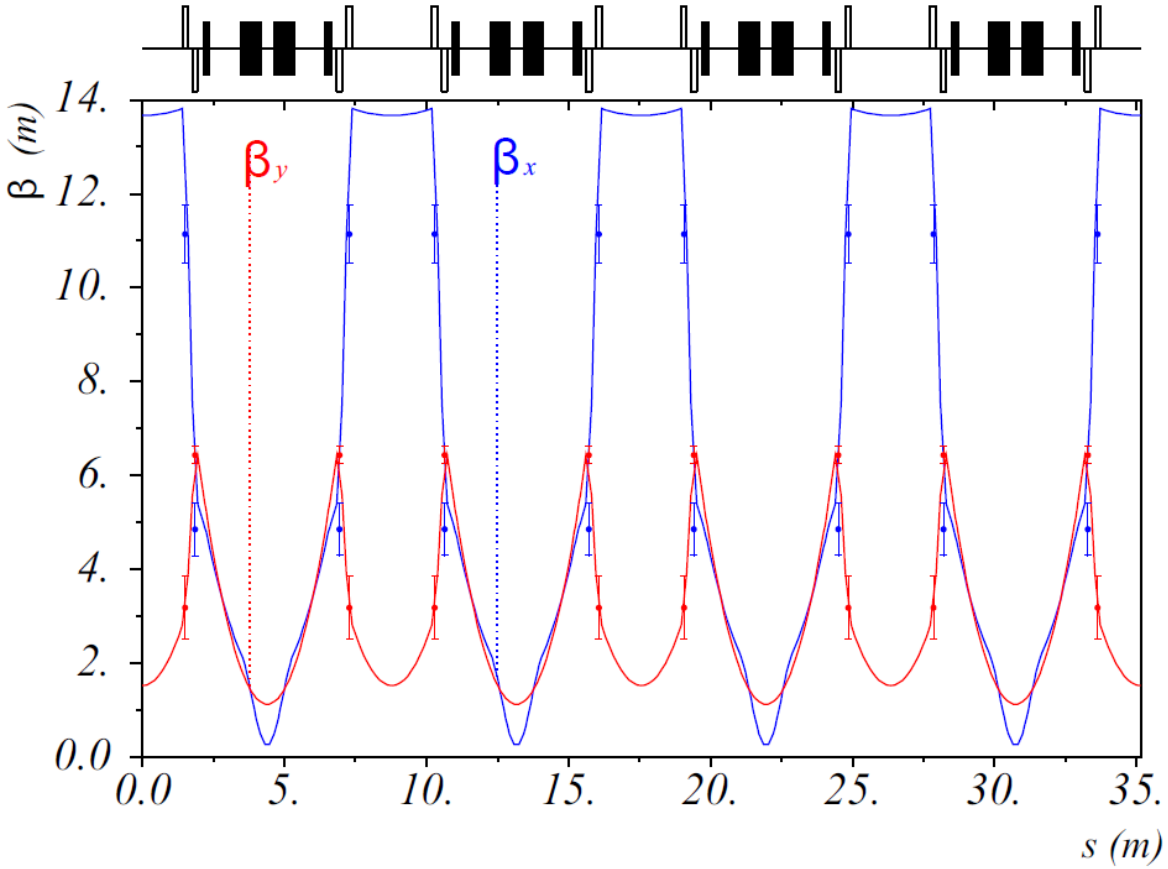

- measured vertical $ß_x$ function
- measured vertical $ß_y$ function

The slip factor η and momentum compaction α_p

slip factor η in the non relativistic approach (γ→1)

different to magnetic storage ring

$$\eta = \frac{\Delta f/f}{\Delta p/p} = 1 - 2\,\alpha_p = 1 - \frac{1}{\gamma_{th}^2}$$

γ_{tr}- gamma transition parameter

α_p-momentum compaction $\alpha_p = \frac{\Delta C/C}{\Delta p/p}$

f- revolution frequency

p- momentum

C- circumference

γ_{tr} as a function as a horizontal tune Q_x

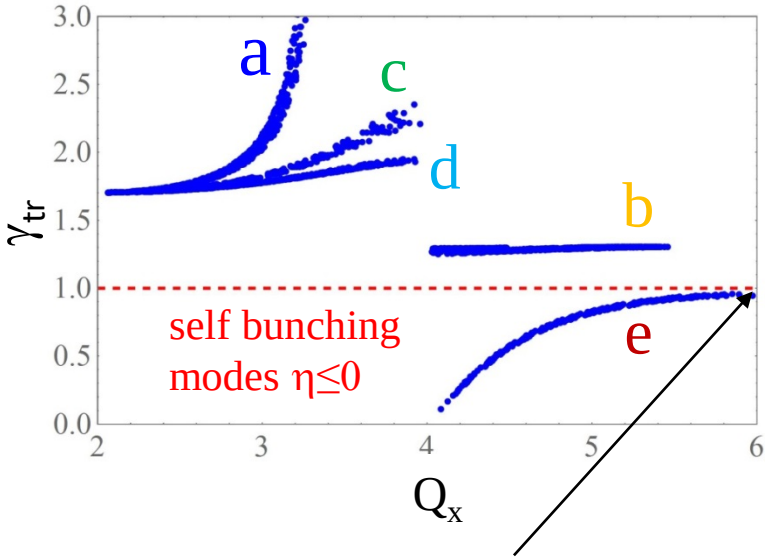

isochronous mode with η=0

unfortunately: $Q_x \approx 6$

strong resonance !

Stability diagram of CSR

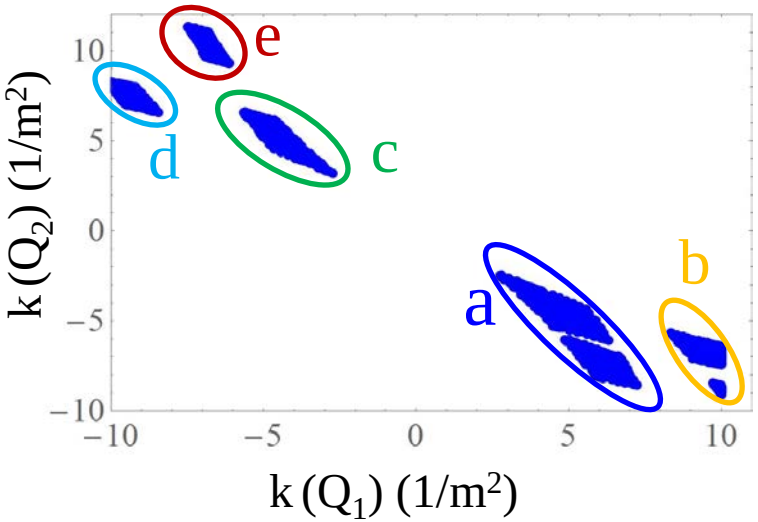

$k(Q_1)$ and $k(Q_2)$ are the quadrupole strength of quadrupole family 1 and quadrupole family 2

Measurement of the slip factor η at the CSR

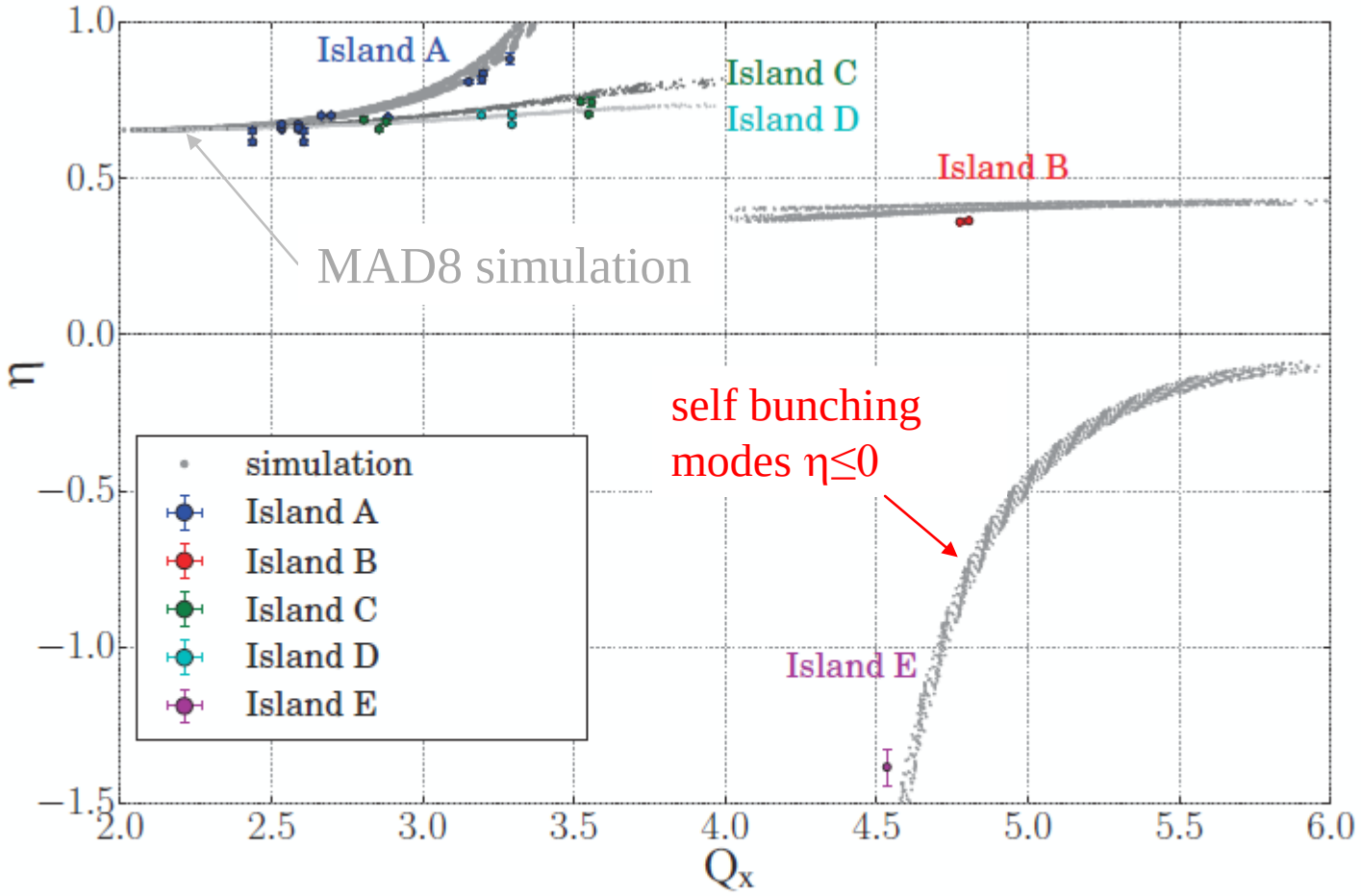

Figure 3. The measured (markers with error bars) and simulated (gray markers) phase slip factors for the cryogenic storage ring CSR as a function of the measured and simulated horizontal tune Q_x, respectively.

published in 8th International Particle Accelerator Conference
IOP Conf. Series: Journal of Physics: Conf. Series **874** (2017) 012049

Self Bunching at η<0 observed at the TSR

pick-up voltage

with beam, without rf U0=0, ECOOL on

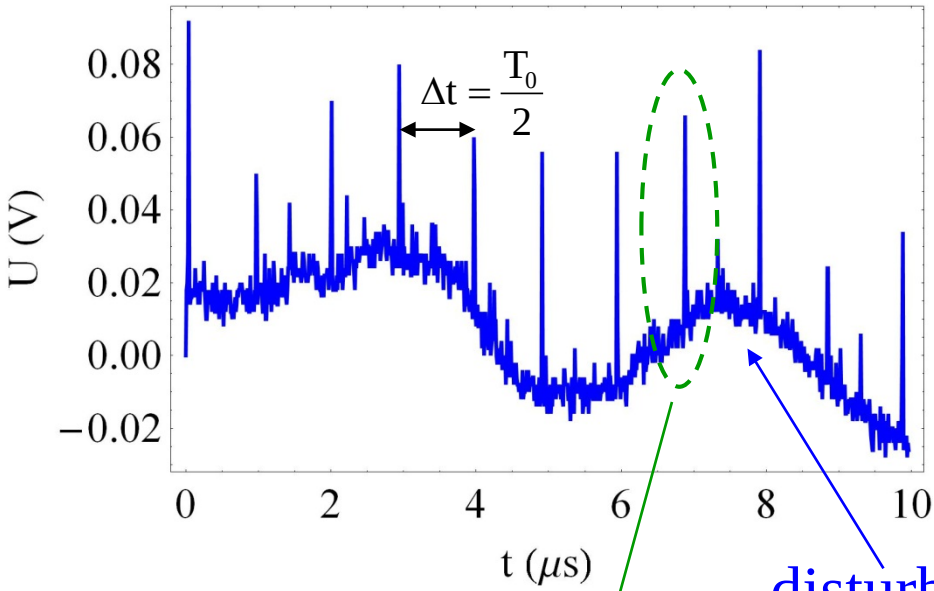

pick-up voltage

without beam, without rf, ECOOL on

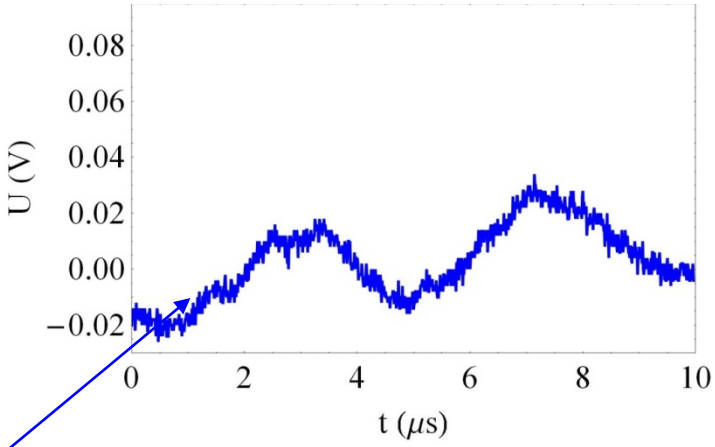

disturbance

synchrotron side band caused by self bunching

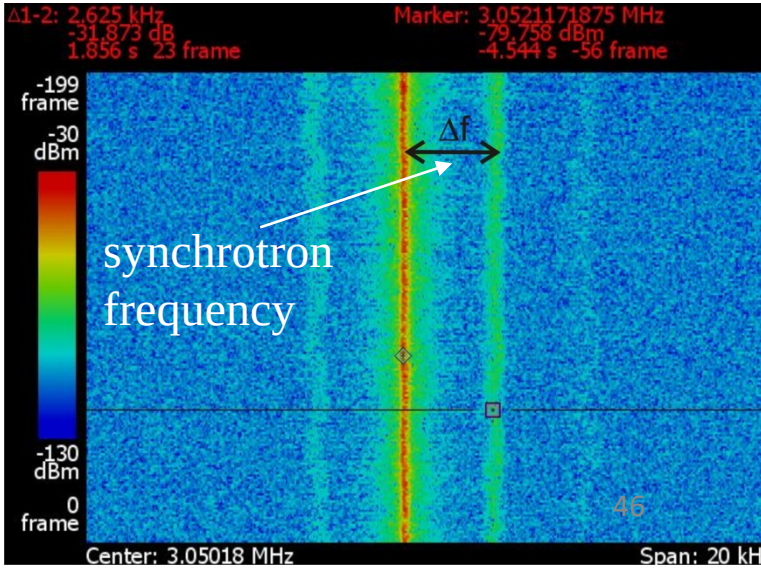

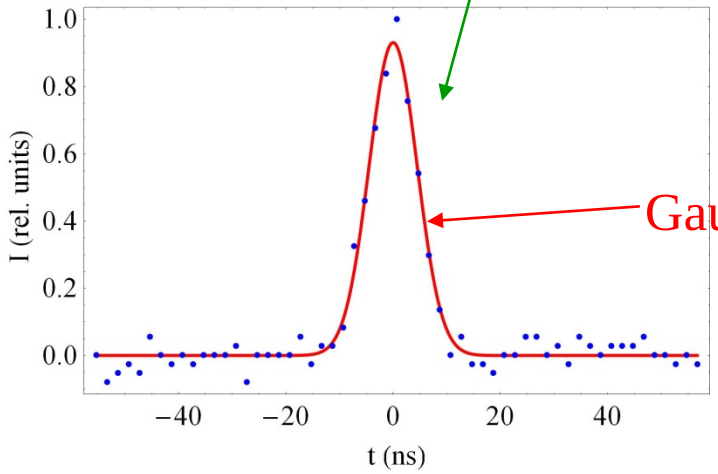

Gaussian Fit

I ≈ 2μA

σ = 4.5 ns

beam: $^{12}C^{6+}$

E=50 MeV

Pick-up signal meaured at f=1 MHz (h=2) as a function of time

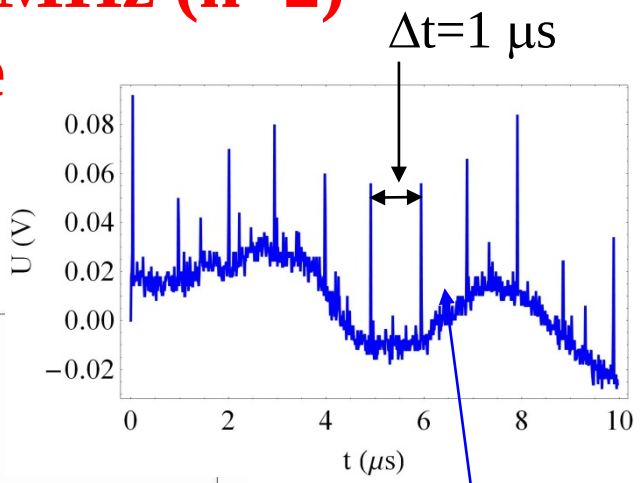

pick-up voltage

observation frequency f = 1.0 MHz

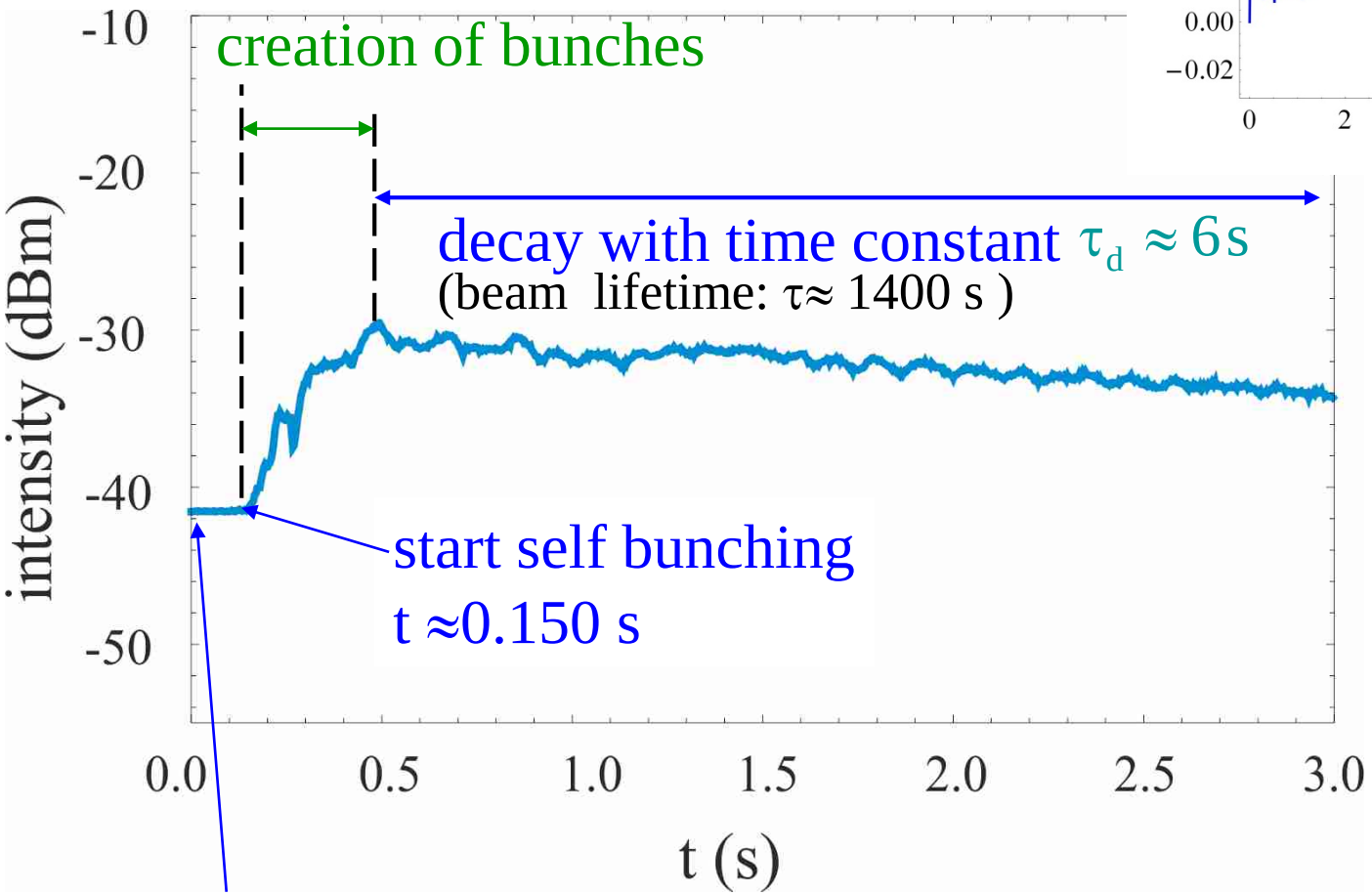

spectrum analyzer in zero span mode

injection at t=0 s and start electron cooling

CSR working point

working point for electron cooling to enable a large incoherent tune shift

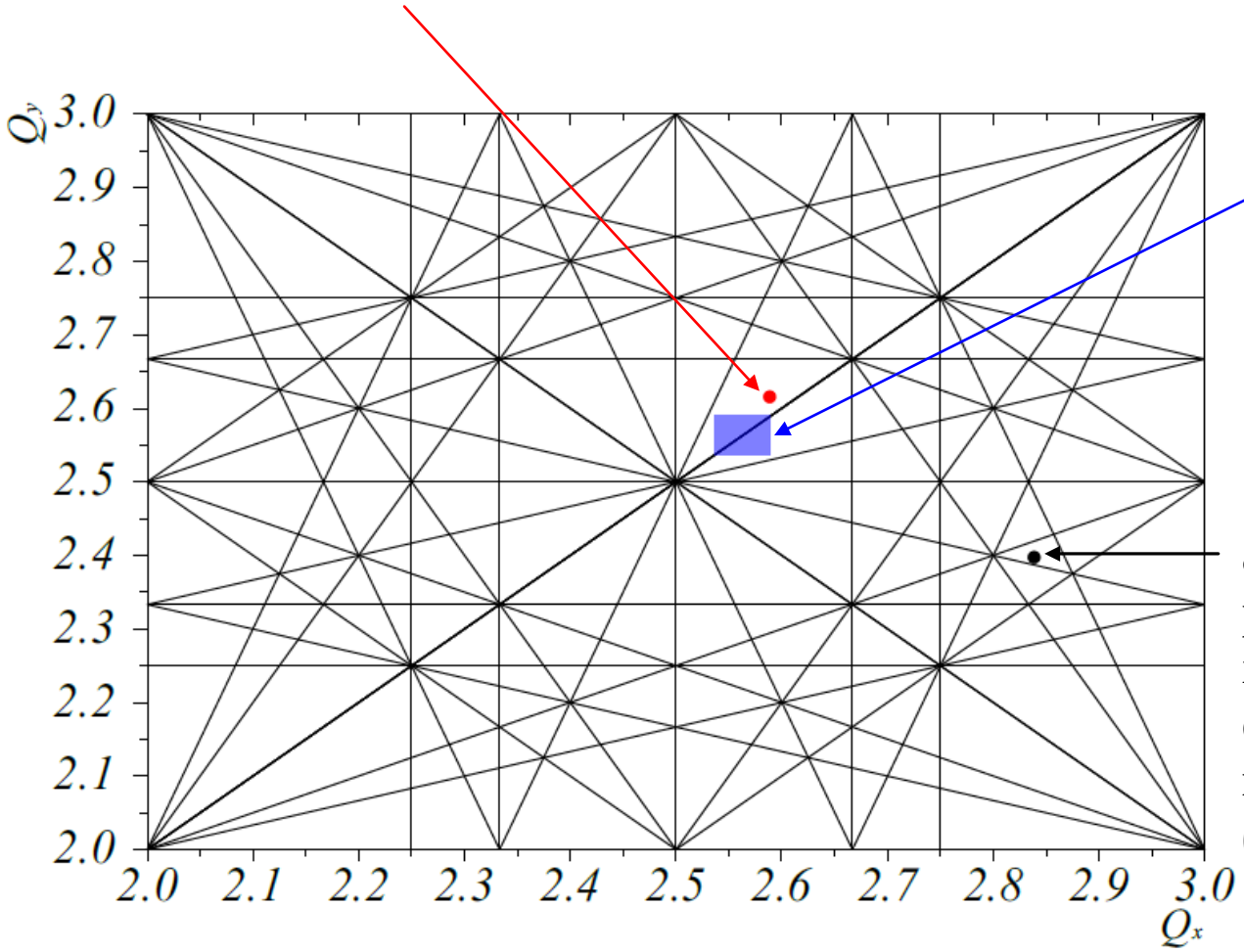

region where coupling effects where studied experimentally

another working point which was investigated for comparison reason (working point II)

Operation of the CSR close to the coupling resonance

(ECOOL magnets off)

$Q_x=q_x+2$
$Q_y=q_y+2$

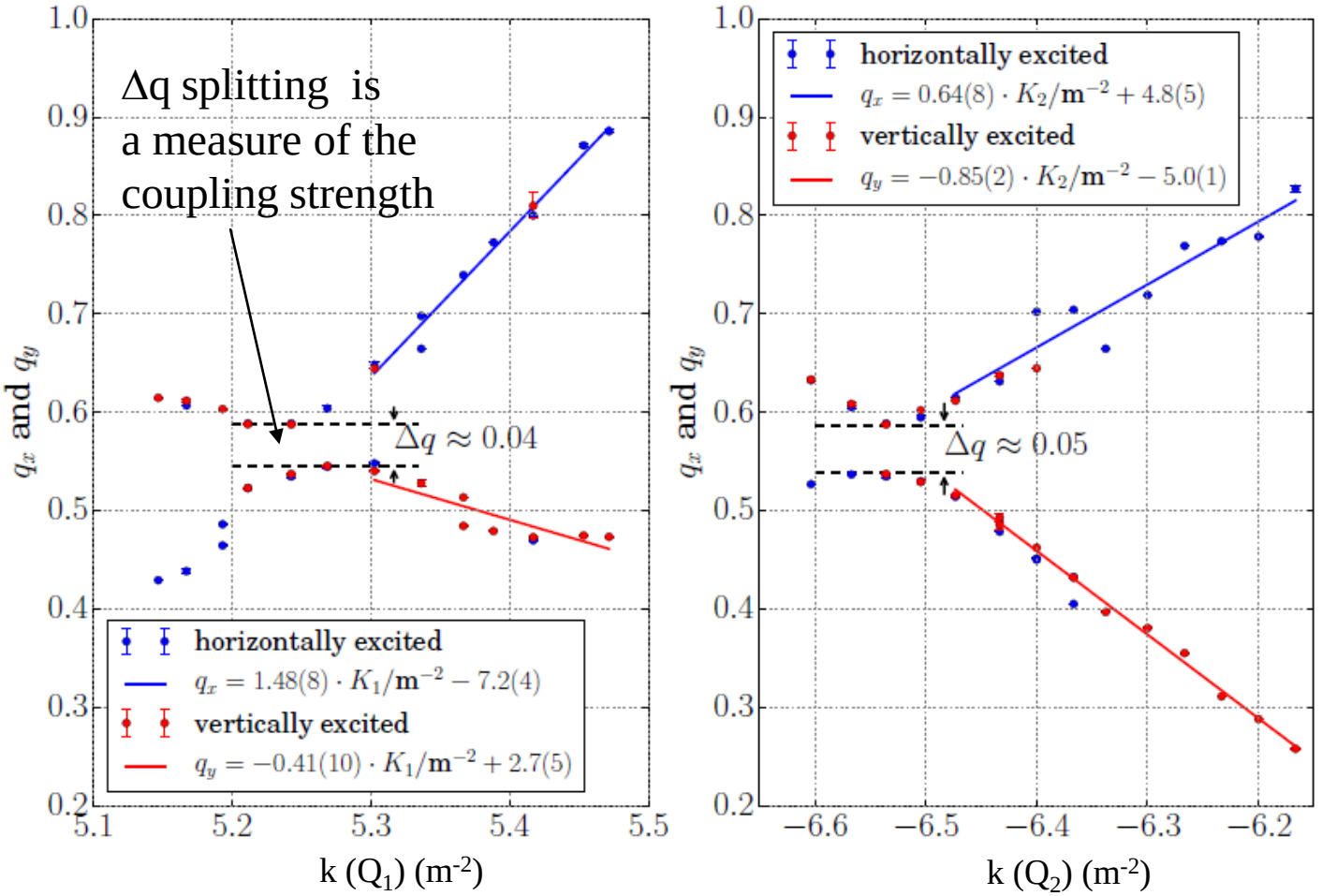

Measured fractional tune values q_x and q_y as a function of the quadrupole strengths of family 1 and 2 close to the coupling resonance. In the left plot $k(Q_2)=-6.54\ m^{-2}$ and in the right plot $k(Q_1)=5.24\ m^{-2}$.

Explanation of the coupling effect

determination of the tune
with ion tracking and FFT of x

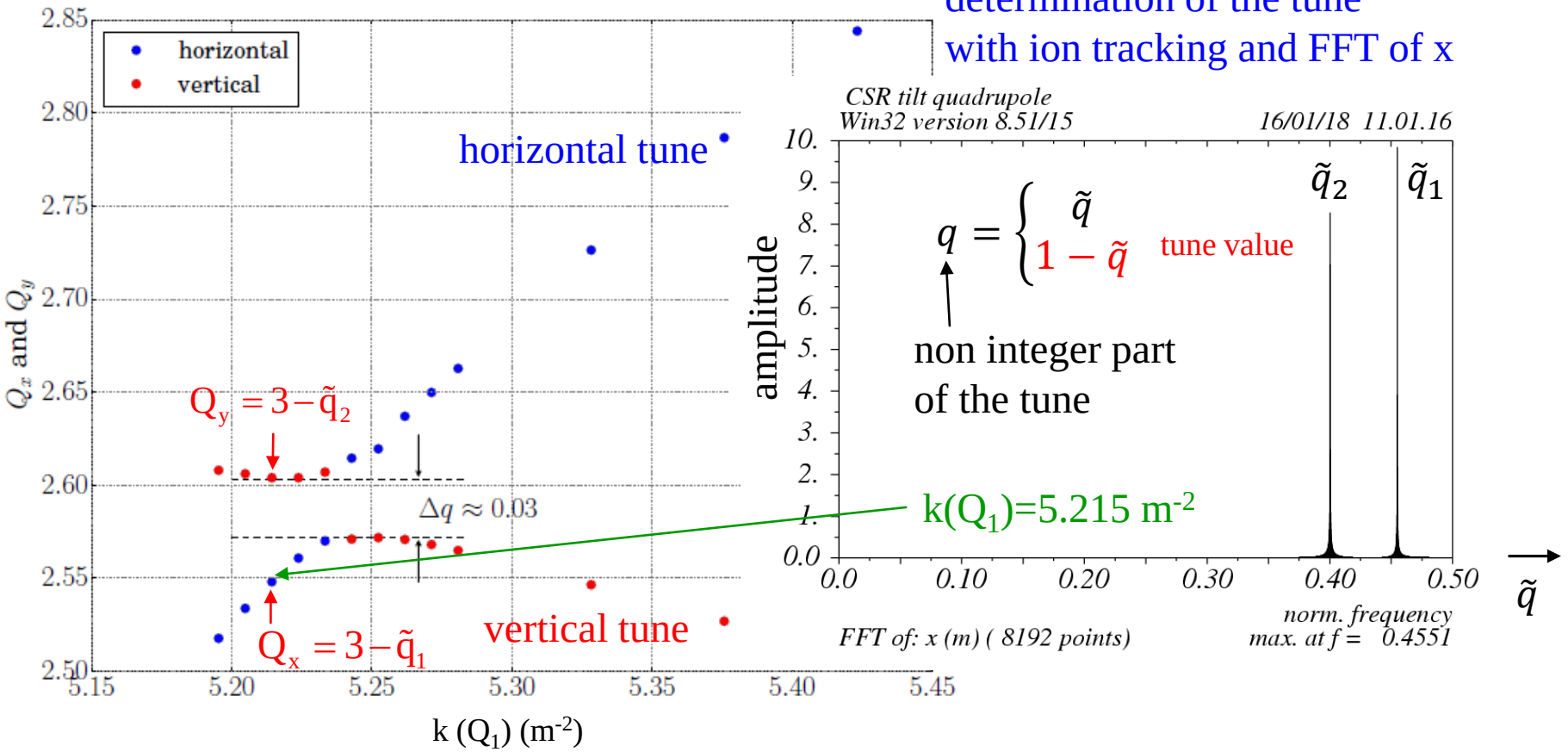

MAD8 simulation of the tune values Q_x and Q_y as a function of the quadrupole strength of family 1. In the simulation one of the quadrupole is rotated by 1^0 around the longitudinal axis.

rotation angle not specified in the CSR design

CSR electron cooler – principle

principle of electron cooling:

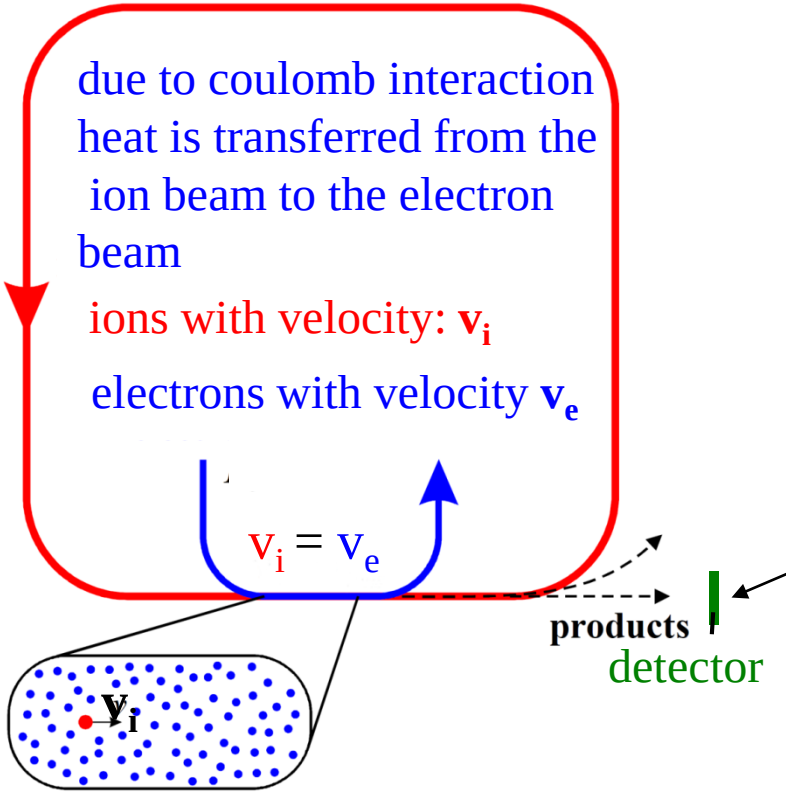

E_e (eV)	ion
163	for 300 keV p^+
~10	for most ions
1	for M_{ion} = 160 u

electron cooling experiment at the TSR

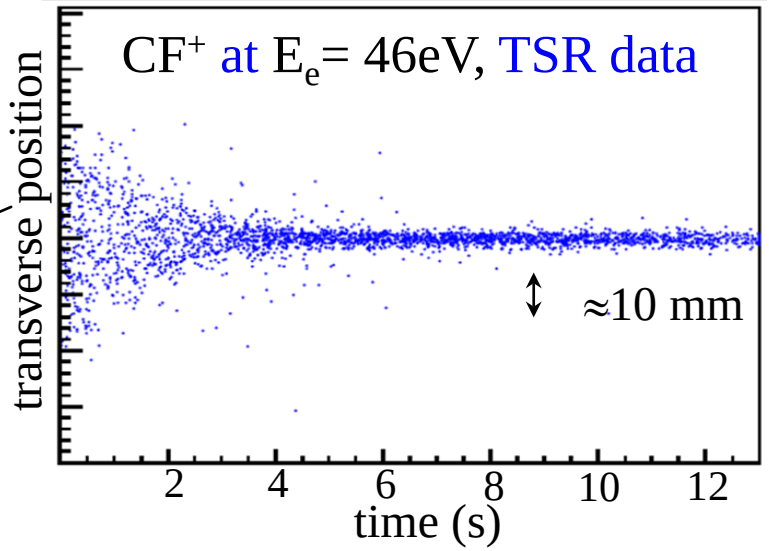

CSR electron cooler – photo-cathode

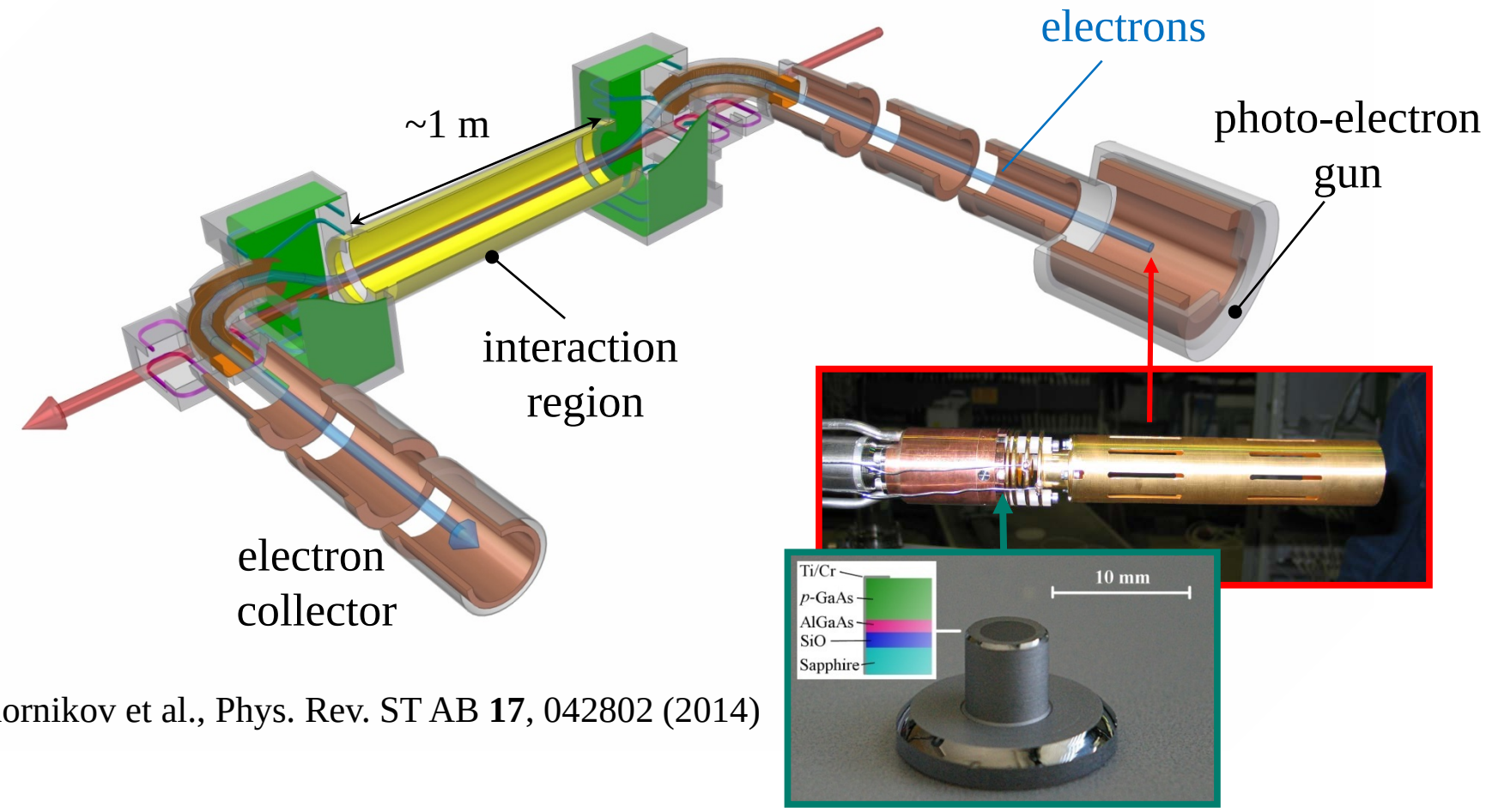

Shornikov et al., Phys. Rev. ST AB **17**, 042802 (2014)

CSR electron cooler – magnetic guiding field

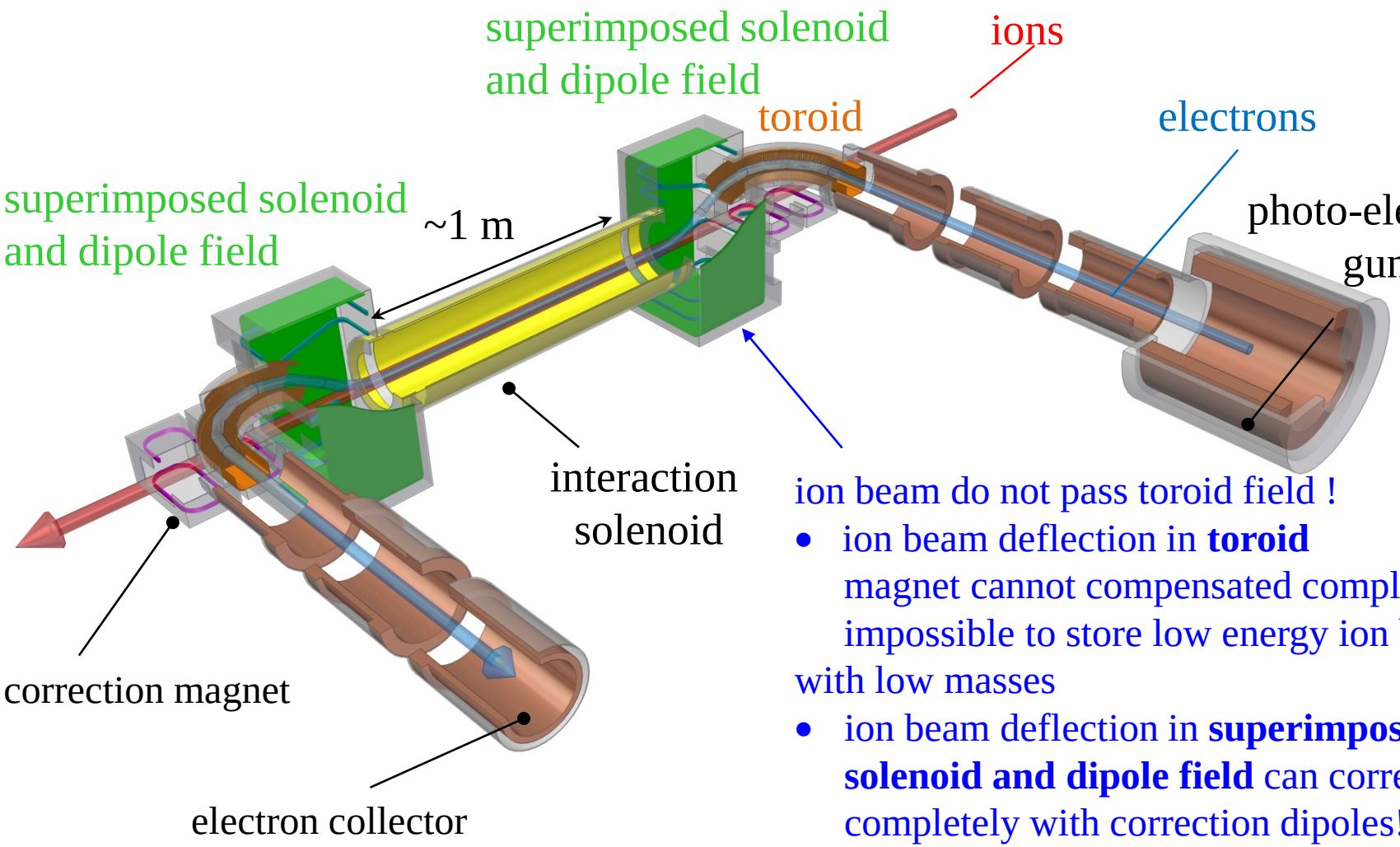

ion beam do not pass toroid field !

- ion beam deflection in **toroid** magnet cannot compensated completely impossible to store low energy ion beams with low masses
- ion beam deflection in **superimposed solenoid and dipole field** can corrected completely with correction dipoles!
- very low interaction with the stored ion beam

Ion deflection in one toroid magnet

usual electron cooler: ion beam has to pass an toroid beam

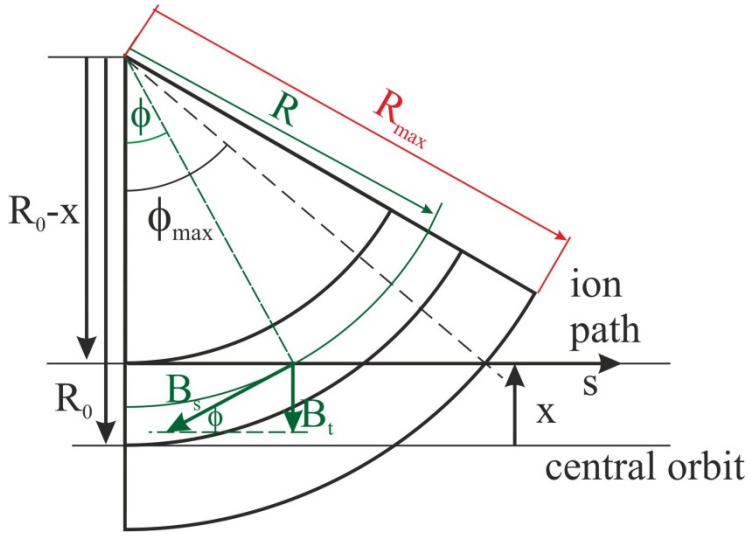

due to interaction with the transverse magnetic field B_t component the ion beam is deflected in the vertical direction:

$$\delta(x) = -\frac{B_0 R_0}{B\rho} \ln\left(\cos\left(\frac{R_0 - x}{R_{max}}\right)\right)$$

horizontal deviation

$$= \delta_0 - \frac{B_0}{B\rho}\frac{R_0}{R_{max}} \tan\left(\frac{R_0}{R_{max}}\right) x + \ldots.$$

can be compensated by correction magnets

can not compensated by correction magnets

$B\rho$-beam rigidity

new cooler design

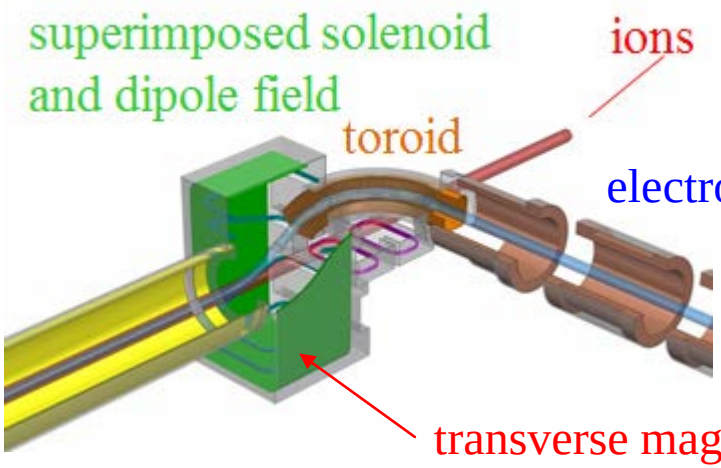

ions with low beam rigidity are kicked out the storage ring !

to avoid the ion loss the ions should not interact with a toroid field

$\Rightarrow$ new electron cooler design

transverse magnetic field B_t do not depend on the horizontal position

The CSR electron cooler

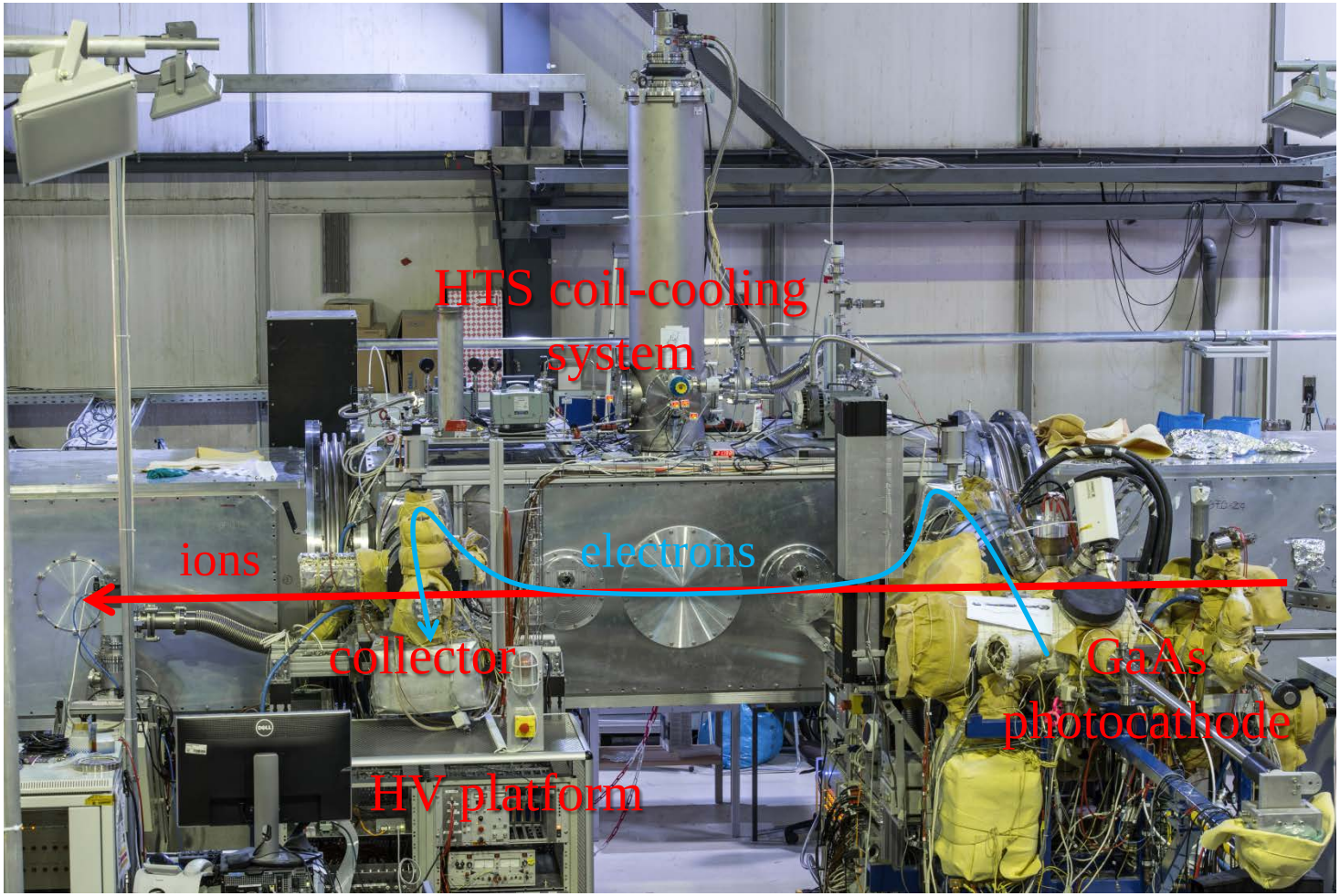

Magnets of the CSR electron cooler

toroid magnet
steering copper coil pairs located inside aluminum body for toroidal drift compensation

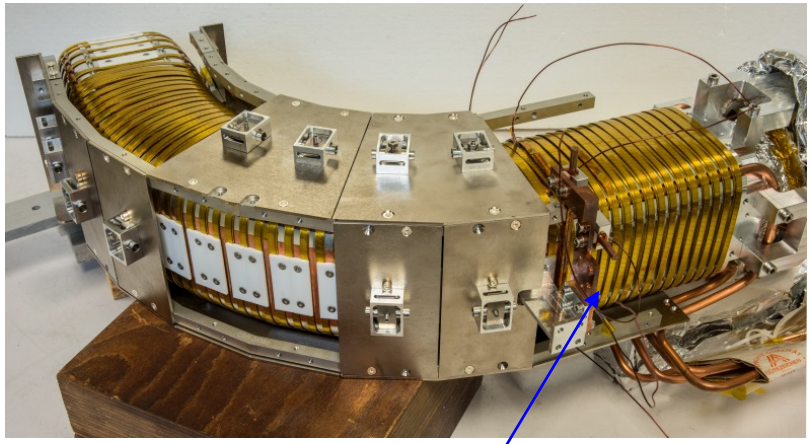

high temperature superconductor

iron shield

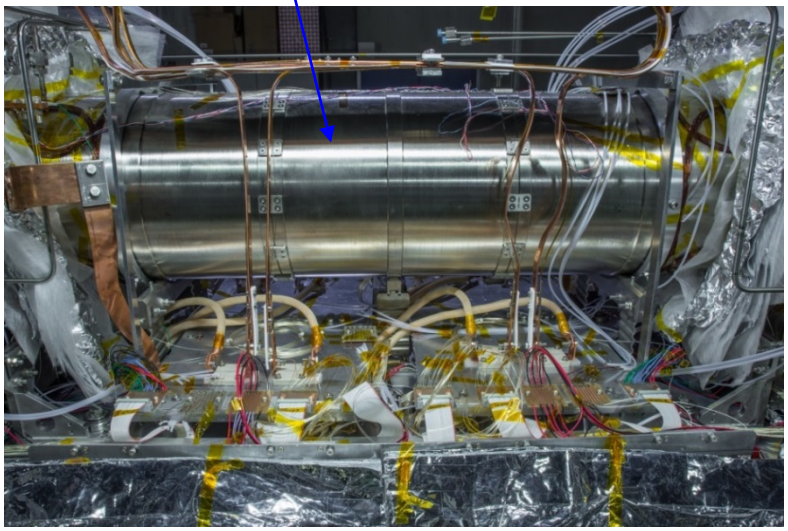

cooling solenoid
High-temperature superconductor attached onto cooled copper strips distributes ≈60 A currents to the magnets

Longitudinal electron cooling of a bunched ion beam

rf system system of the CSR

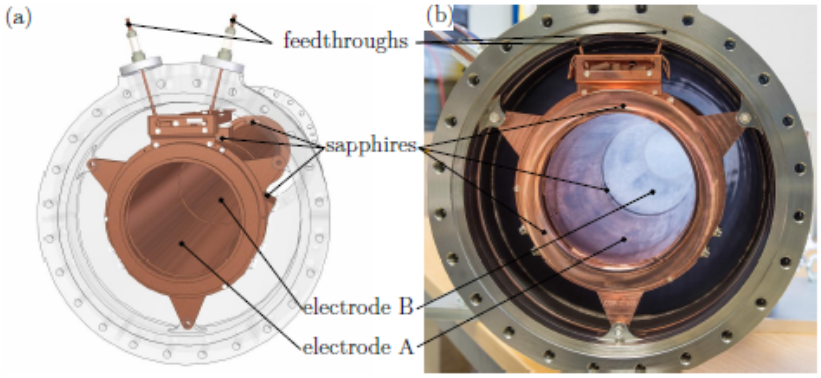

Figure 3.28: The rf system as a (a) CAD-model and (b) photograph mounted in its CSR vacuum chamber. The length of the electrodes A and B are 340 mm and 736 mm, respectively, and the aperture diameter is 100 mm.

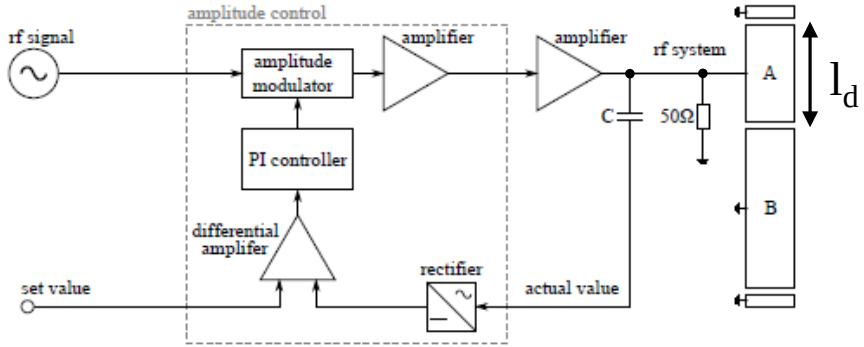

Figure 3.29: Schematic layout of the amplitude regulation system of the rf system.

effective voltage: $U_{eff} = 2U_d \sin\left(\frac{\pi h l_d}{C_0}\right)$

pick-up signal as a function of time

beam: $^{19}F^{6+}$

ion energy: E = 1.34 MeV

electron energy: E_e = 38.7 eV

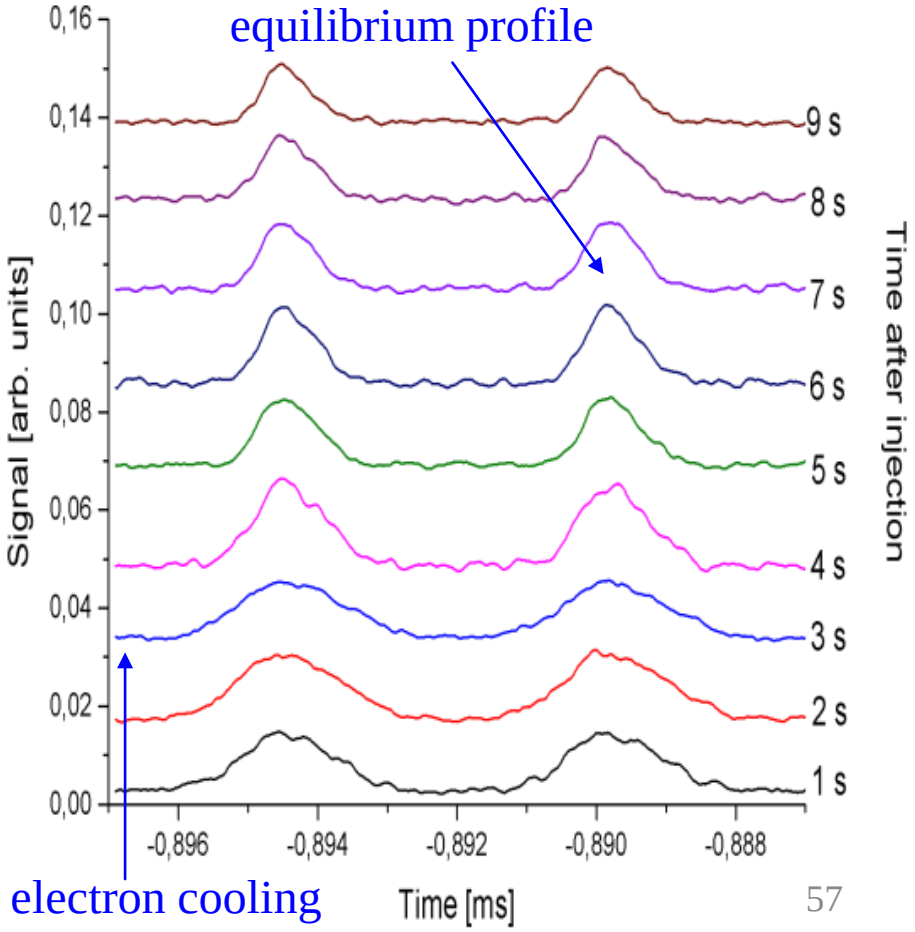

First electron cooling results of a bunched ion beam

beam width at space charge limit:

$$w = C_0 \frac{\sqrt[3]{3(1+2\ln(\frac{R}{r}))\,I}}{\sqrt[3]{2^4\,\pi^2\,c^4\,\varepsilon_0\,\gamma^2\,h^2\,\beta^4\,U}}$$

beam: $^{19}F^{6+}$
ion energy: E = 1.34 MeV
electron energy: E_e = 38.7 eV
ion current: I ≈ 300 nA
ion number: N ≈ 10^6 particles
Solenoid field: 100 Gauss
rf bunching frequency = 2nd (h=2) harmonic of revolution frequency = 214 kHz
drifttube voltage: U_d= 3.25 V
effective bunch voltage: U_{eff}=0.4 V

$$U = U_{eff} = 2U_d \sin\left(\frac{\pi h l_d}{C_0}\right)$$

Equilibrium longitudinal beam profile

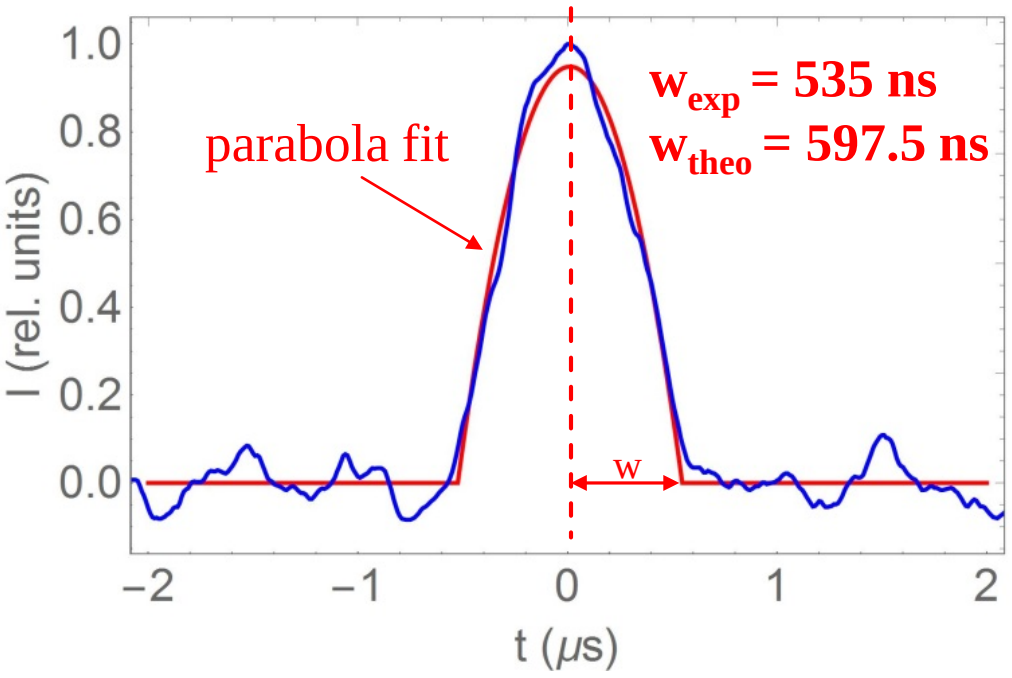

10 sec after injection,
7 sec after cooling

Principle of the longitudinal cooling time measurements

capacitive current pick up

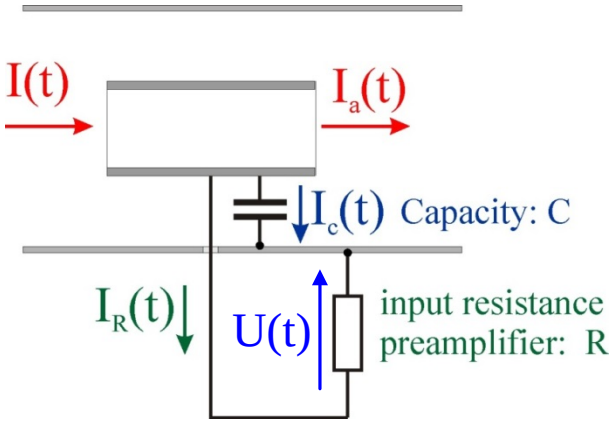

T – RF period
U(t)-pick-up voltage
A_n- spectrum
A_2-second harmonic of the pick-up spectrum

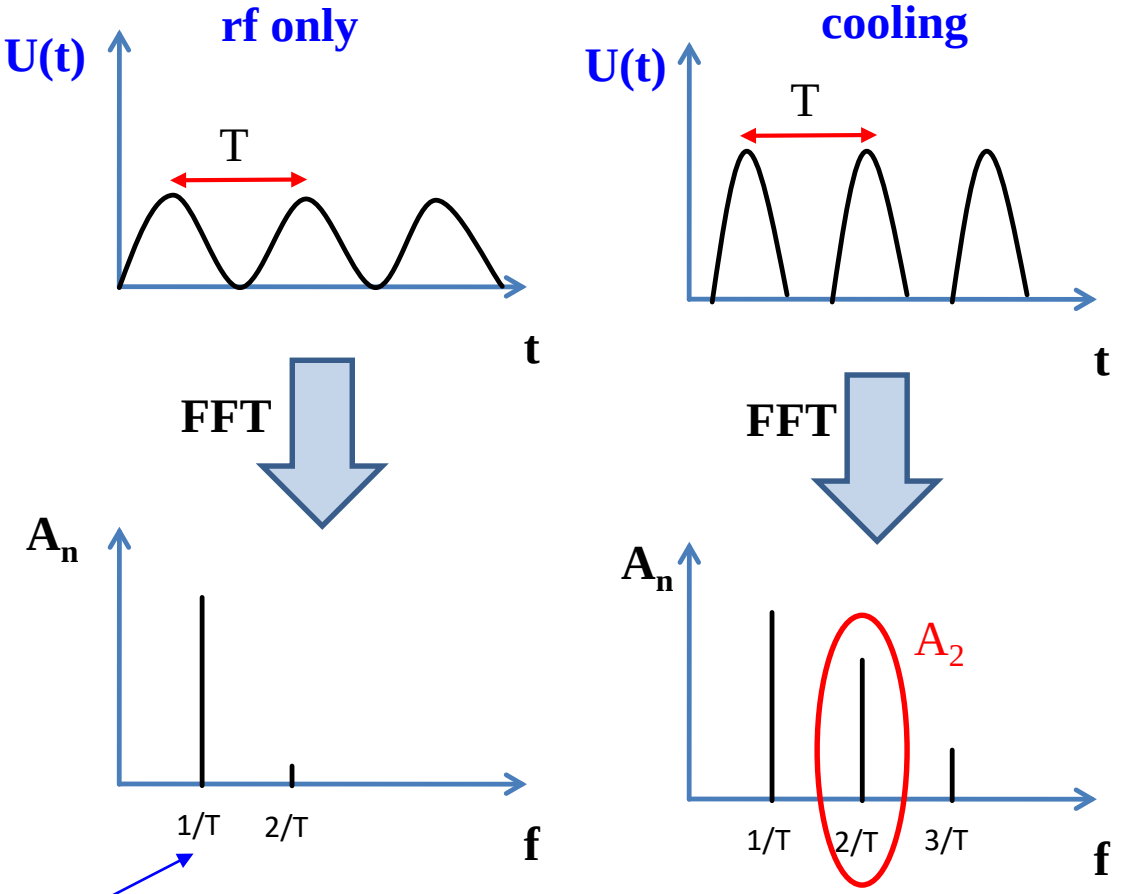

RF frequency

measurement:
observation of A_2 as a function of time with a spectrum analyzer in span 0 mode

Longitudinal cooling time of a bunched ion beam

beam: $^{19}F^{6+}$

ion energy: E = 1.34 MeV

electron energy: E_e = 38.7 eV

ion current: I ≈ 300 nA

ion number: N ≈ 10^6 particles

solenoid field: 100 Gauss

rf bunching frequency = 2nd harmonic of revolution frequency = 214 kHz

pick-up signal spectrum measured at the second harmonic of the rf frequency (f=428 kHz)

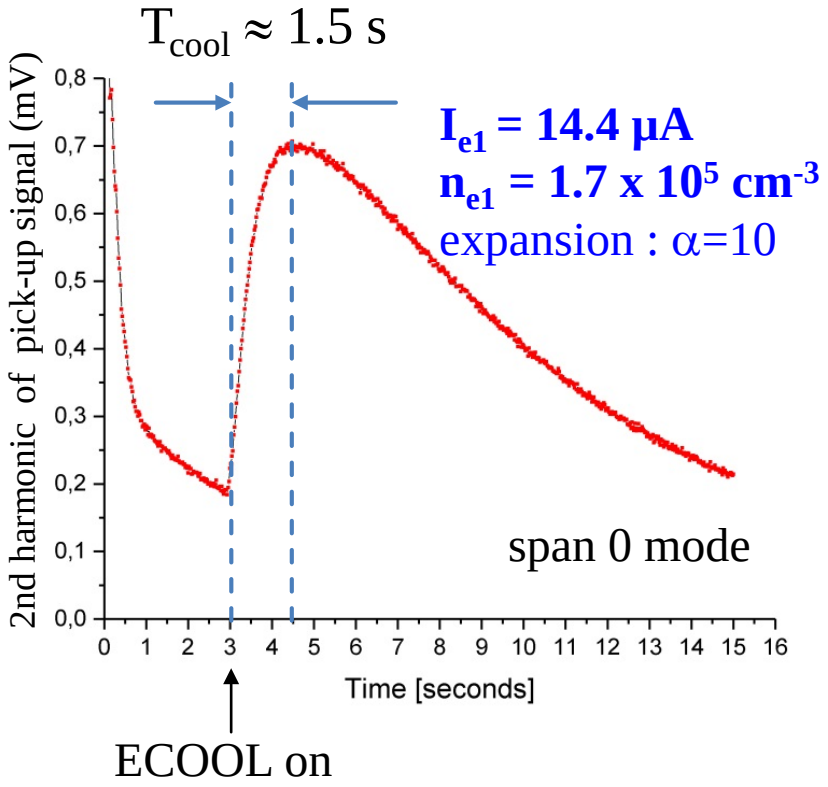

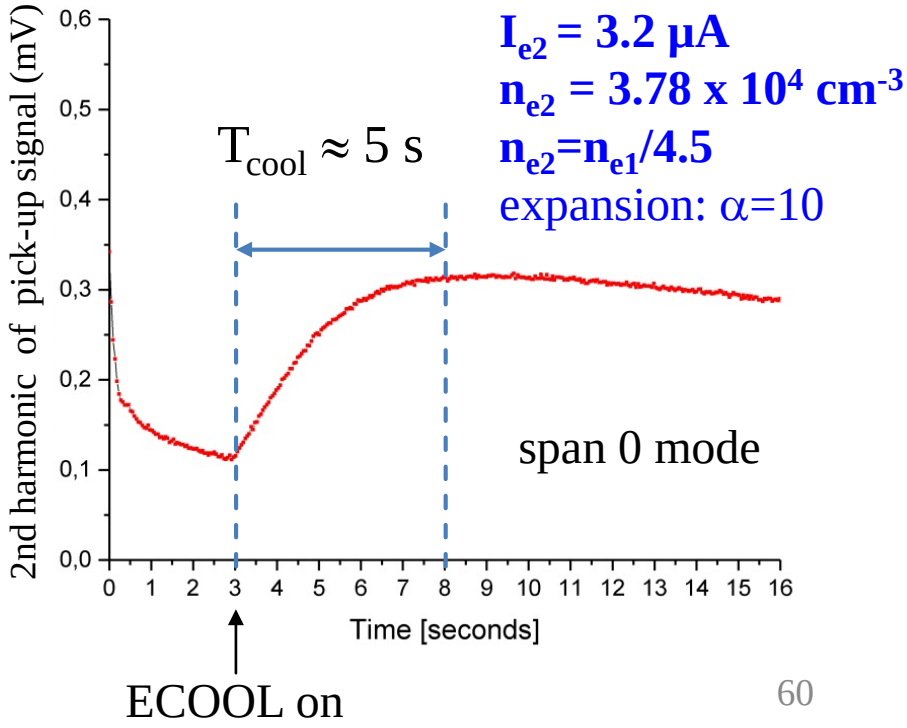

Merged beam experiments

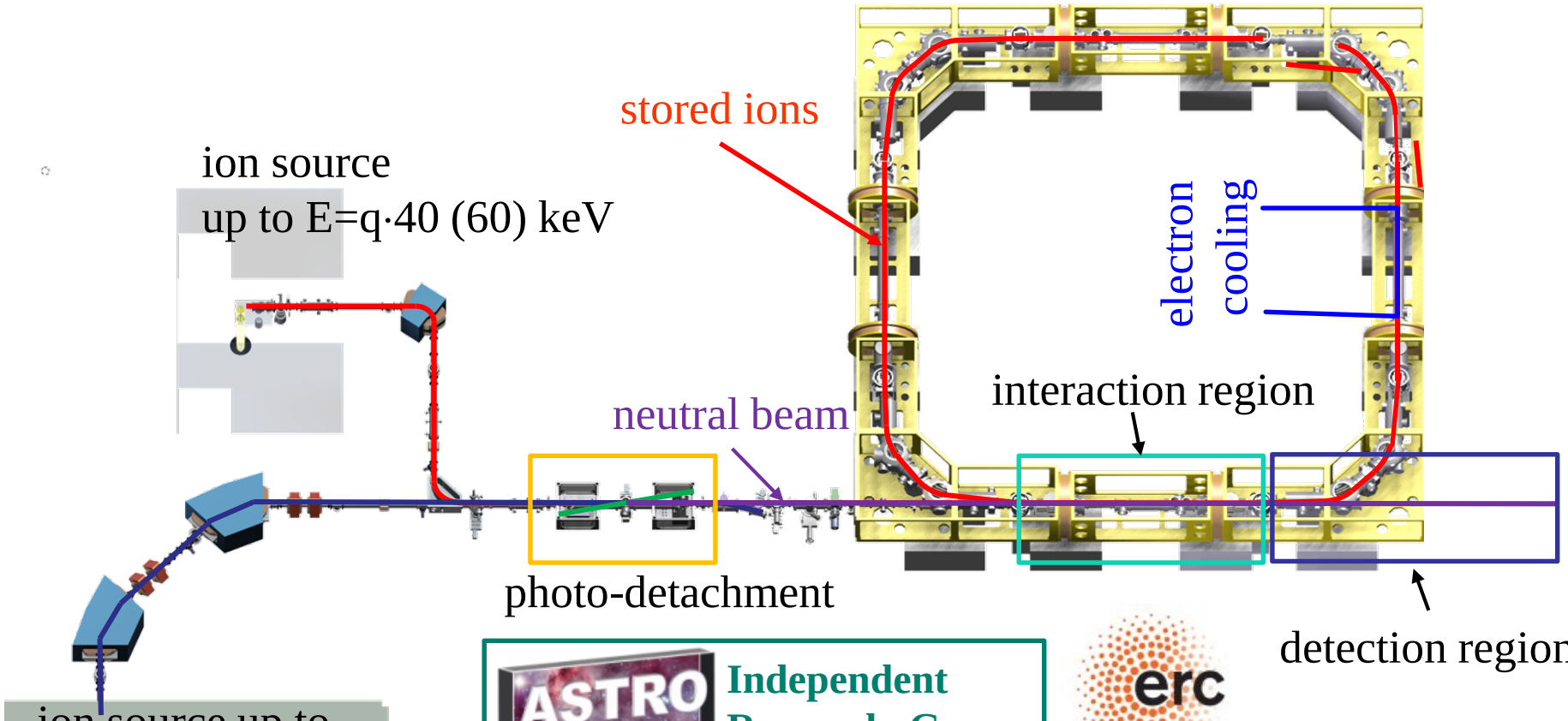

ASTRO LAB **Independent Research Group of H. Kreckel**

erc European Research Council

The reaction microscope

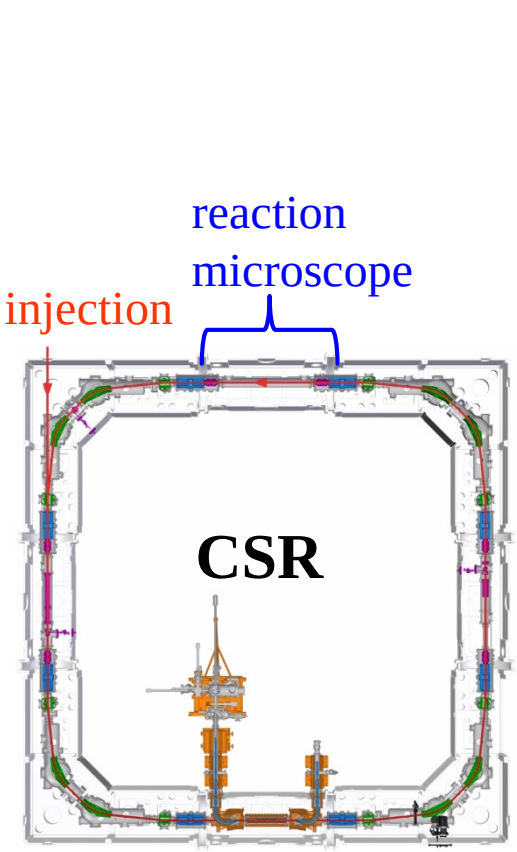

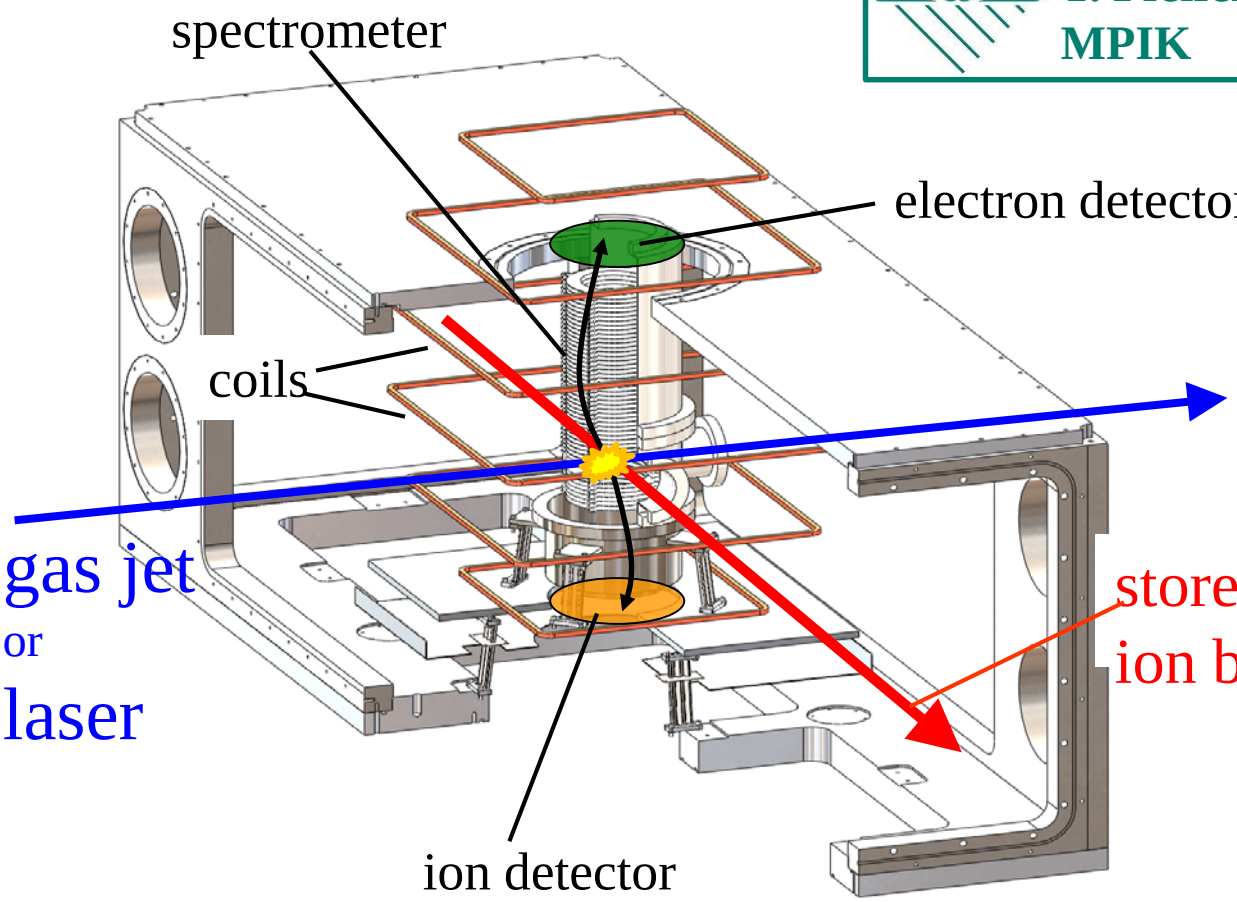

Division of
T. Pfeifer,
MPIK

Thanks for your attention!

CSR team

A. Becker
K. Blaum
C. Breitenfeldt
F. Fellenberger
S. George
J. Göck
M. Grieser
F. Grussie
R. von Hahn
P. Herwig
J. Karthein
C. Krantz
H. Kreckel
S. Kumar S.
M. Lange
J. Lion
S. Lohmann
C. Meyer
P. M. Mishra
O. Novotný
P. O'Connor
R. Repnow
S. Saurabh
S. Schippers
C. D. Schröter
D. Schwalm
L. Schweikhard
K. Spruck
X. Urbain
S. Vogel
P. Wilhelm
A. Wolf
D. Zajfman

back-up

Isolators

High voltage Isolators of 39^0 deflector electrodes

old design

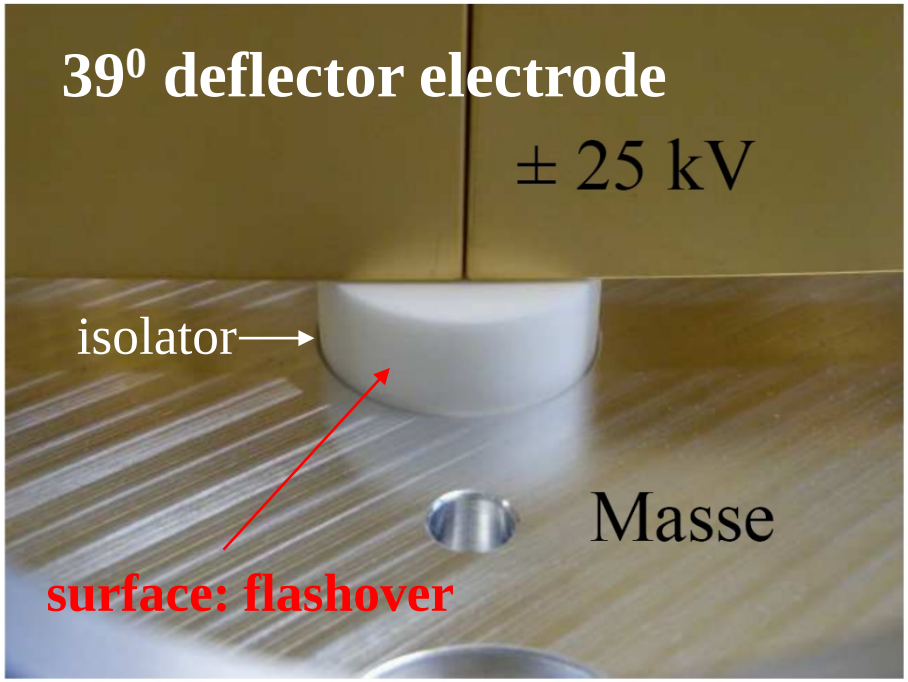

new design

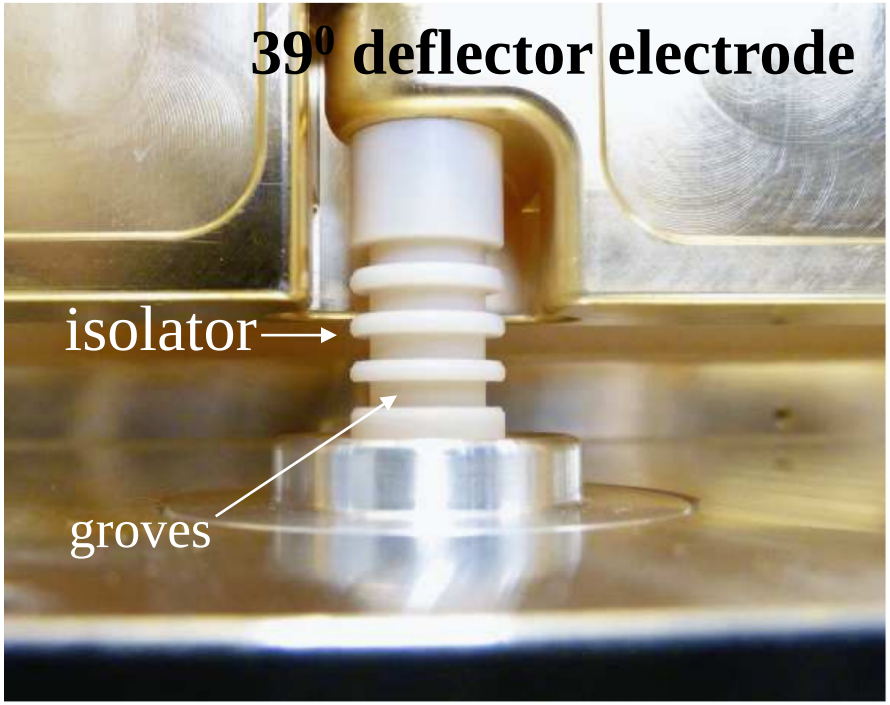

Prevent of flashover

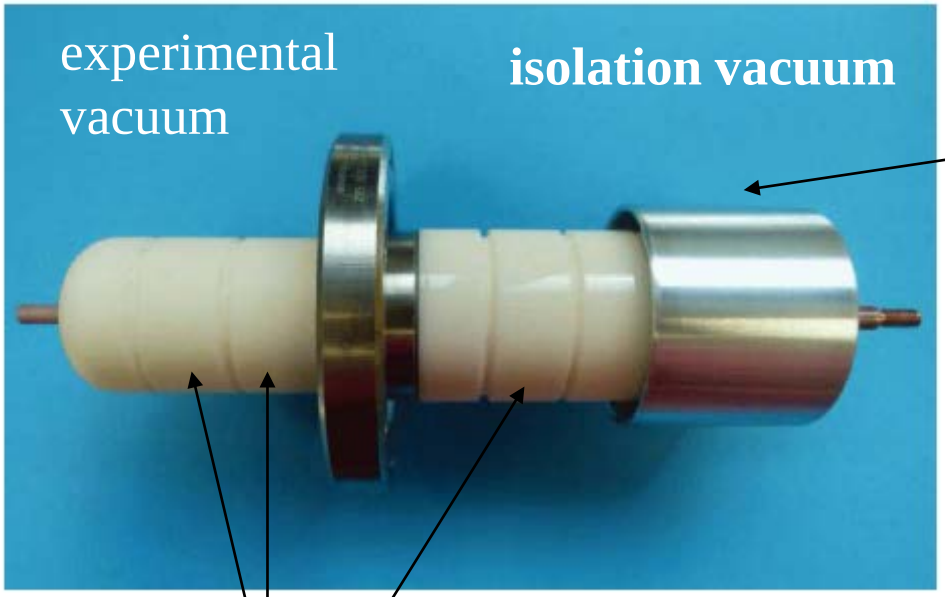

modification of the high voltage feed through

Grooves to avoid flashover

old design

new design

ceramic isolator of the quadrupoles

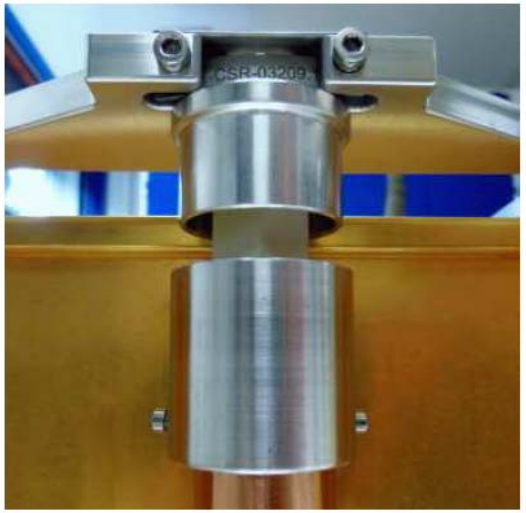

(a)

(b)

COSYINFINITY calculations

ß function and envelopes (standard mode)

COSY infinity calculation

horizontal beam envelope

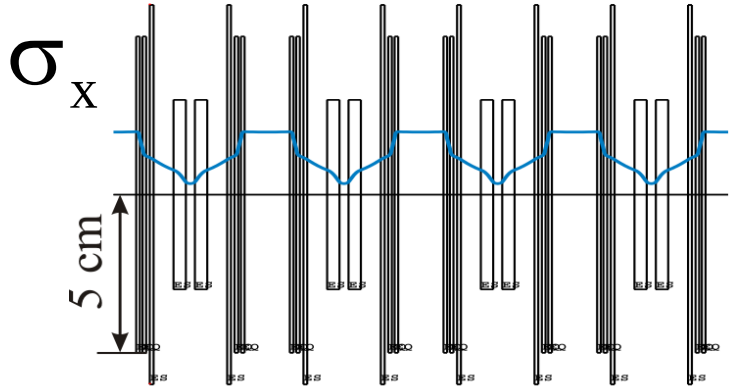

vertical beam envelope

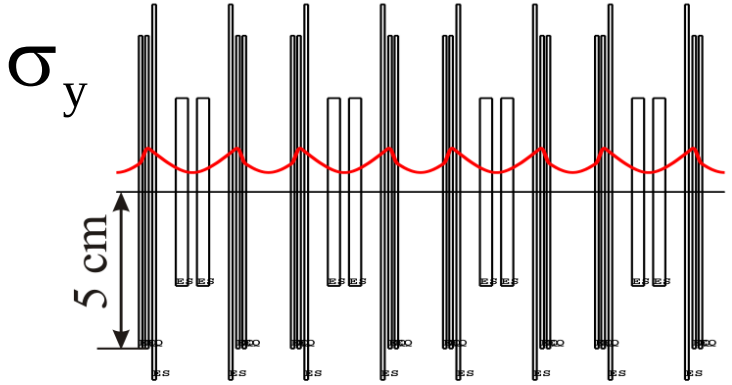

MAD8 calculation

horizontal and vertical ß function

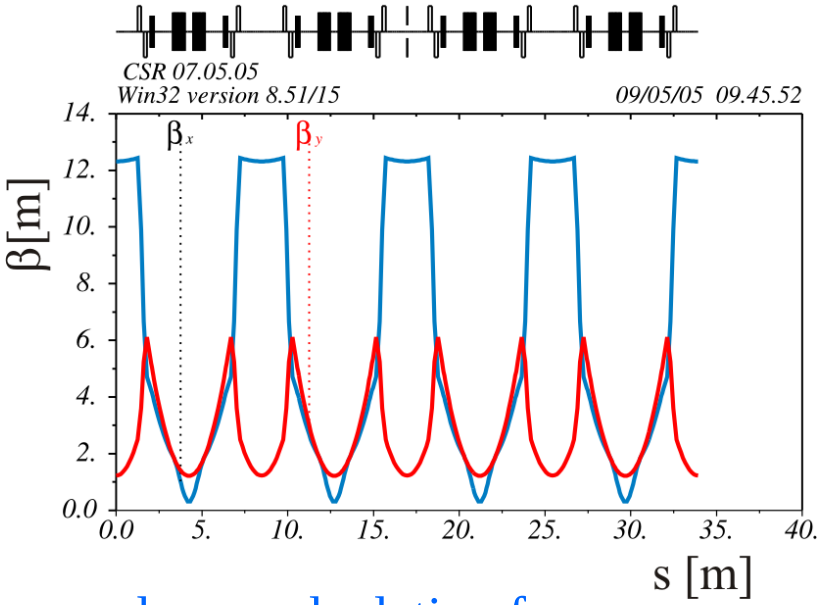

envelopes calculation for

$\varepsilon_x = 100$ mm·mrad $\quad \varepsilon_y = 100$ mm·mrad

$$\varepsilon_x = \frac{(2\cdot\sigma_x)^2}{\beta_x} \qquad \varepsilon_y = \frac{(2\cdot\sigma_y)^2}{\beta_y}$$

quadrupole settings:

Q_1: k= 5.58 1/m^2 ⇔ 4.19 kV (E/Q=300 kV)

Q_2: k=-7.04 1/m^2 ⇔ -5.28 kV (E/Q=300 kV)

Dispersion (standard mode)

COSY infinity calculation

closed orbit x_c for $\Delta E/E=0.01$

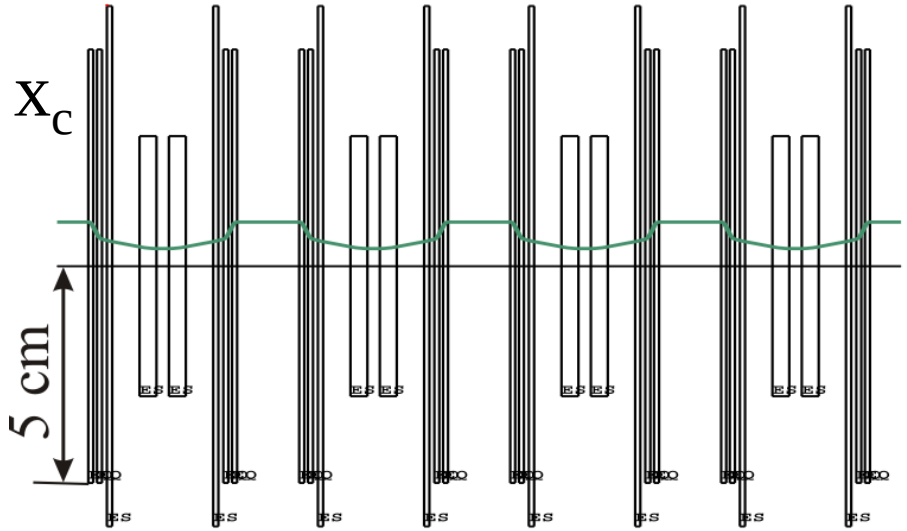

$$x_c = D_E \cdot \frac{\Delta E}{E} \quad \Rightarrow D_{E,max} = 1.04 \text{ m}$$
$$\Leftrightarrow D_{p,max} = 2.08 \text{ m}$$

quadrupole settings:

MAD8 calculation

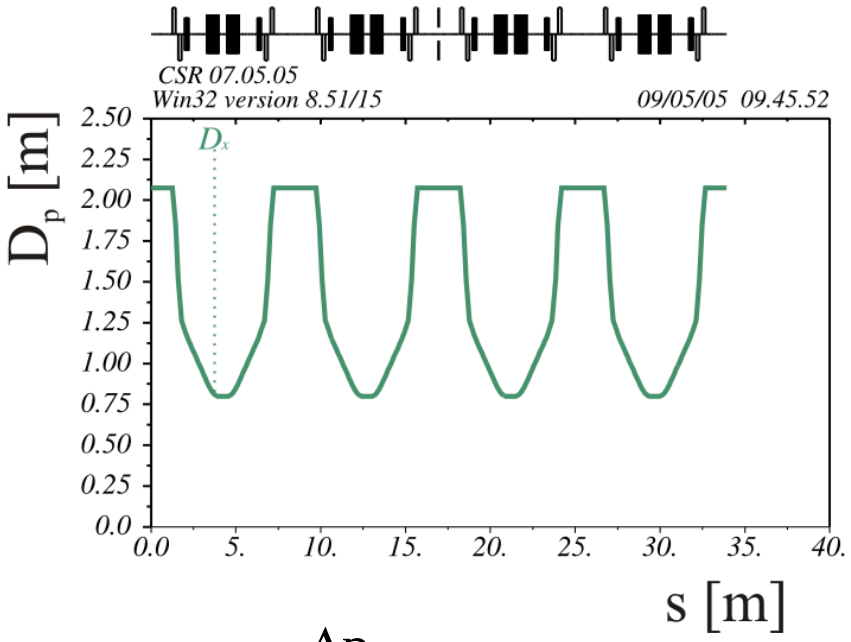

$$x_c = D_p \cdot \frac{\Delta p}{p}$$

$D_{p,max}=2.08$ m

Q_1: k= 5.58 1/m^2 $\Leftrightarrow$ 4.19 kV (E/Q=300 kV)

Q_2: k=-7.04 1/m^2 $\Leftrightarrow$ -5.28 kV (E/Q=300 kV)

Misalignment

Determination of misalignment effects with COSY Infinity

Misalignment of the 39^0 deflector

1^0 horizontal deflector rotation around the y-axes

horizontal closed orbit

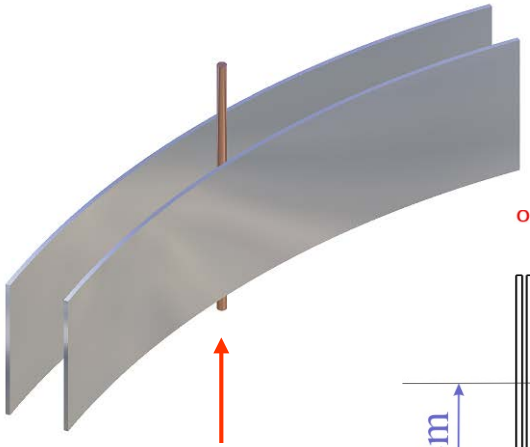

rotation axes

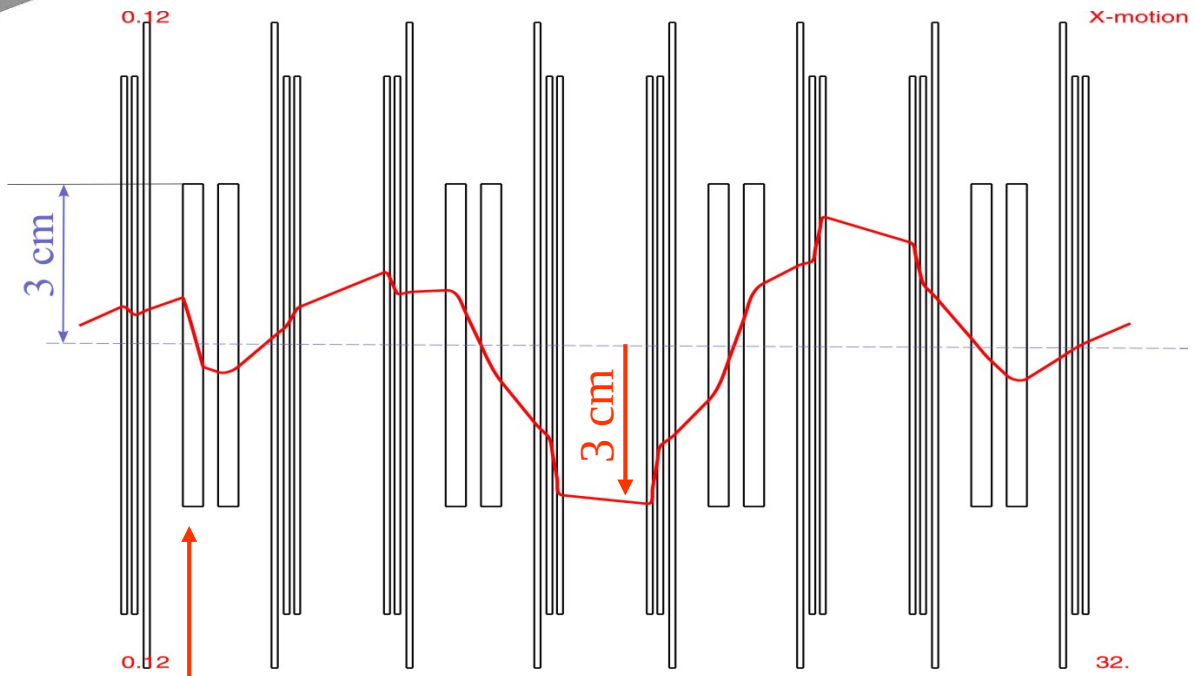

39^0 deflector rotation $\alpha = 1^0$

maximum closed orbit distortion should be less then 1 mm

$\Rightarrow$ alignment error $\alpha \leq \pm 0.03^0$

Alignment precision

Calculated for a maximum closed orbit shift of 1 mm

element	**degree of freedom**	nominal value	measurements*
6°-Deflektor	Rot. horiz.	$\leq 0{,}15\,°$	$0{,}095° \pm 0{,}058°$
6°-Deflektor	Rot. vert.	$\leq 0{,}15\,°$	$0{,}022° \pm 0{,}001°$
6°-Deflektor	Transl. horiz.	$\leq 1{,}0$ mm	$0{,}40$ mm $\pm\, 0{,}05$ mm
39°-Deflektor	Rot. horiz.	$\leq 0{,}03\,°$	$0{,}000° \pm 0{,}004°$
39°-Deflektor	Rot. vert.	$\leq 0{,}06\,°$	$0{,}016° \pm 0{,}004°$
39°-Deflektor	Transl. horiz.	$\leq 0{,}5$ mm	$0{,}20$ mm $\pm\, 0{,}03$ mm
Quadrupoldublett	Rot. horiz.	$\leq 0{,}015°$	$0{,}000° \pm 0{,}010°$
Quadrupoldublett	Rot. vert.	$\leq 0{,}03°$	$0{,}040° \pm 0{,}016°$
Quadrupoldublett	Transl. horiz.	$\leq 0{,}50$ mm	$0{,}30$ mm $\pm\, 0{,}05$ mm
Quadrupoldublett	Transl. vert.	$\leq 0{,}40$ mm	$0{,}16$ mm $\pm\, 0{,}05$ mm

*Alignment change measurements of the ion optical elements during the cool down process from room temperatures below T=40 K

Single turn injection

Single turn injection

pulsed injector beam

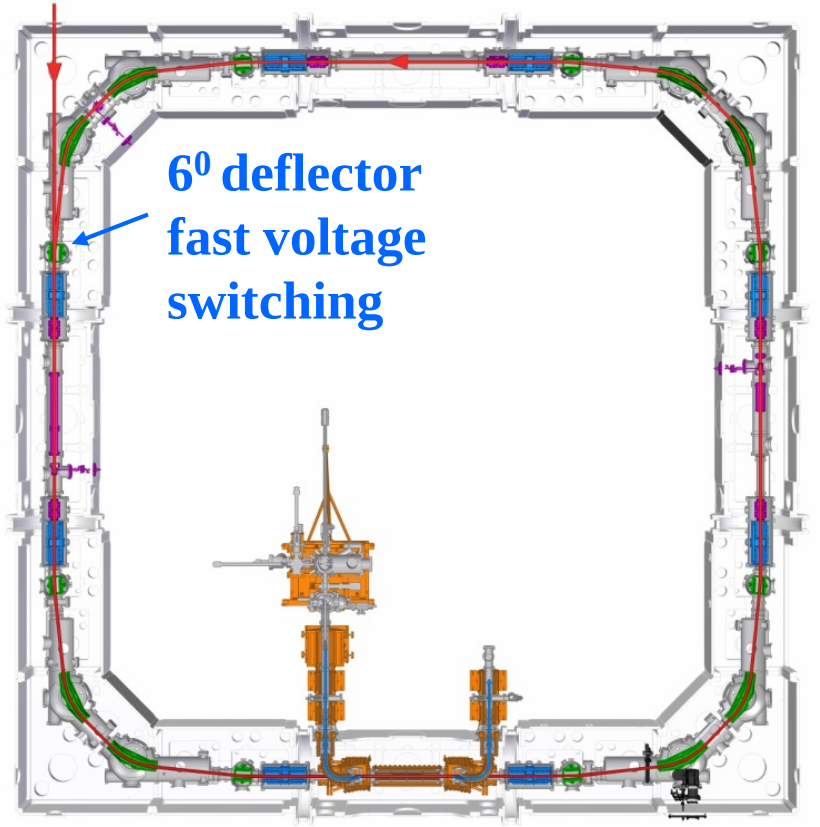

T_0 - revolution time

T_i - injector beam pulse length

$T_i > T_0$

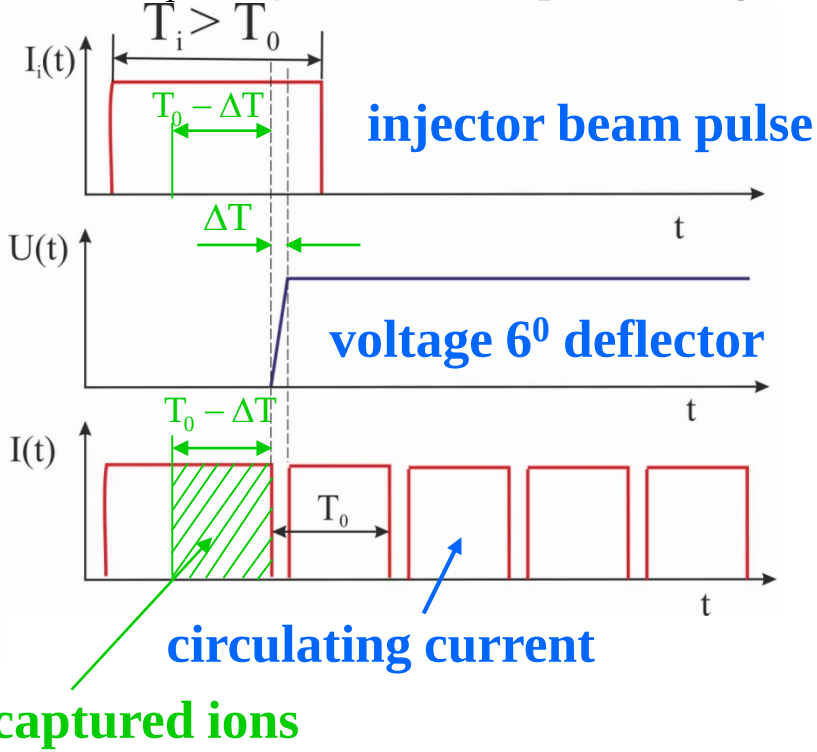

Fast switching of the 6^0 deflector voltage

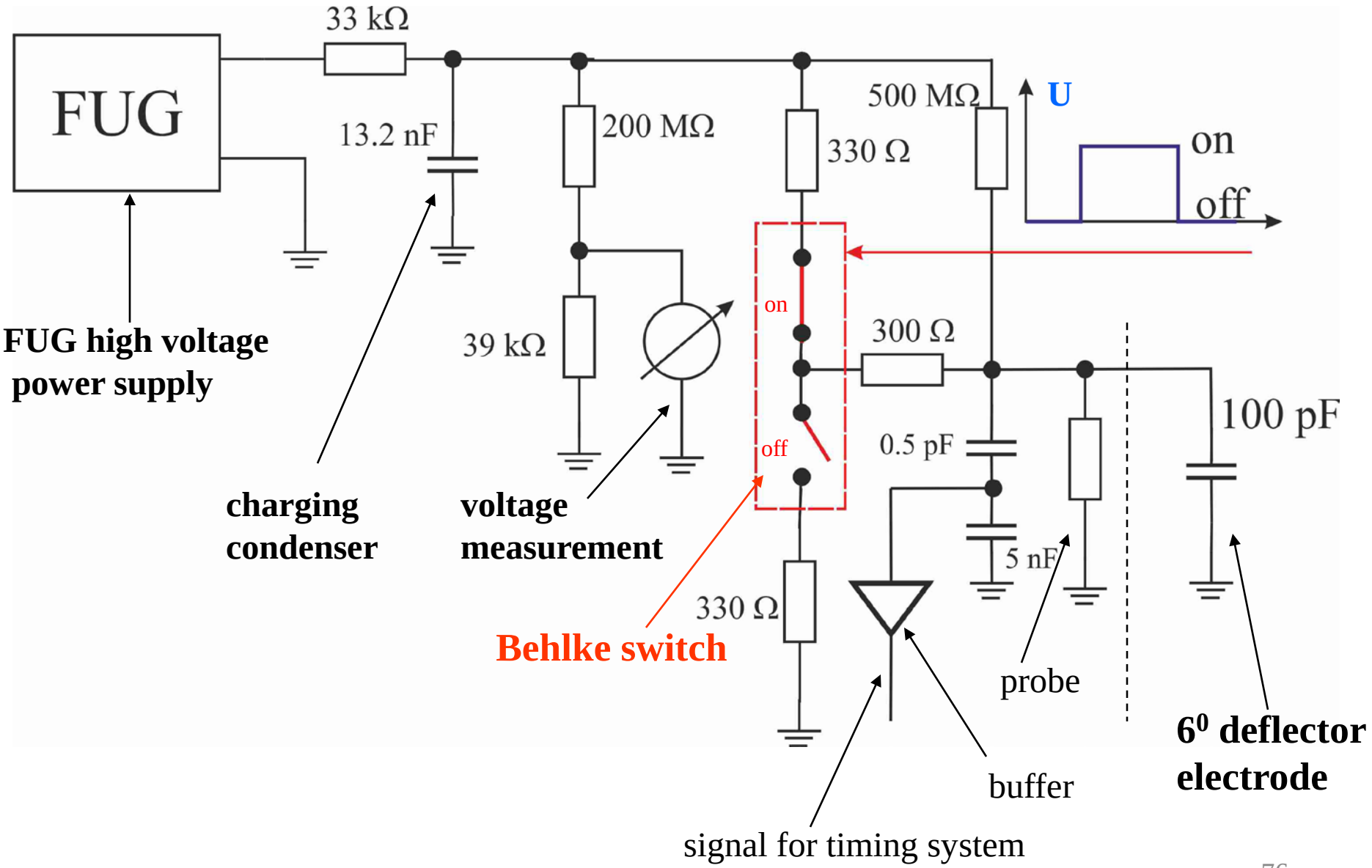

Switching time of Behlke switch

electrode voltage as a function of time

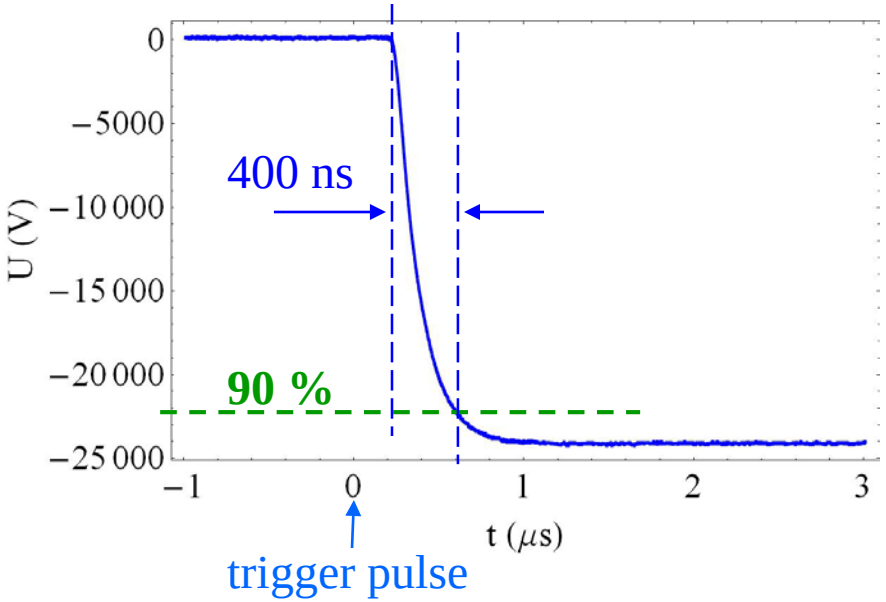

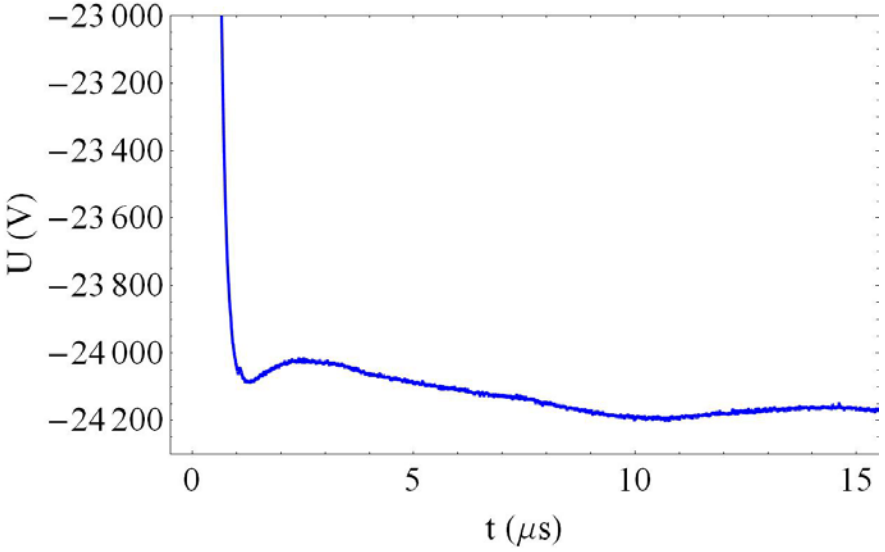

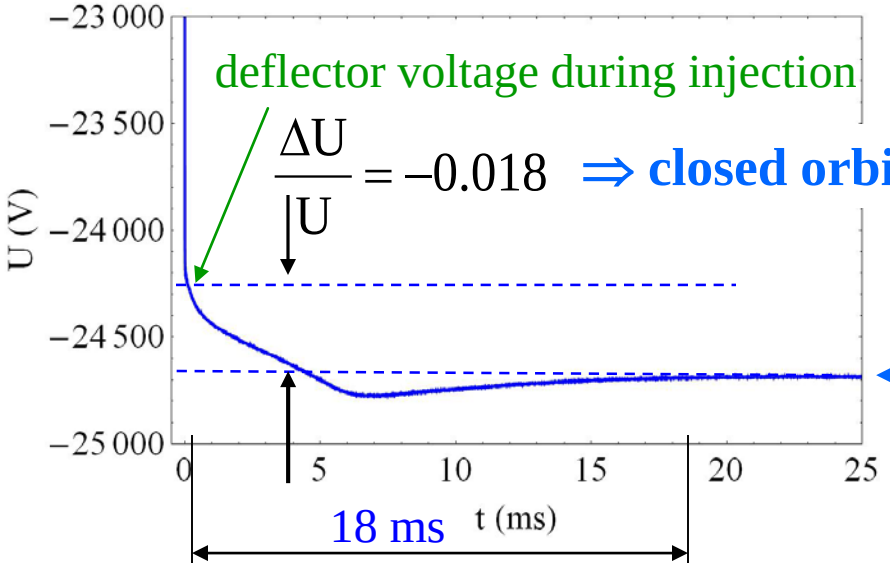

⇒ closed orbit during injection !!!!!!

Final voltage U_f=-24685 V

Closed Orbit shift during injection injection

6^0 deflector change of the deflection angle by: $\frac{\Delta\alpha}{\alpha} = -\frac{\Delta U}{U} = 0.018$

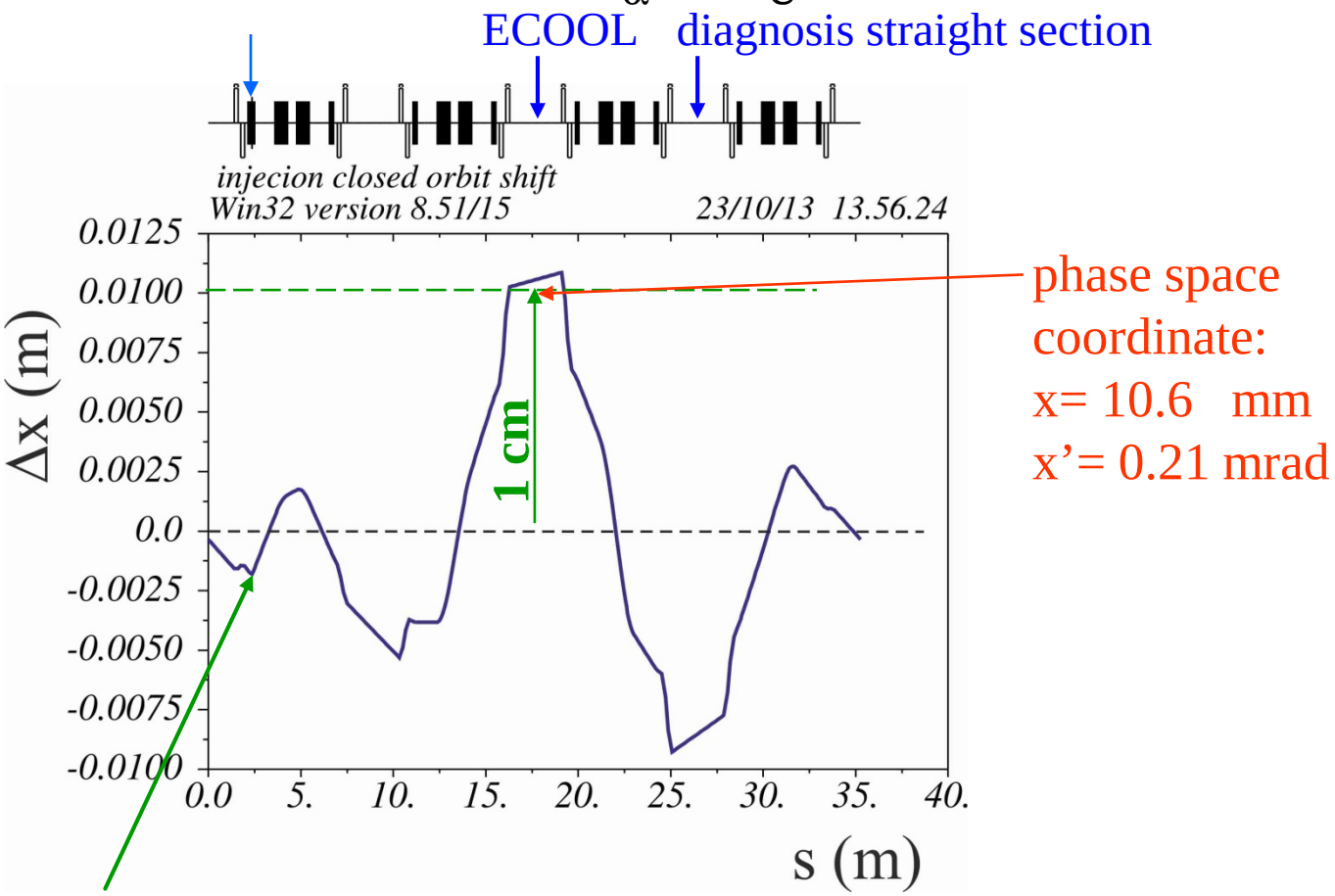

phase space coordinate:
x= 10.6 mm
x'= 0.21 mrad

theoretical injection orbit (injector beam),not realizable due to aperture limitations in the transfer line ⇒ excitation of dipole oscillations of stored ion beam

Horizontal dynamical acceptance of the CSR

ECOOL OFF

Horizontal acceptance at the center of a straight section

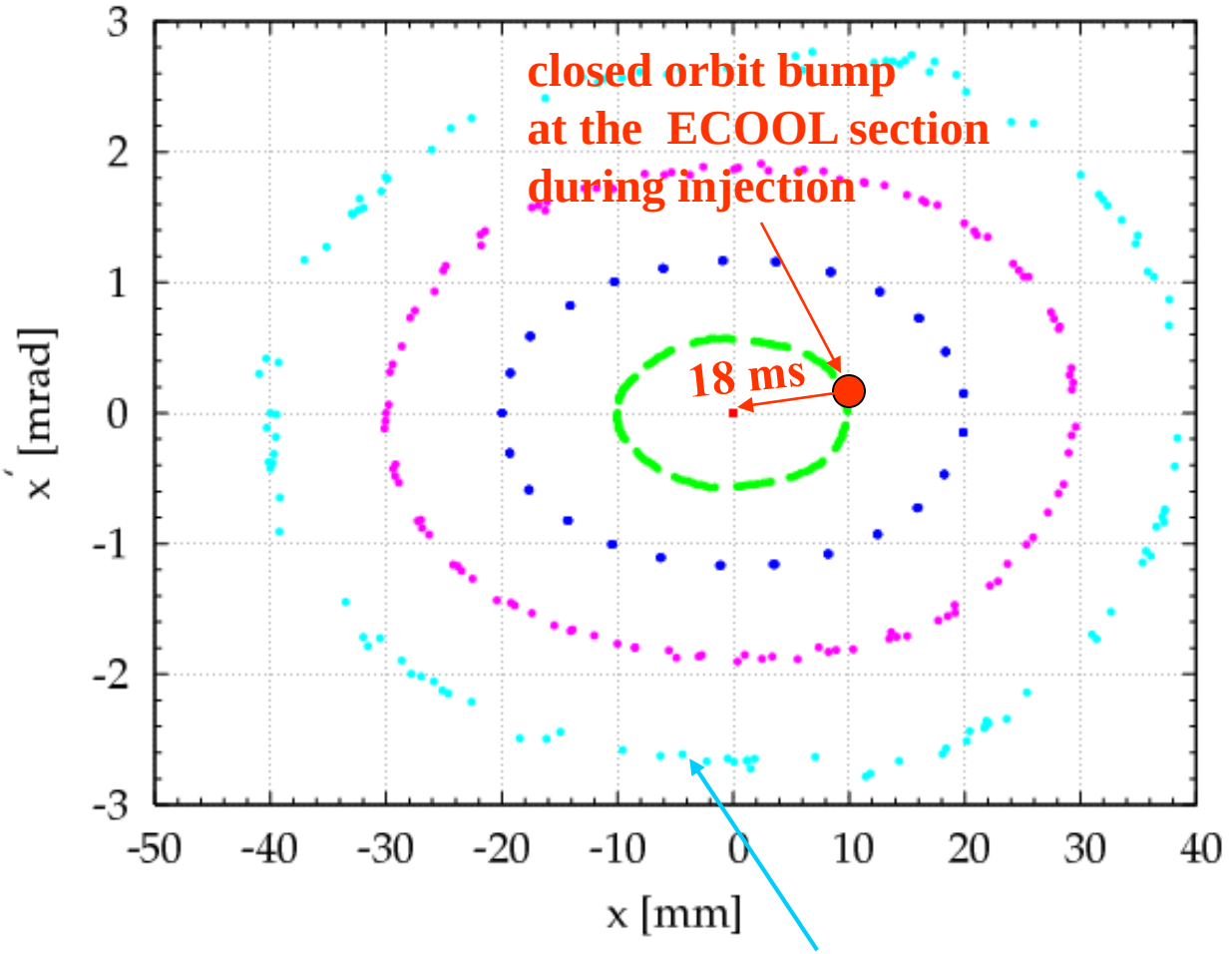

X_i=0
X_i=10
X_i=20
X_i=30
X_i=40

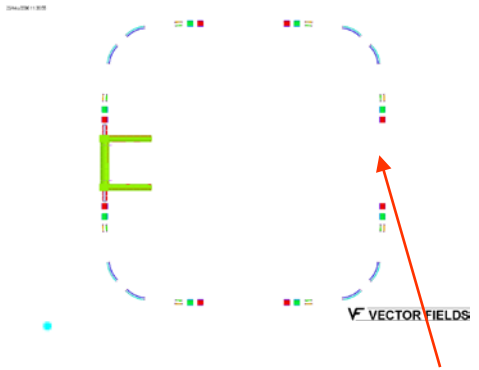

starting point

maximum beam Size in the center of the straight section

$$|x|_{max} \approx 4\text{cm}$$

ions lost for x>4 cm
reason: good field region of the quadrupole

dynamical acceptance at center of each straight section

A_x=120 mm·mrad

Current pick-up

Pick-up signal of a bunched ion beam

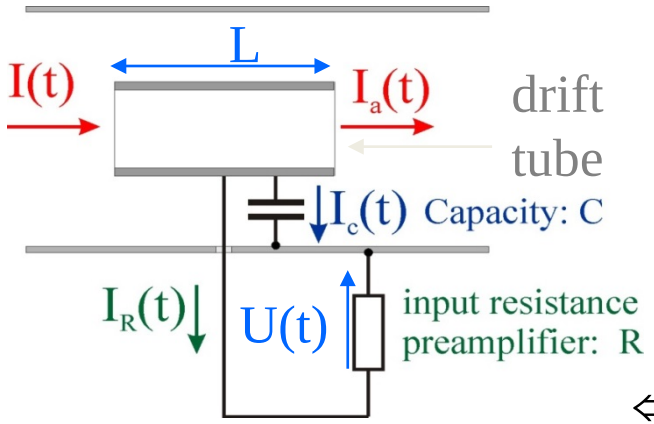

current of the stored ion beam

$$I_a(t) = I(t - \Delta t)$$

after the drift tube — flight time inside the drift tube

node theorem:

$$I(t) = I_a(t) + I_R(t) + I_C(t)$$

$$\Leftrightarrow \; I(t) = I(t - \Delta t) + I_R(t) + I_C(t)$$

With bunch length $l_b >> L$:

$$I(t-\Delta t) = I(t) - \frac{dI}{dt}\Delta t = I(t) - \dot{I}(t)\frac{L}{v}$$

with $I_R(t) = \frac{U}{R}$ and $I_C(t) = C \cdot \dot{U}(t)$ differential equation for drift tube voltage U(t)

$$\frac{L}{v}\dot{I}(t) = C \cdot \dot{U}(t) + \frac{U(t)}{R}$$

for $R \to \infty$ drift tube voltage: $U(t) = \frac{1}{C}\frac{L}{v} I(t) \;\Rightarrow\; U(t) \propto I(t)$

Calculated Pick-up signal

circulating beam current

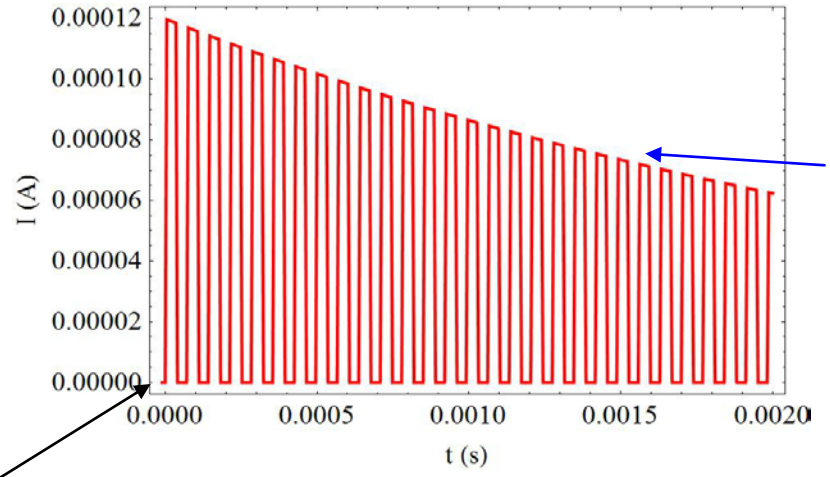

circulating ion pulse
calculated for $p \approx 10^{-7}$ mbar

intensity decrease
due to life-time

injection

pick-up signal

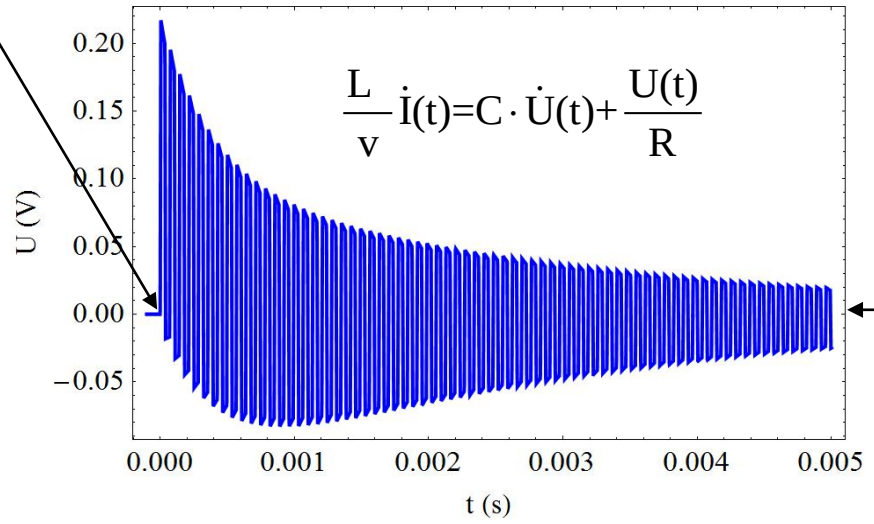

DC part
disappeared

Comparison between calculated and measured pick-up signal

calculated

$$\frac{L}{v}\dot{I}(t) = C \cdot \dot{U}(t) + \frac{U(t)}{R}$$

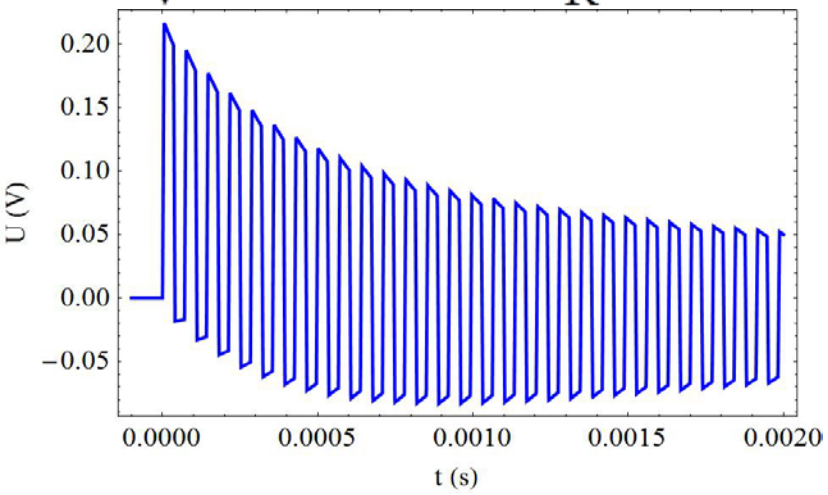

calculated for C=400 pF
and R=1 MΩ

measured

Schottky pick-up used as current pick-up

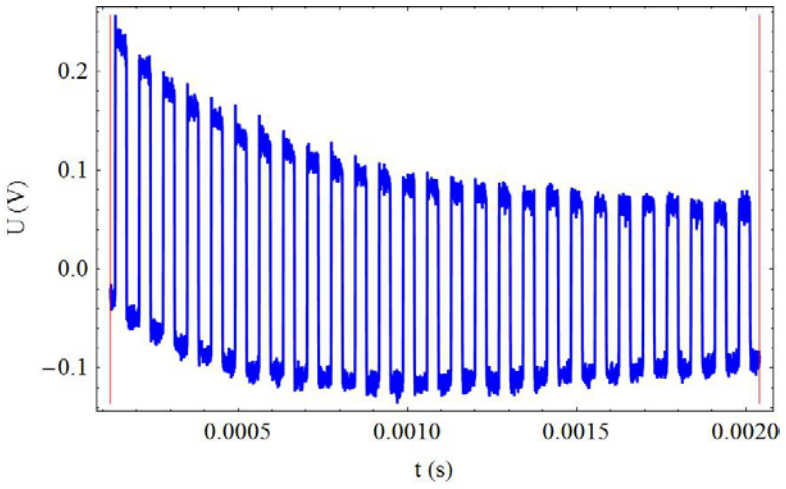

Life time determination with current pick-up

-used to measure the **absolute number** of the injected ion number (pulsed current)
-sensitivity 10^6 singly charged ions

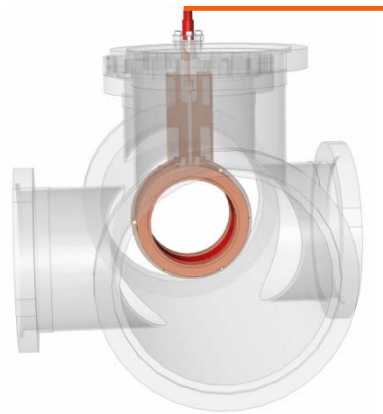

$$U(t) = \frac{1}{C}\frac{L}{v} I(t)$$

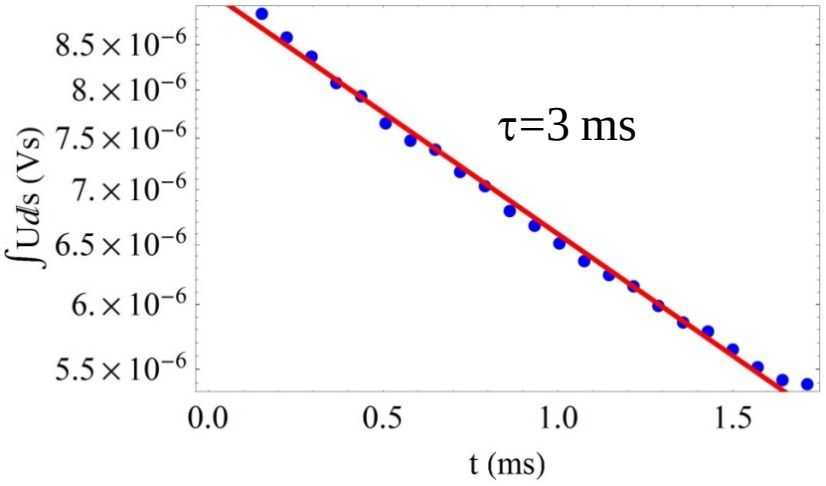

pick-up signal at at ≈**10^{-7} mbar** (room temperature, no out-backing) for 50 keV Ar^+ ions

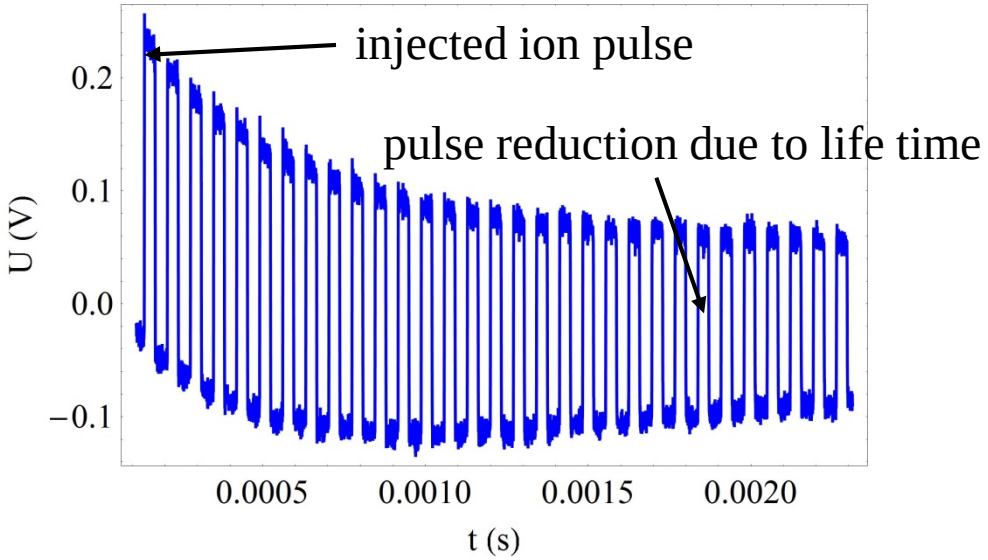

measured lifetime at ≈**10^{-7} mbar**
(room temperature operation, **March 2014**)

Schottky-pickup

The Schottky pick up of the CSR

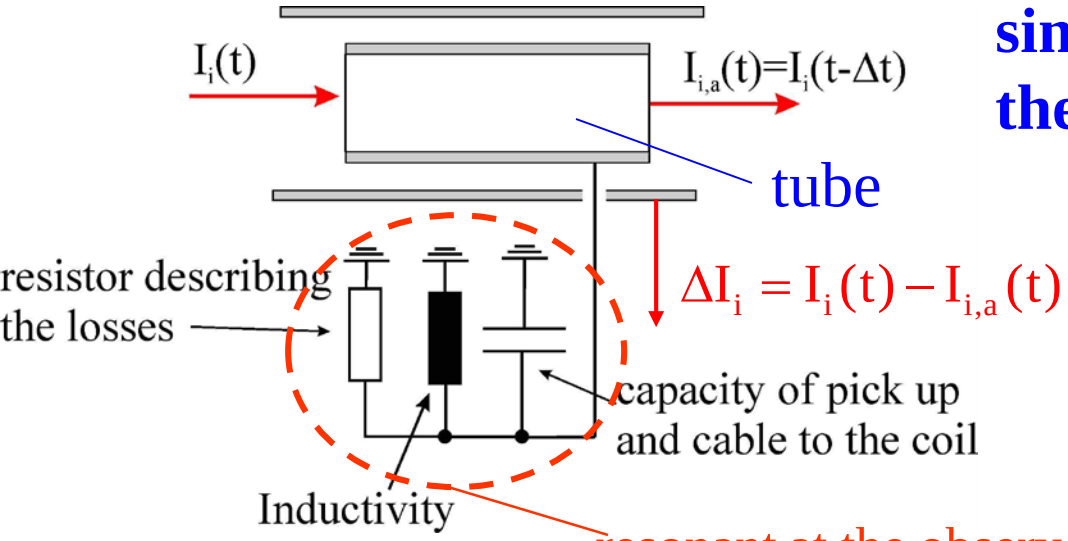

single ion interaction with the Schottky pick up

flying time through the pick up

$$I_i(t) = Q\sum_n \delta(t - nT)$$

$$I_{i,a}(t) = I_i(t-\Delta t) = Q\sum_n \delta(t - nT + \Delta t)$$

resonant at the observed Schottky band

$$\Delta t = \frac{L}{v}$$

L- pick up length

v- ion velocity

Fourier row

$$I_i(t) = Q\left(\frac{a_0}{2} + \sum_{n=1}^{\infty}\frac{2}{T}\cos(n\,\omega_0\,t)\right)$$

T -revolution time of the ion

$$I_{i,a}(t) = Q\left(\frac{a_0}{2} + \sum_{n=1}^{\infty}\frac{2}{T}\cos(-n\,\omega_0\,\Delta t)\cdot\cos(n\,\omega_0\,t) + \frac{2}{T}\cdot\sin(-n\,\omega_0\,\Delta t)\sin(n\,\omega_0\,t)\right)$$

current into LC circuit $\Delta I_i(t) = I_i(t) - I_{i,a}(t)$ with $\omega_n = n\,\omega_0$

$$\Delta I_i(t) = Q\frac{2}{T}\sum_{n=1}^{\infty}\left(\left(1-\cos(\omega_n\,\Delta t)\right)\cos(\omega_n t) + \sin(\omega_n\,\Delta t)\sin(\omega_n t)\right)$$

Spectrum of the Schottky signal coming from a single ion

$$\Delta t = \frac{L}{v}$$

$$\Delta I_i(t) = Q\frac{2}{T}\sum_{n=1}^{\infty}\left(\left(1-\cos(\omega_n \Delta t)\right)\cos(\omega_n t) + \sin(\omega_n \Delta t)\sin(\omega_n t)\right)$$

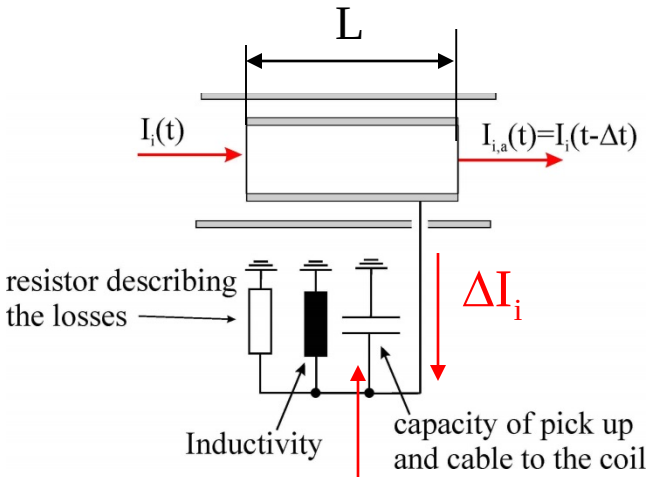

$\Rightarrow$ spectrum of ΔI_i $\quad \omega_n = n\,\omega_0$

$$\Delta\hat{I}_i(\omega_n) = \frac{2Q}{T}\sqrt{\left(1-\cos(\omega_n \Delta t)\right)^2 + \sin^2(\omega_n \Delta t)} = \frac{2\sqrt{2}\,Q}{T}\sqrt{1-\cos(\omega_n \Delta t)}$$

resonant at f_n

$f_n = n\,f_0$

$\Delta\hat{I}_i(\omega_n)$ is maximum at $\omega_n \Delta t = \pi, 3\pi, \ldots$

$\Delta\hat{I}_i(\omega_n)$ is 0 at $\omega_n \Delta t = m \cdot \pi$ $\quad \Delta t = \frac{L}{v}$

$\omega_n = 2\pi n f_0$ ← revolution frequency of the ion

integer number

Spectrum of the Schottky signal coming from a single ion

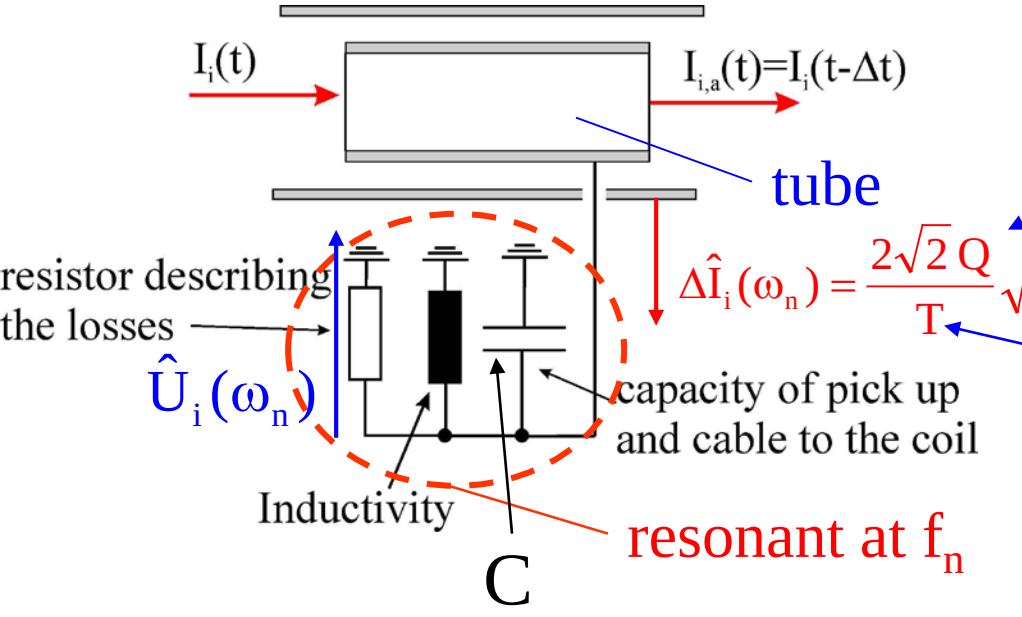

ion charge

$$\Delta\hat{I}_i(\omega_n)=\frac{2\sqrt{2}\,Q}{T}\sqrt{1-\cos(\omega_n\Delta t)}$$

T revolution time

Q value of the LC circuit

signal on LC circuit from a single ion：

$$\hat{U}_i(\omega_n)=\frac{Q_w}{\omega_n C}\frac{2\sqrt{2}\,Q}{T}\sqrt{1-\cos(\omega_n\frac{L}{v})}$$

$\Rightarrow$ signal from a single ion proportion to the Q-value (Q_w) of the LC circuit！

Schottky signal of the ion beam

Schottky signal from a single ion: $$\hat{U}_i(\omega_n) = \frac{Q_w}{\omega_n C}\frac{2\sqrt{2}\,Q}{T}\sqrt{1-\cos(\omega_n \frac{L}{v})}$$

Schottky signal from a ion beam: $$\hat{U}(\omega_n) = \sum_{i=1}^{N} \hat{U}_i(\omega_n)\cos(\varphi_i)$$

statistical distributed

Schotty Power : $$P_0(\omega_n) = \left(\sum_{i=1}^{N} \hat{U}_i(\omega_n)\cos(\varphi_i)\right)^2$$

hence in the time average: $$\overline{\left(\sum_{i=1}^{N}\cos(\varphi_i)\right)^2} = \frac{N}{2}$$

we obtain for the Schottky power:

$$\overline{P}_0(n) = \hat{U}_i^2\frac{N}{2} = \left(Q_w\frac{\sqrt{2}}{\pi}\frac{1}{n}\frac{Q}{C}\sqrt{1-\cos(n\,2\pi\frac{L}{C_0})}\right)^2\frac{N}{2}$$

Improvement of noise signal ratio at resonant measurement

P_{res}- noise of preamplifier (resonant measurement)

$P_{nonresonant}$- noise of pre amplifier (non resonant measurement)

pre amplifier: ULNA

pre amplifier noise

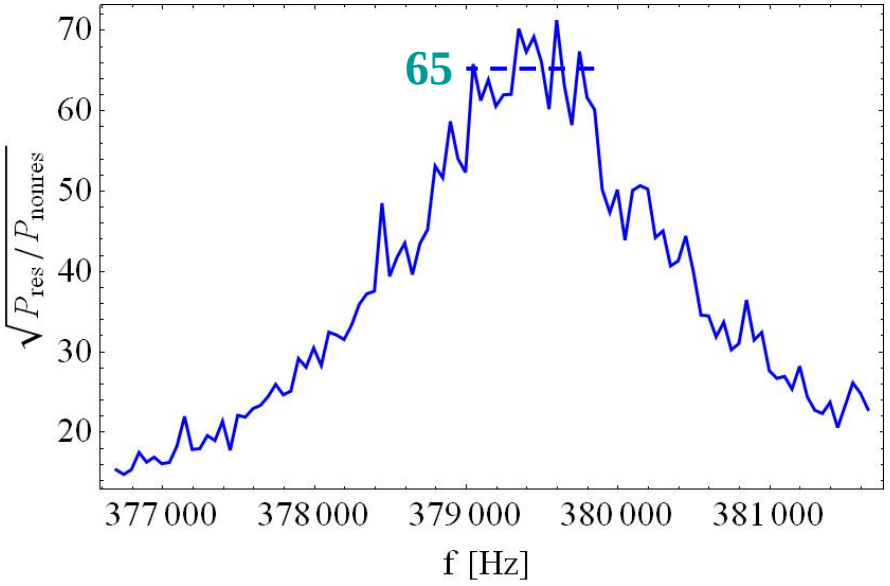

Q_w value measurement

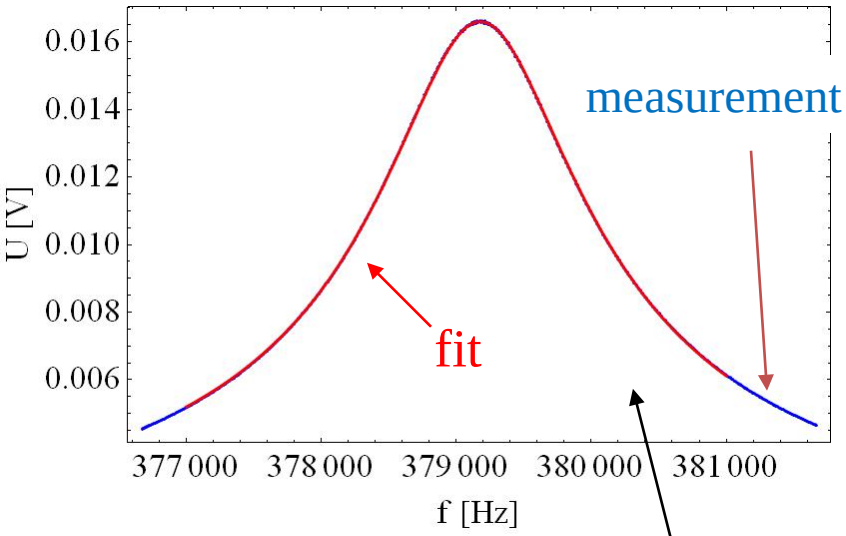

Q_w value : **Q_w=263**

normal conducting coil

$$\Rightarrow \text{improvement of SNR} = \frac{Q}{\sqrt{P_{res}/P_{nonres}}} = \frac{263}{65} = 4$$

$$\text{detection limit } N \sim \frac{1}{SNR^2} = \frac{1}{16}$$

Schottky pick –up of the CSR

52

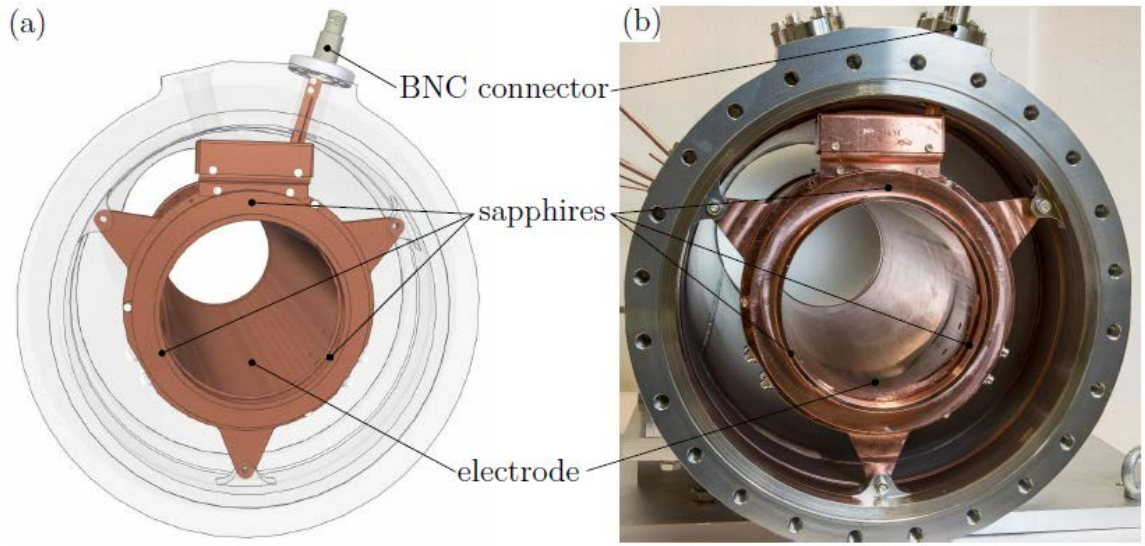

Figure 3.15: The SCHOTTKY pick-up electrode as a (a) CAD-model and (b) photograph mounted in its CSR vacuum chamber. The electrode has a length of 350 mm and aperture diameter of 100 mm.

Schottky pick-up

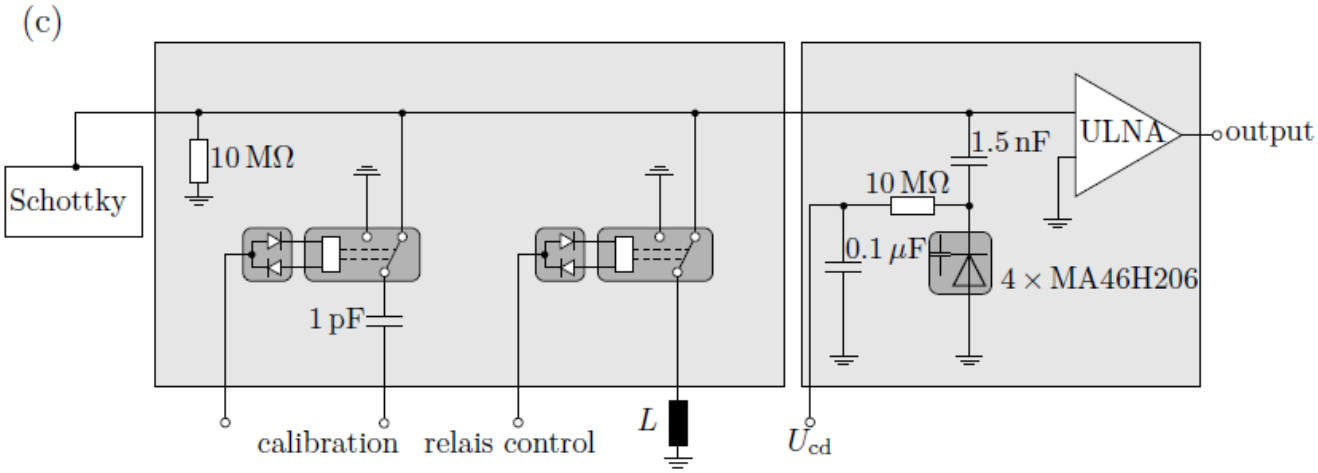

Layout of the cryogenic electronic of the Schottky pick-up

Cryogenic amplifier box of the Schottky pick-up

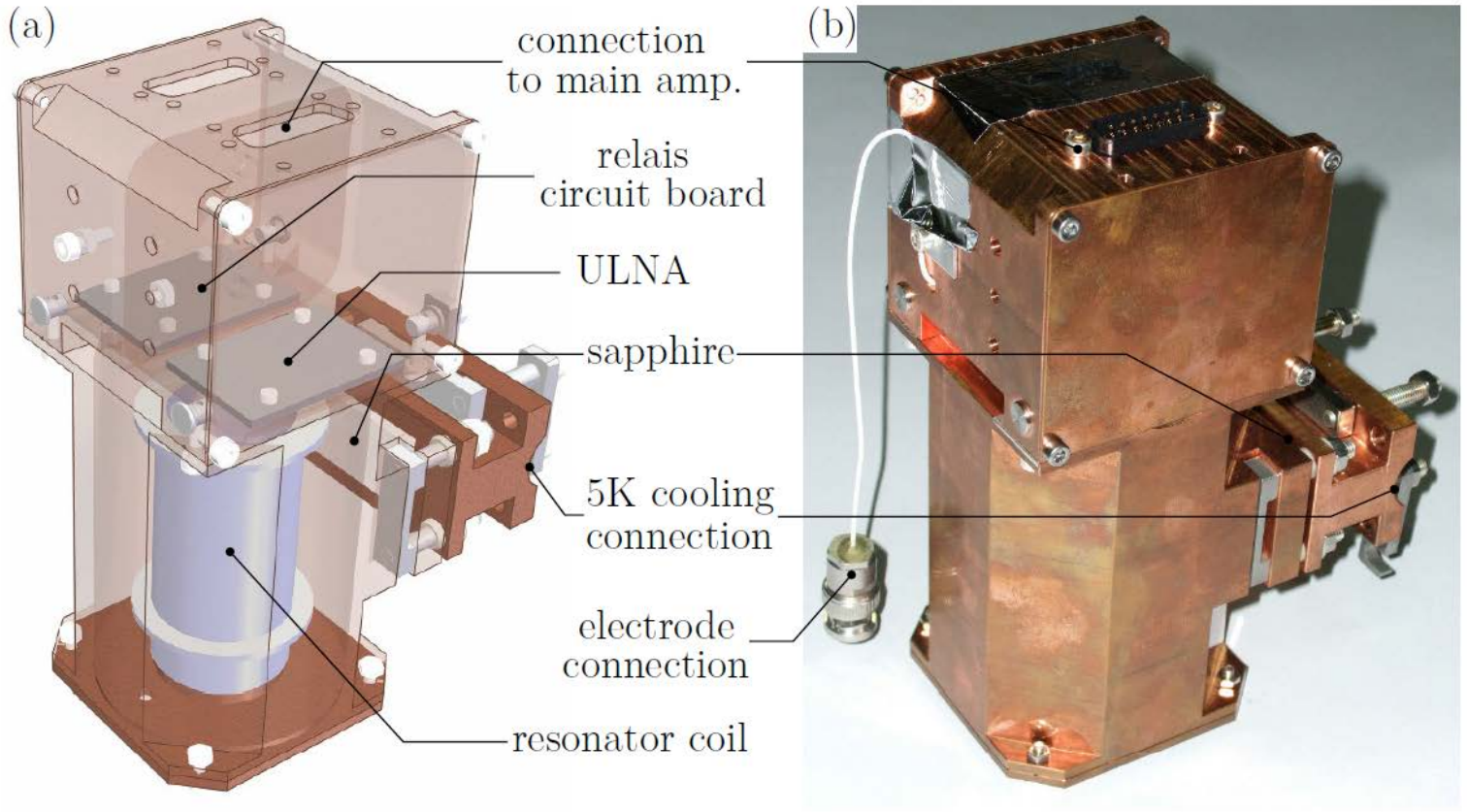

CAD-model

Photograph

Detection Limit of Schottky pick-up

detection is possible:

Schottky power > amplifier noise in the Schottky band width:

$$\overline{P}_0(n) = \hat{U}_i^2 \frac{N}{2} > U_n^2 \Delta f_n \qquad U_n \approx 1\,\mathrm{nV}/\sqrt{\mathrm{Hz}}$$

← noise of pre amplifier

detection limit calculated for Co_2^- (E=60 keV)

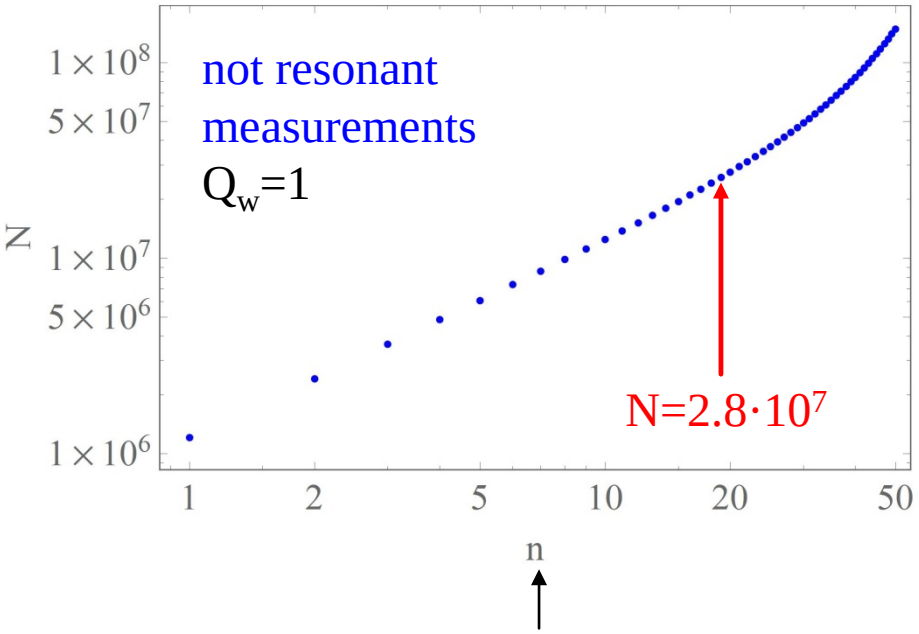

harmonic number of the revolution frequency

Schottky spectrum not clear visible

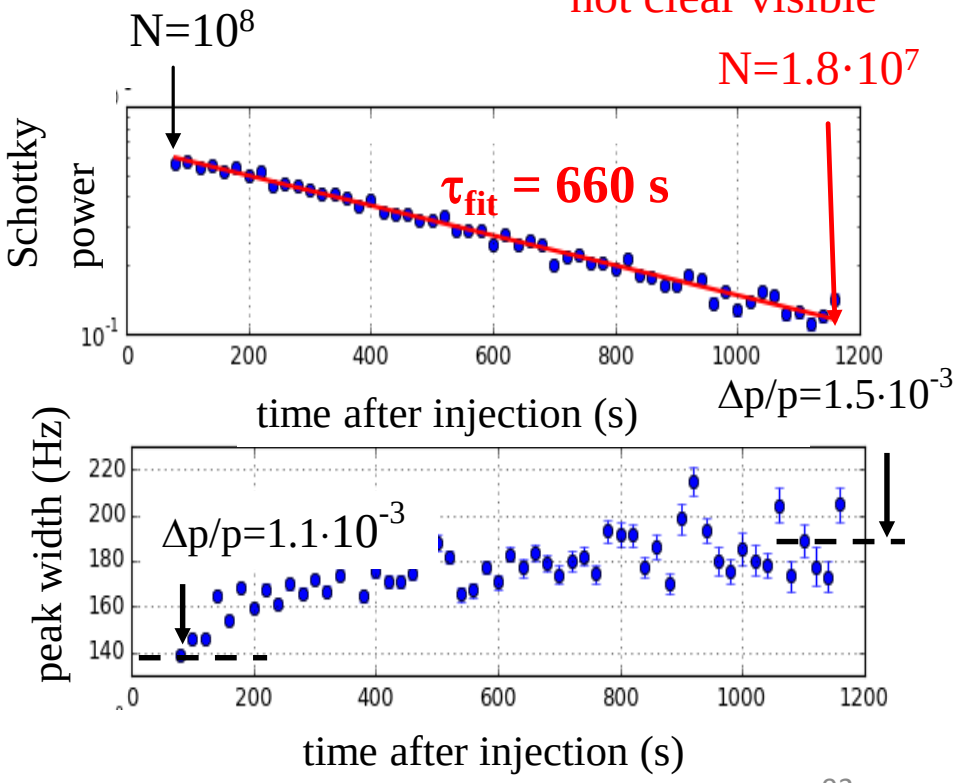

Some thoughts about the pick-up length L

consider pick-up with capacity C

one single ion will produce a voltage during one passage

in our simple model

$$I_c(t) = \begin{cases} Q\,\delta(t - t_0) & t \le t_0 \\ -Q\,\delta(t - (t_0 + \Delta t)) & t > t_0 \end{cases}$$

$$U(t) = \frac{\int_{t_0}^{t_0+t} I(t')\,dt'}{C}$$

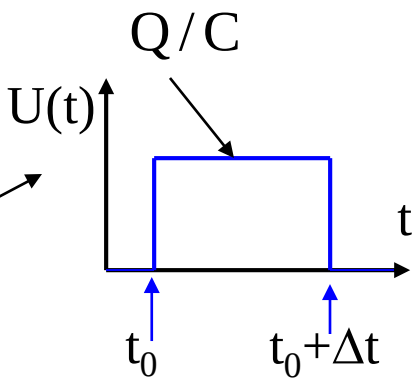

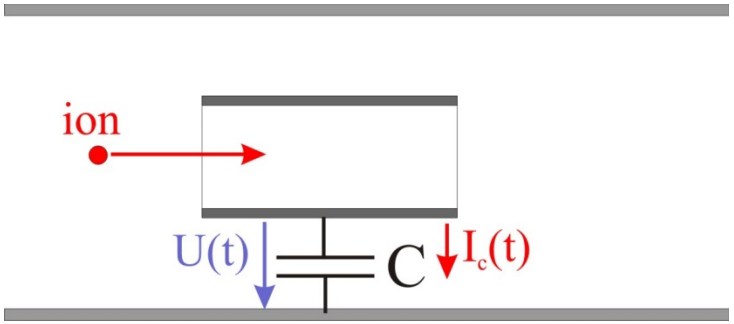

---

induced charge distribution Λ(s)

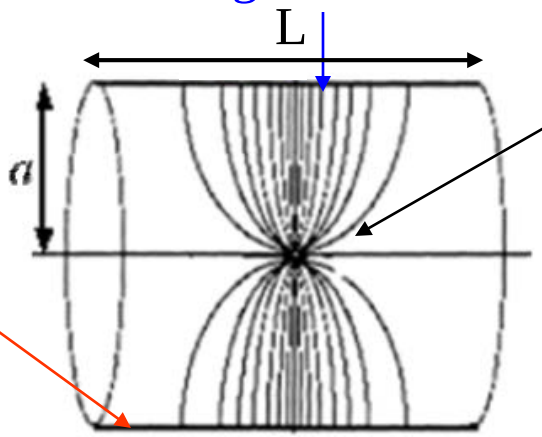

ion with charge Q

tube

Electrical field lines from a point charge

σ_{rms} -RMS value of Λ(s)

$$\sigma_{rms} = \frac{a}{\gamma\sqrt{2}}$$

a ← radius of the tube

γ -relativistic γ

CSR: γ=1

If $L >> \sigma_{rms}$

induced charge on the outside of the cylinder

$$Q = \int_{-L/2}^{L/2} \Lambda(s)\cdot ds \quad \Rightarrow U = Q/C$$

voltage rise time: $t_{rise} \approx \frac{\sigma_{rms}}{v}$ ← ion velocity

CSR: a=5 cm $L \ge 6\cdot\sigma_{rms} \approx$ 20 cm better $L \approx 35$ cm $\Leftrightarrow L/C_0 = 0.01$

ECOOL

CSR electron cooler – Design

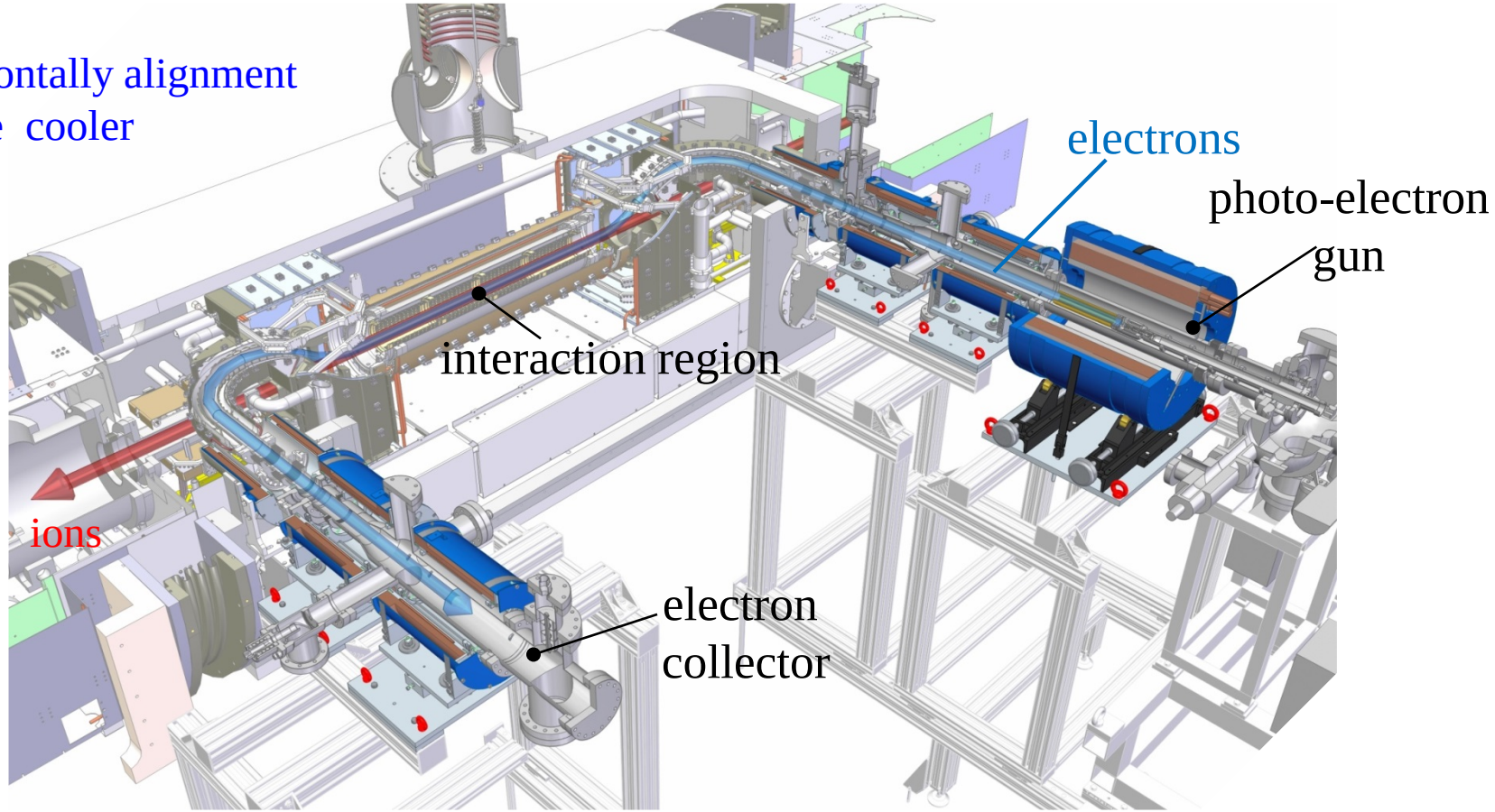

Merging and interaction sections of the electron cooler

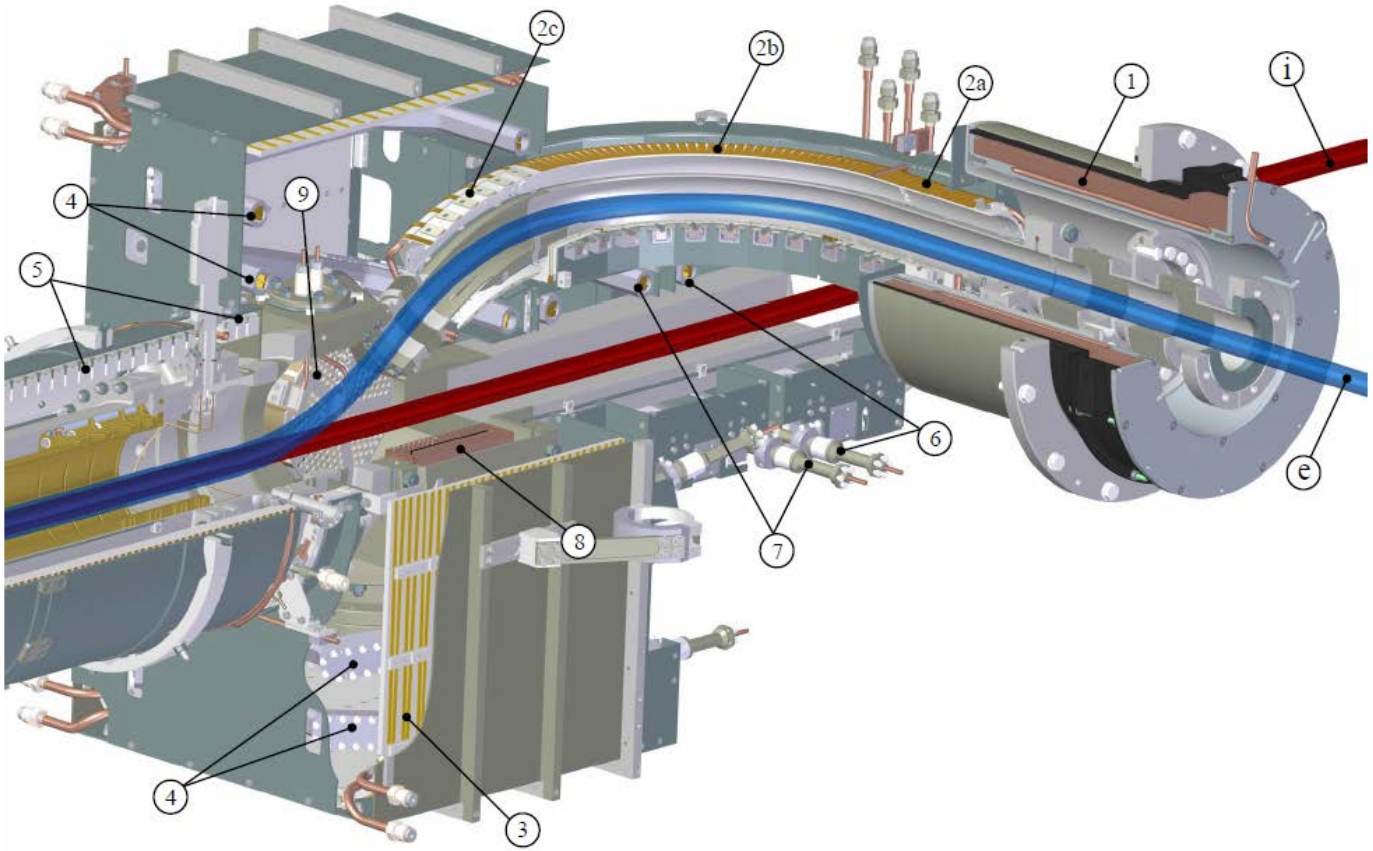

Figure 4.8: Mechanical design of the electron and ion beam merging section with the (e) electron and (i) ion beam, (1) the last low-field guiding magnet, the toroid, consisting of (2a) a solenoidal extension, (2b) the horizontal 90° bend, and (2c) a vertical 30° bending, (3) the longitudinal merging solenoid, (4) four vertical merging coils, (5) the interaction solenoid, (6-7) two pairs of ion beam compensation coils, (8) a charcoal cryopump, and (9) a NEG-pump.

Electron and ion beam Interaction Section

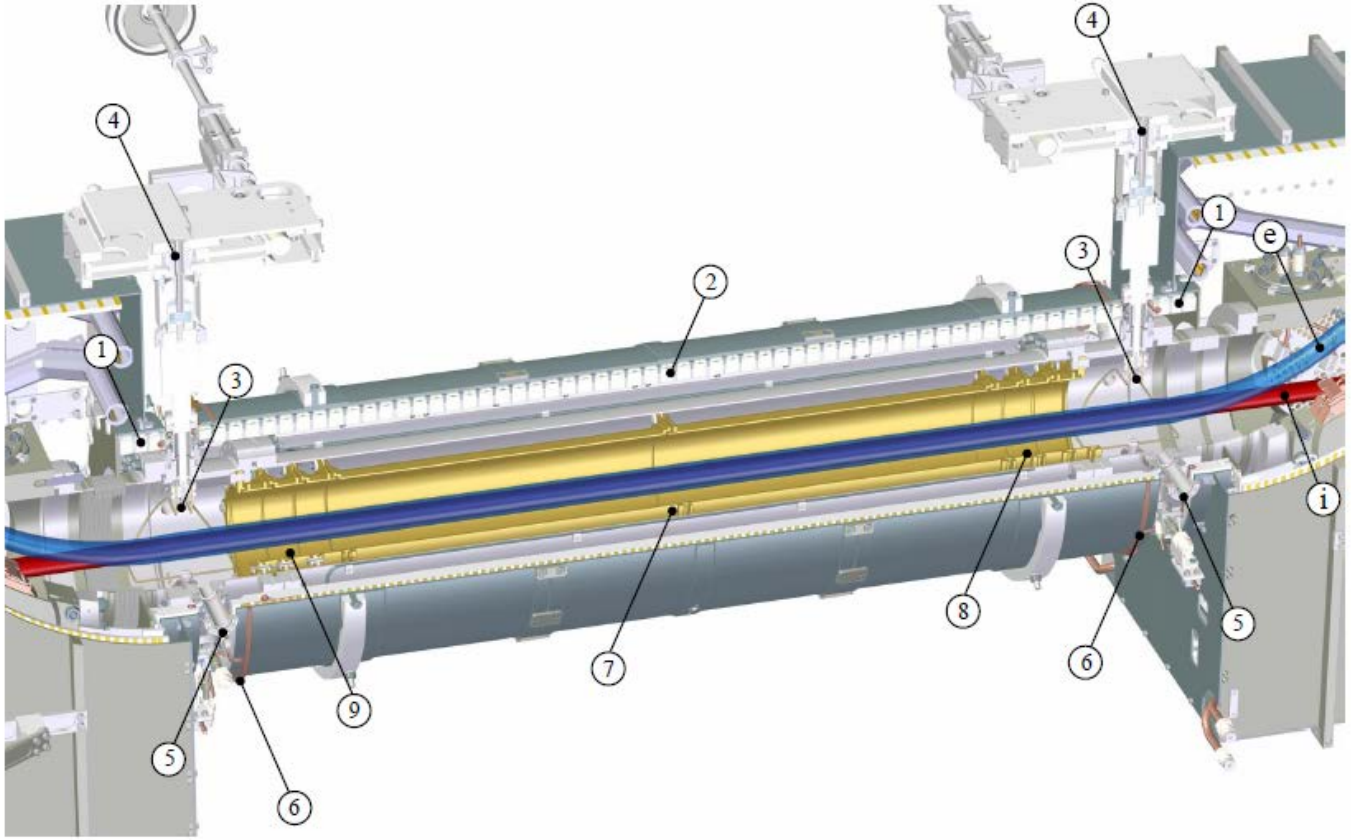

Figure 4.9: Mechanical design of the electron and ion beam interaction section with the (e) electron and (i) ion beam, the interaction solenoid, which is split in (1) two 47 mm and (2) one 944 mm long parts, providing two 34 mm wide gaps for electrical feedthroughs, (3) two wire scanners with (4) their rotational stages, and (5) two crossed laser beam viewports, (6) the transverse steering coils, and (7-9) drift tube consisting of different electrodes.

Acceptance Calculations with TOSCA

Determination of the dynamic acceptance

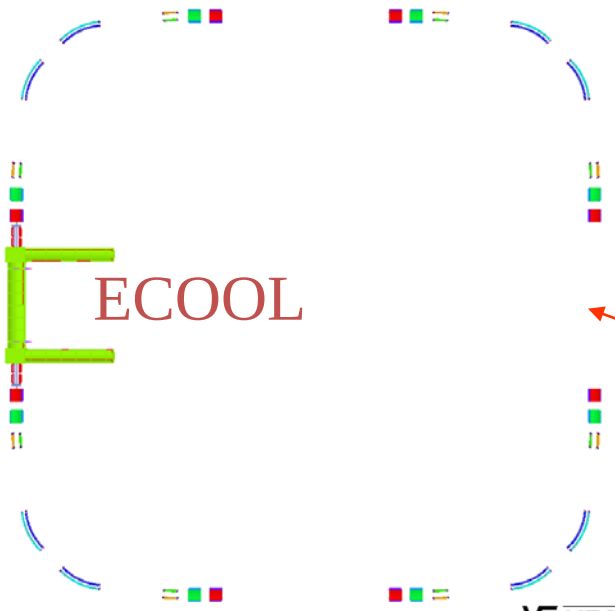

the hole storage ring was
modeled with TOSCA
orbit calculation with real fields
for several hundreds turns

starting point

calculation were done
with and without ECOOL

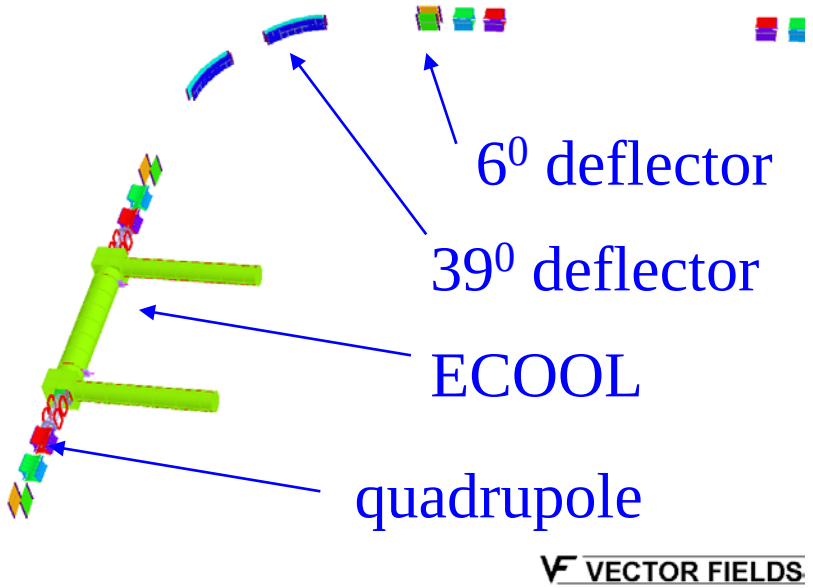

Horizontal Acceptance of the CSR (p 300 keV)

ECOOL OFF

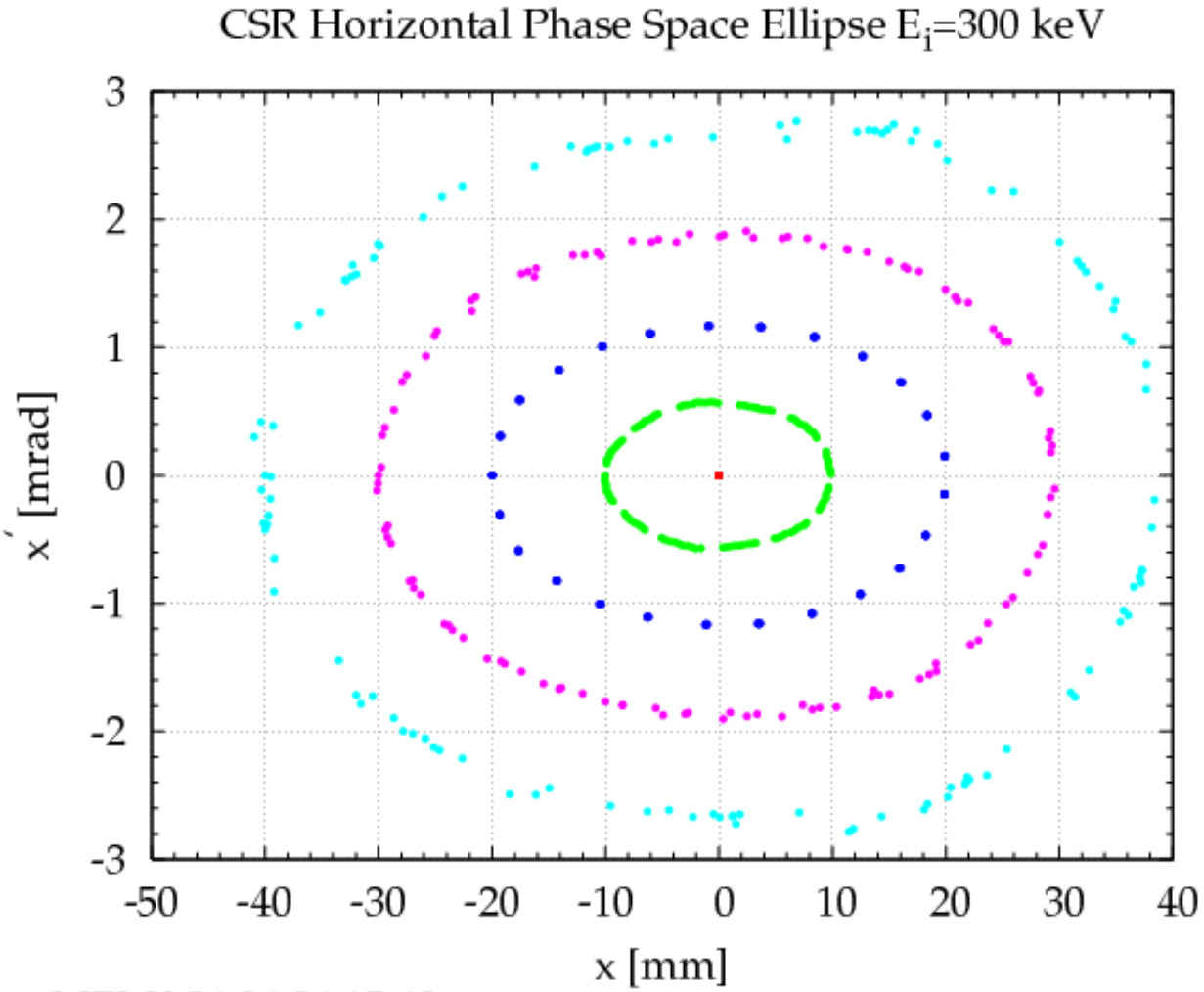

X_i=0
X_i=10
X_i=20
X_i=30
X_i=40

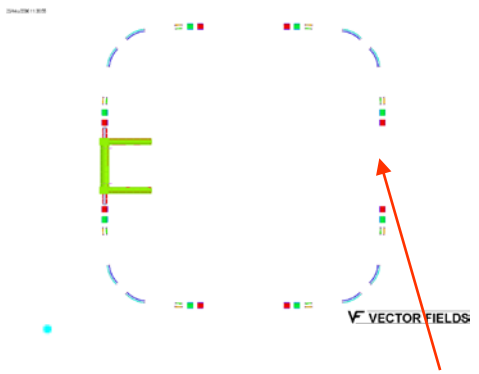

starting point

Maximum Beam Size in the center of the straight section

$$|x|_{max} \approx 4\text{cm}$$

ions lost for x>4 cm
reason: property of the quadrupole

Horizontal acceptance and quadrupole gradient

Orbit calculations with real fields: ion lost for x>4cm

gradient G(x) deviation in quadrupole

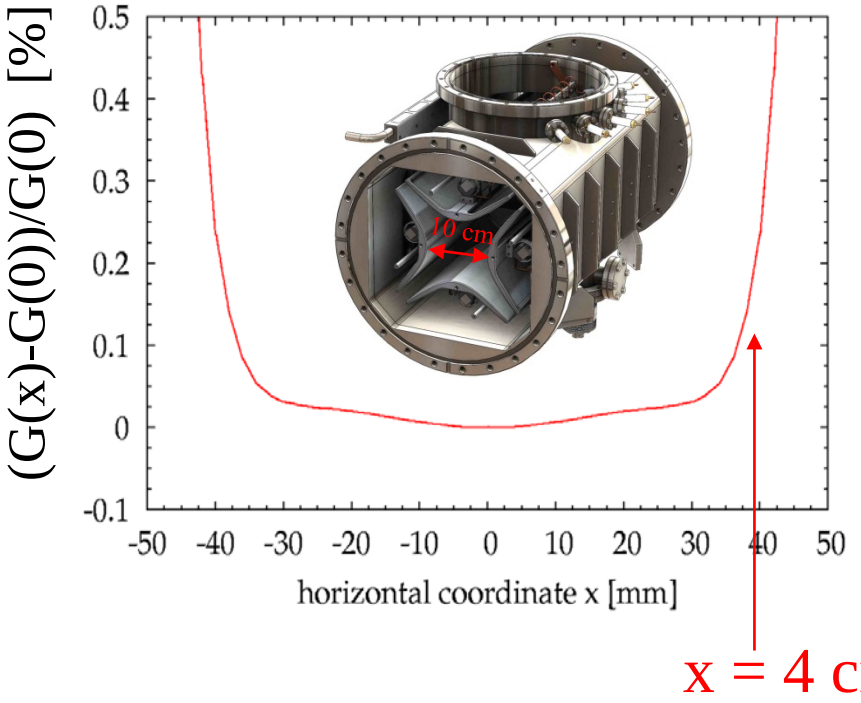

observation point

quadrupole

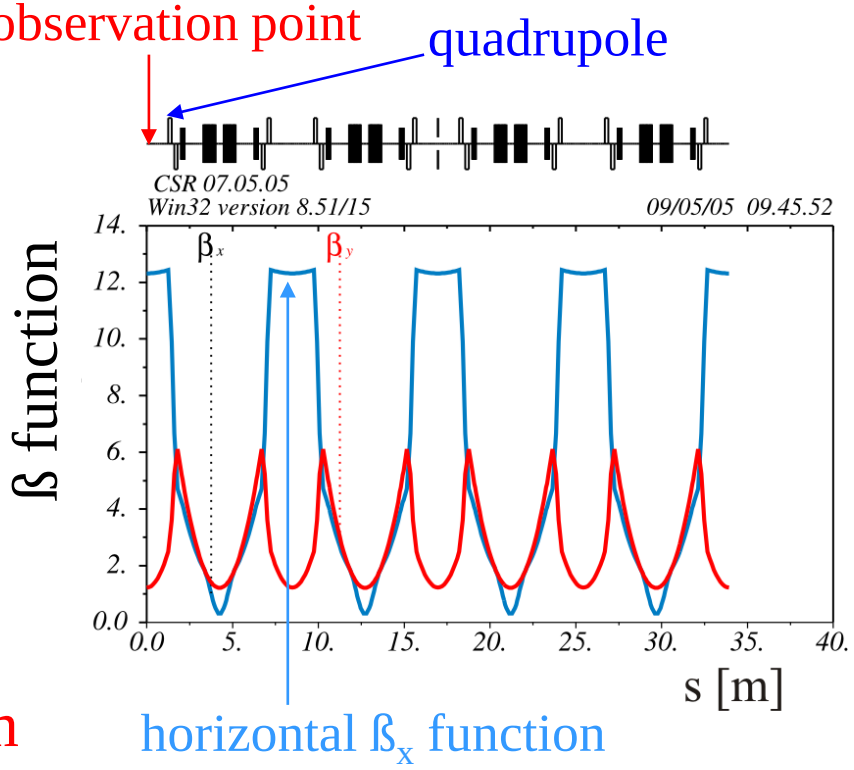

horizontal $ß_x$ function

if x reaches 4 cm ions see a dramatically change of the quadrupole gradient
⇒ tune change ⇒ ions lost due to resonances

horizontal beam size
centre straight section
≈ beam size in quadrupole

Acceptance of the CSR (p 300 keV)

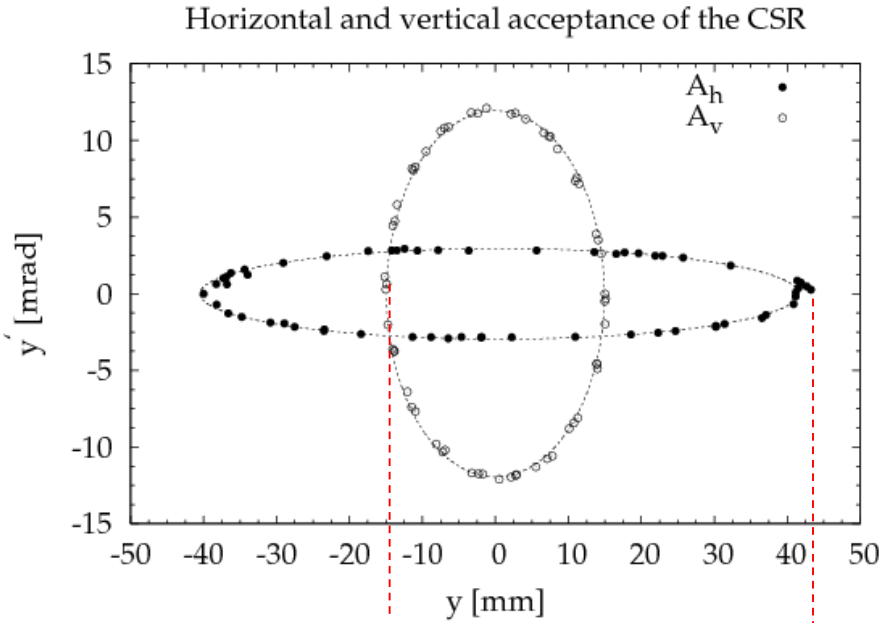

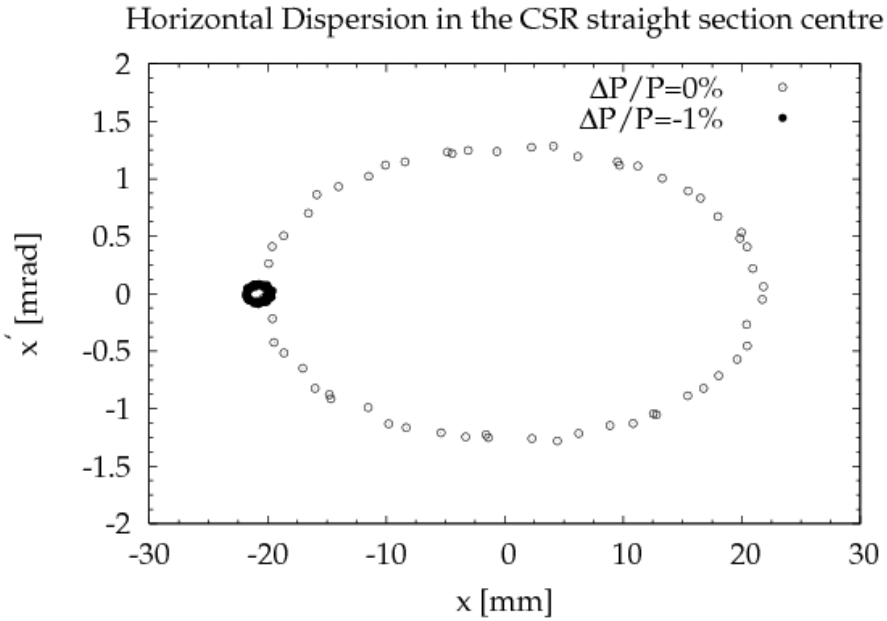

±15mm

±40mm

Lattice	Linear	Realistic	
Horizontal β function	12.3	12.1	m
Vertical β function	1.2	1.3	m
Dispersion	2.1	2.1	m
Acceptance horizontal	–	120	$mm \cdot mrad$
Acceptance vertical	–	180	$mm \cdot mrad$

MAD8 calculations

Tosca

Calculation done without ECOOL

First design of the electron cooler

first design of the electron cooler at CSR

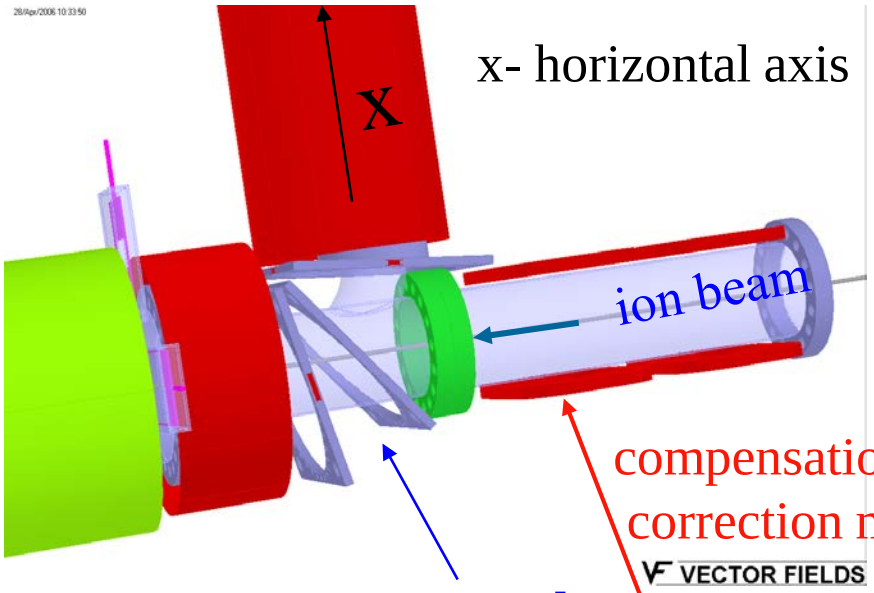

vertical ion deflection
in the toroid fields

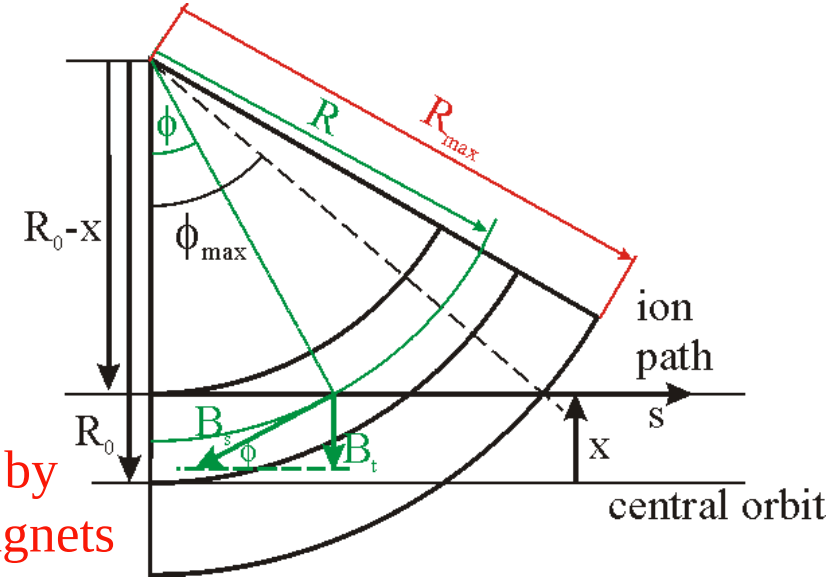

vertical deflection $\delta(x) = \delta(0) - \frac{B_0}{(B\cdot\rho)}\frac{R_0}{R_{max}}\tan\left(\frac{R_0}{R_{max}}\right)\cdot x + ...$

result tracking calculations 20 keV protons can not stored at 30 G ,only on axis ions stored at 10 G

$\Rightarrow$ new electron cooler concept

New Concept for the CSR Electron Cooler/Target

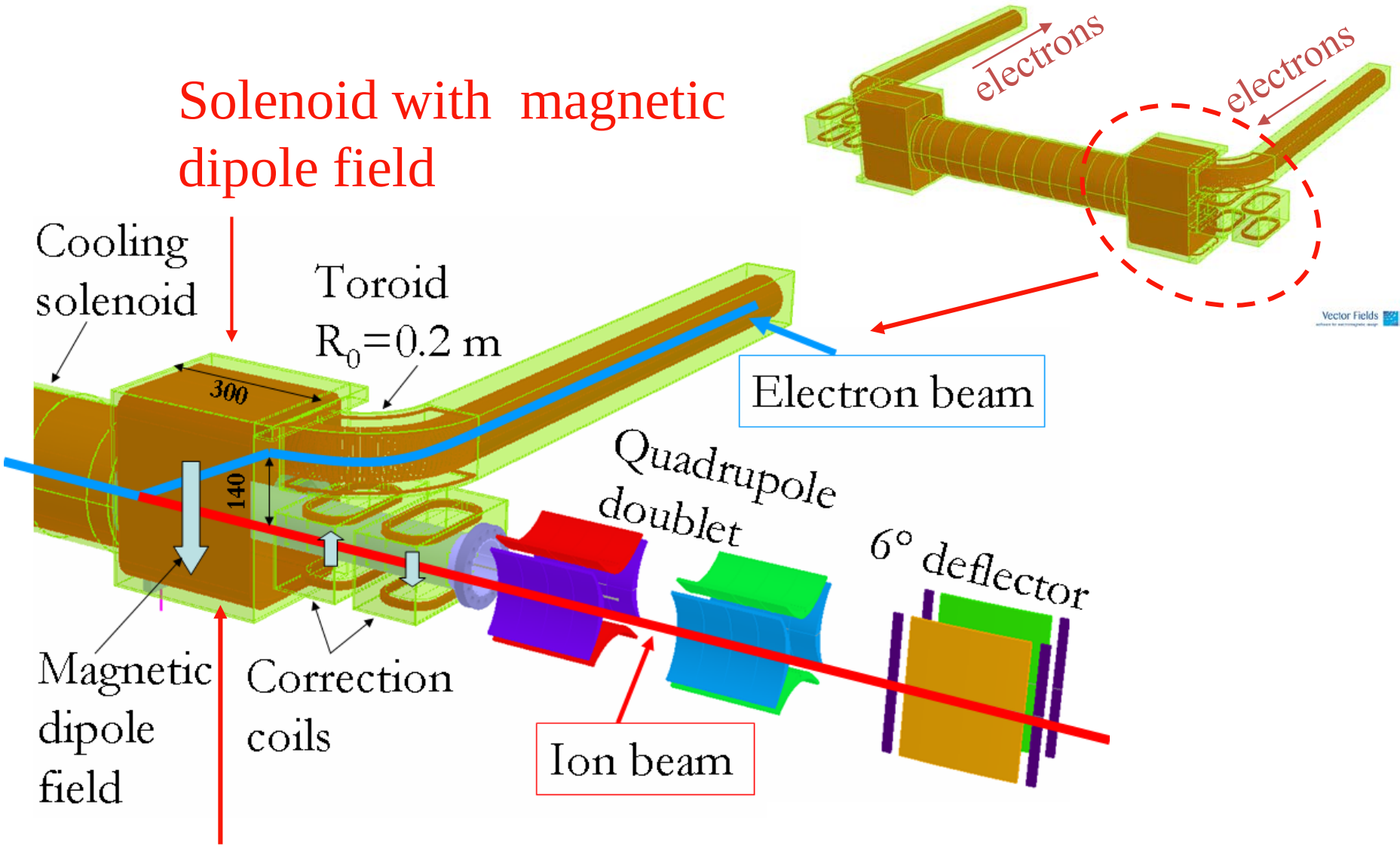

The deflection of low energy ions in the dipole magnetic field can be corrected completely by correction cools.

Ion motion of 20 keV proton with ECOOL

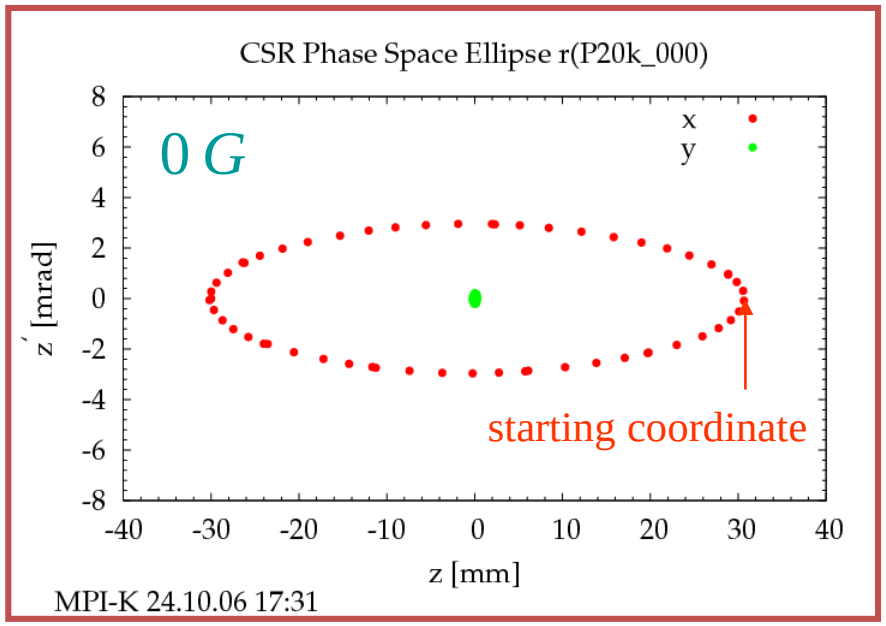

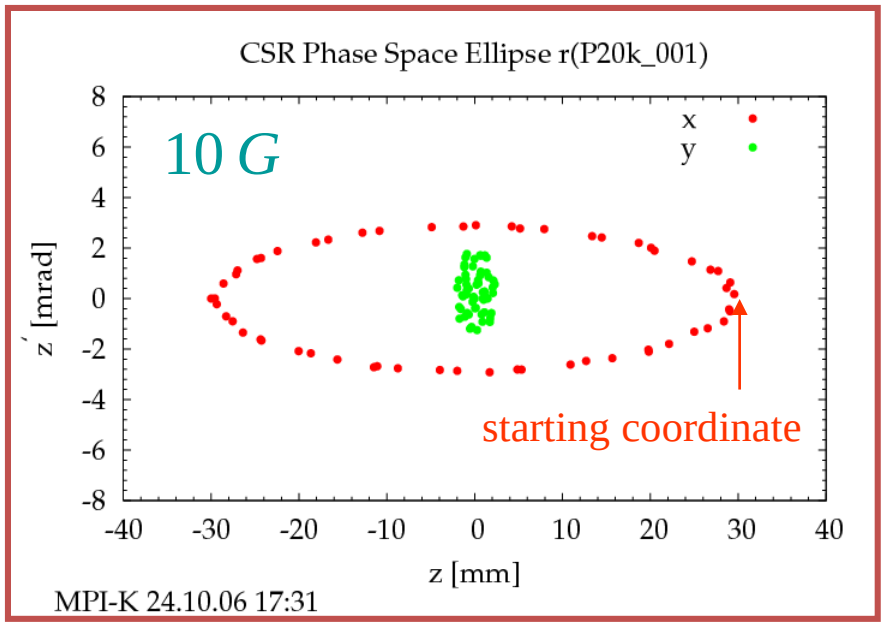

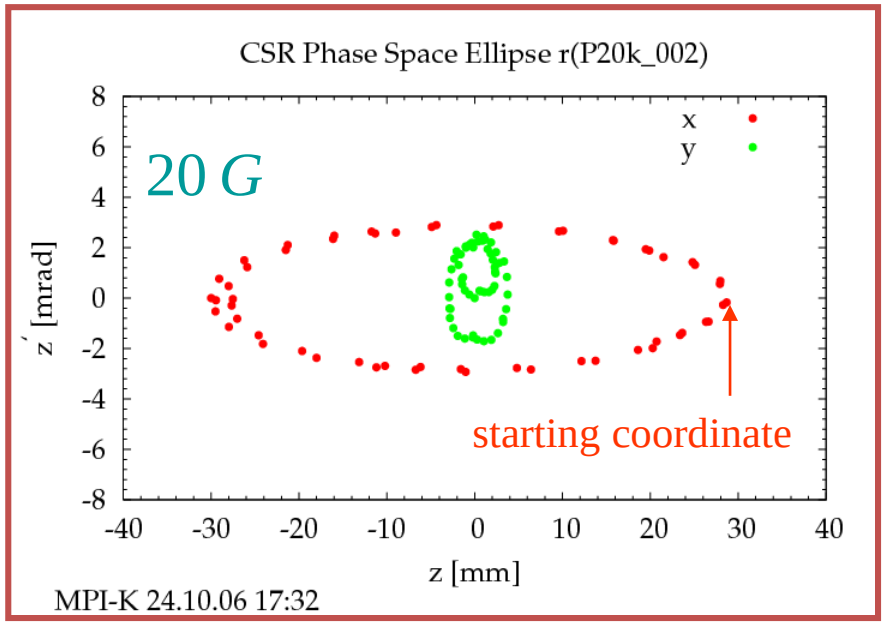

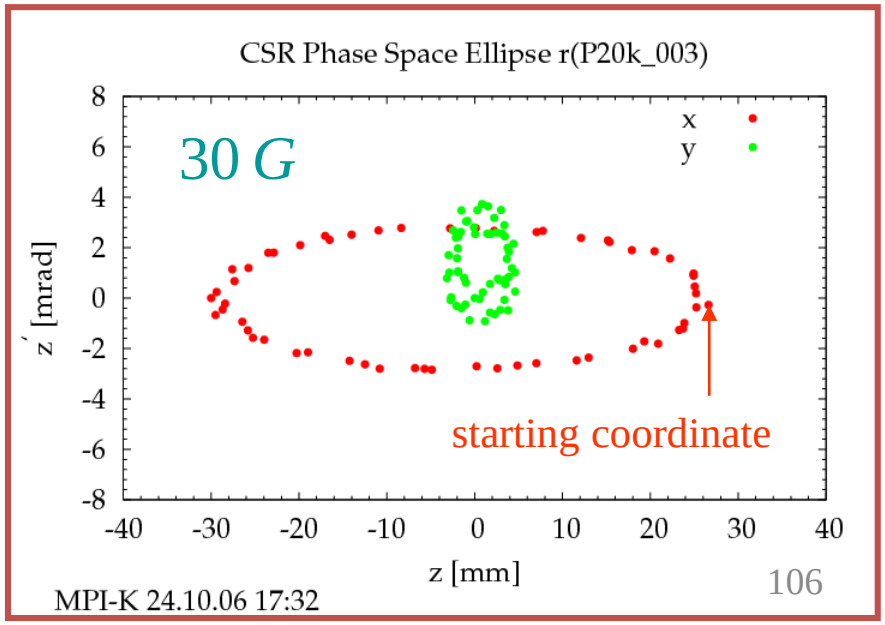

influence of magnetic field of the earth

Influence of the magnetic field of the earth

Horizontal phase space at the center of the injection straight section calculated for **protons** and x_{start}=-15 mm

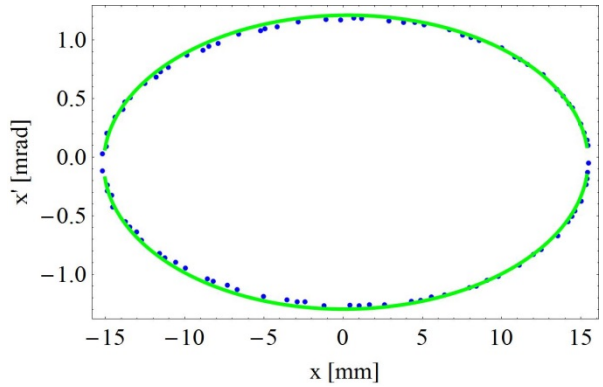

without earth magnetic field
E=300 keV
Δx_s= 0.172 mm $\Delta x_s'$= -0.04 mrad

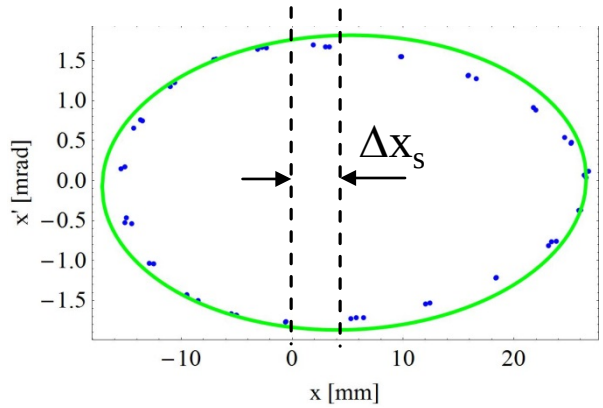

with earth magnetic field
E= 300 keV
Δx_s=4.69 mm $\Delta x_s'$=-0.025 mrad

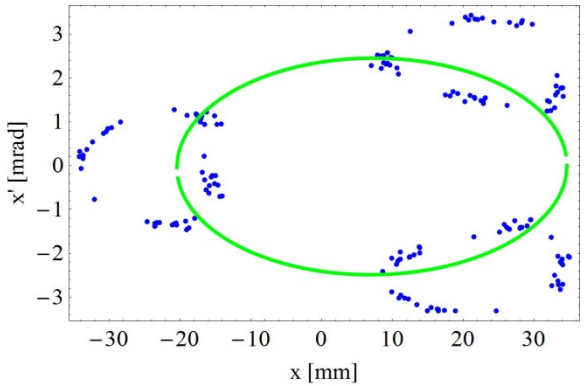

with earth magnetic field
E= 100 keV
Δx_s=7.11 mm $\Delta x_s'$= -0.019 mrad

Influence of the magnetic field of the earth II

Horizontal phase space at the center of the injection straight section
Calculated for proton and x_{start}=-15 mm

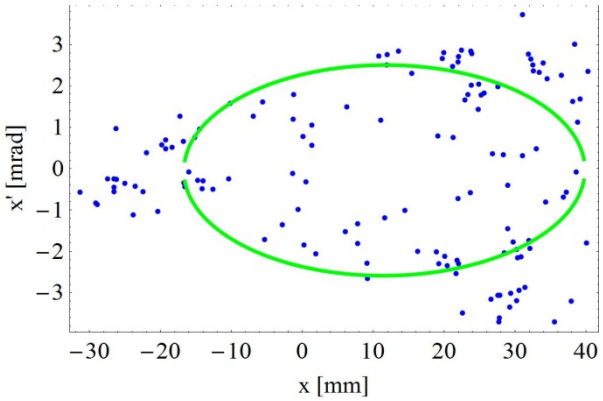

with earth magnetic field
E= 50 keV
Δx_s= 11.55 mm $\Delta x_s'$= -0.158 mrad

beam lost !

with earth magnetic field
and proton energy of E= 20 keV

for small proton energies (E<300 keV) proton motion are not linear at the CSR.

Effect of the magnetic field of the earth is more or less negligible
if the proton energy $E_p \geq 0.5$ MeV

Minimum Energy where earth magnet field is neglect able

ion deflection in magnetic field of the earth $\delta = \frac{\int_a^b B_\perp ds}{B\rho}$ ← beam rigidity

transverse magnetic field of the earth

$B\rho = \frac{p}{Q}$ ← ion momentum ← ion charge

Magnetic field of the earth is negligible if: $B\rho > B\rho_{lim}$

⇒ion energy E where magnetic field of the earth is negligible:

$$E > E_p \frac{q^2}{A}$$

E_p-minimum proton energy where earth magnetic field is negligible at the CSR:
$E_p \approx 0.5$ MeV (determined with G4beamline tracking calculations)
A-ion mass
q- ion charge in units of e

For example $^{40}Ar^+$ with E=50 keV is well above the limit and chosen for the first CSR beam times carried out in the year **2014**

First stored ion beam at the CSR

$^{40}Ar^{+}$ with E= 20…100 keV

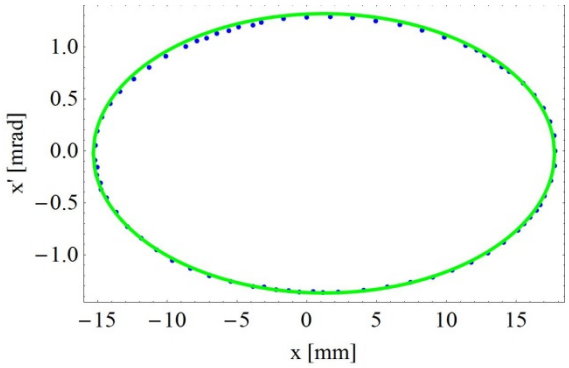

start coordinate: x=-15 mm

with earth magnetic field
E= 100 keV
Δx_s=1.22 mm $\Delta x_s'$= -0.0241 mrad

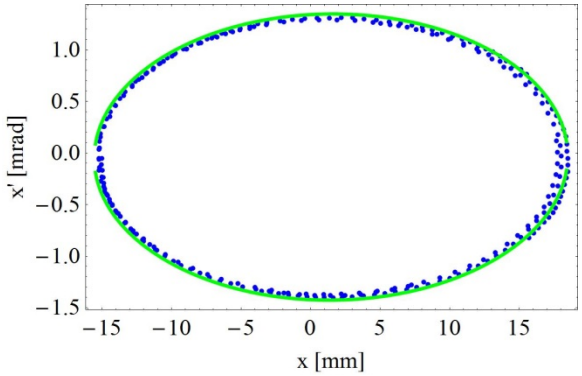

with earth magnetic field
E= 50 keV
Δx_s=1.47 mm $\Delta x_s'$=-0.039 mrad

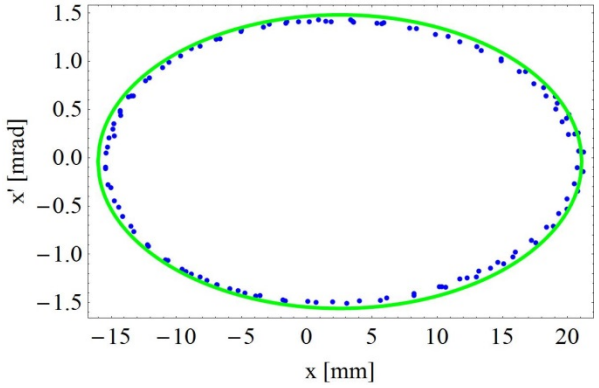

with earth magnetic field
E= 20 keV
Δx_s= 2.53 mm $\Delta x_s'$= -0.04 mrad

Field Calculations with TOSCA

Calculation of the 39^0 deflector with Opera3D/Tosca

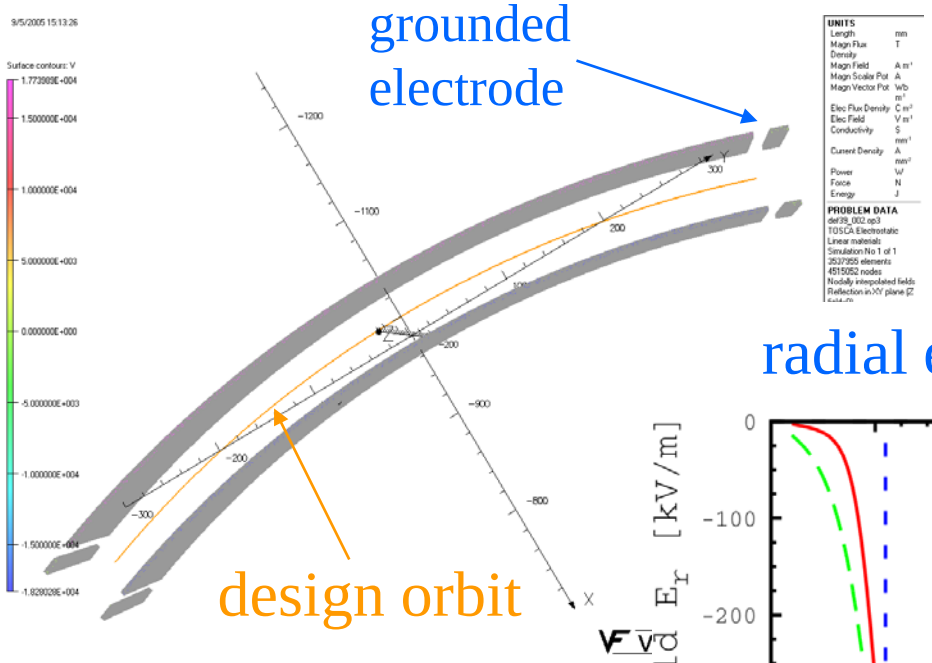

calculation done for
ions with E/Q=300 kV

radial electric E_r field of the 39^0 deflector

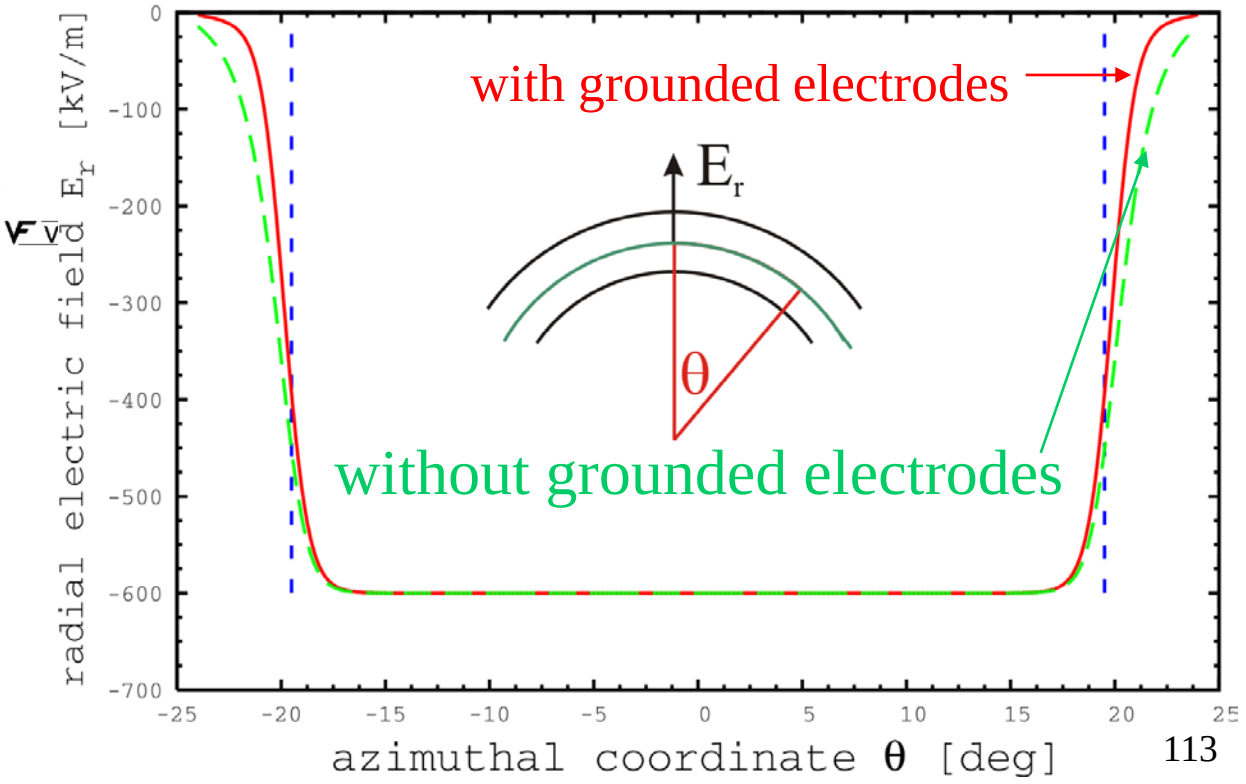

$\theta = 39^0$
r =1m
gap = 6 cm
height =16 cm

Determination of the deflection angle of 39^0 deflector

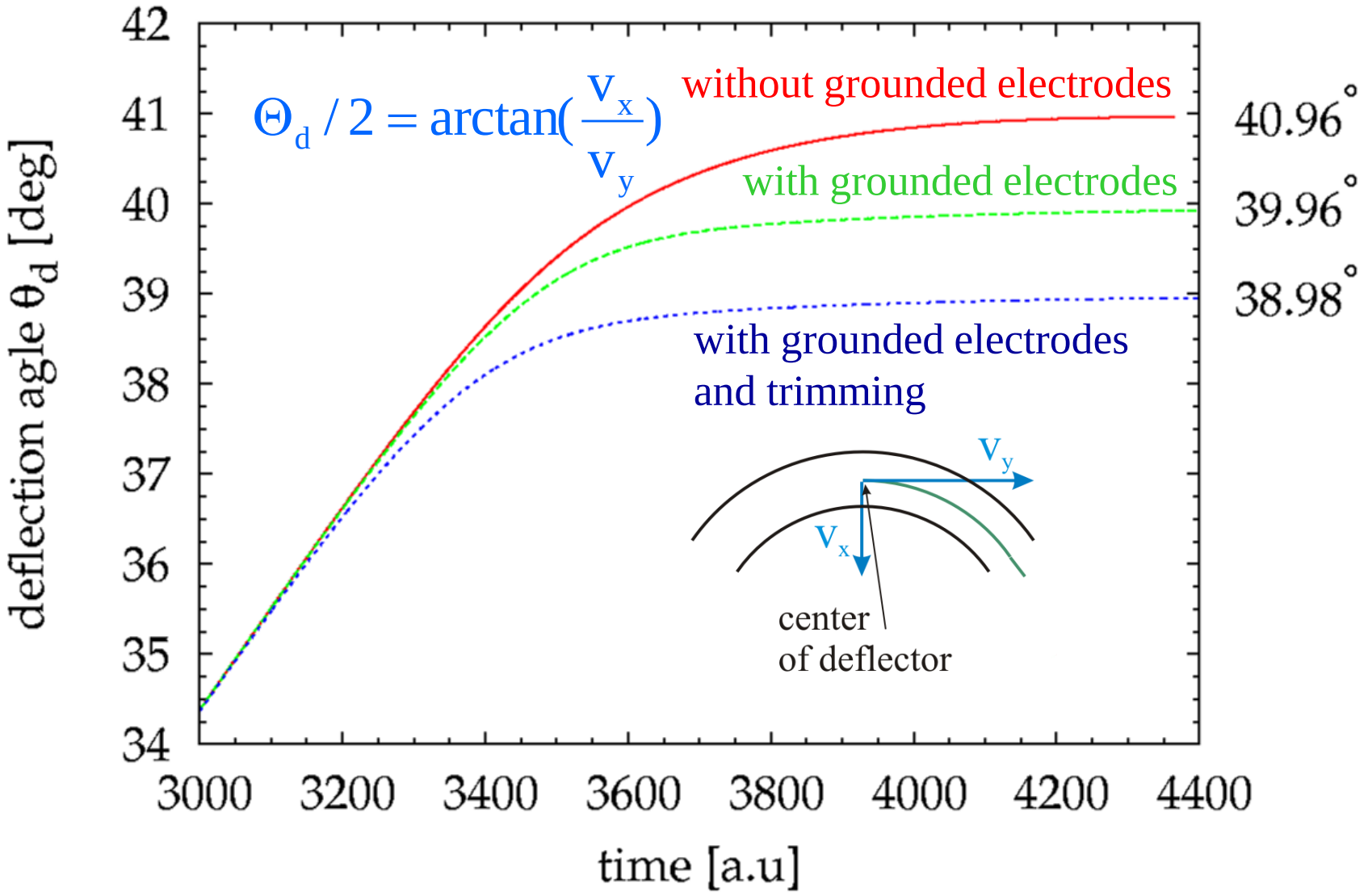

Radial electrical field E_r of the 39^0 CSR deflector

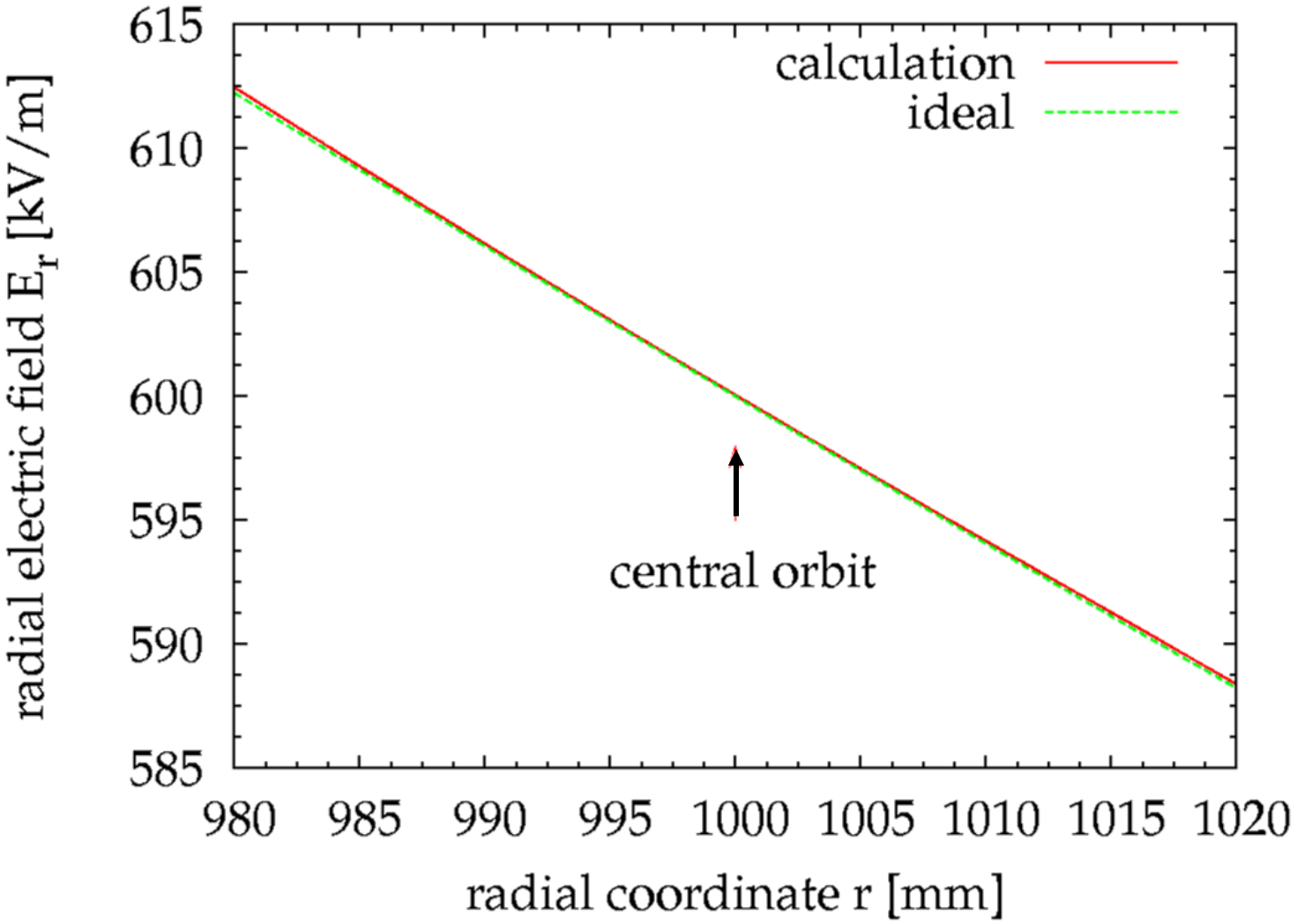

Radial electrical field E_r of the 6^0 CSR deflector

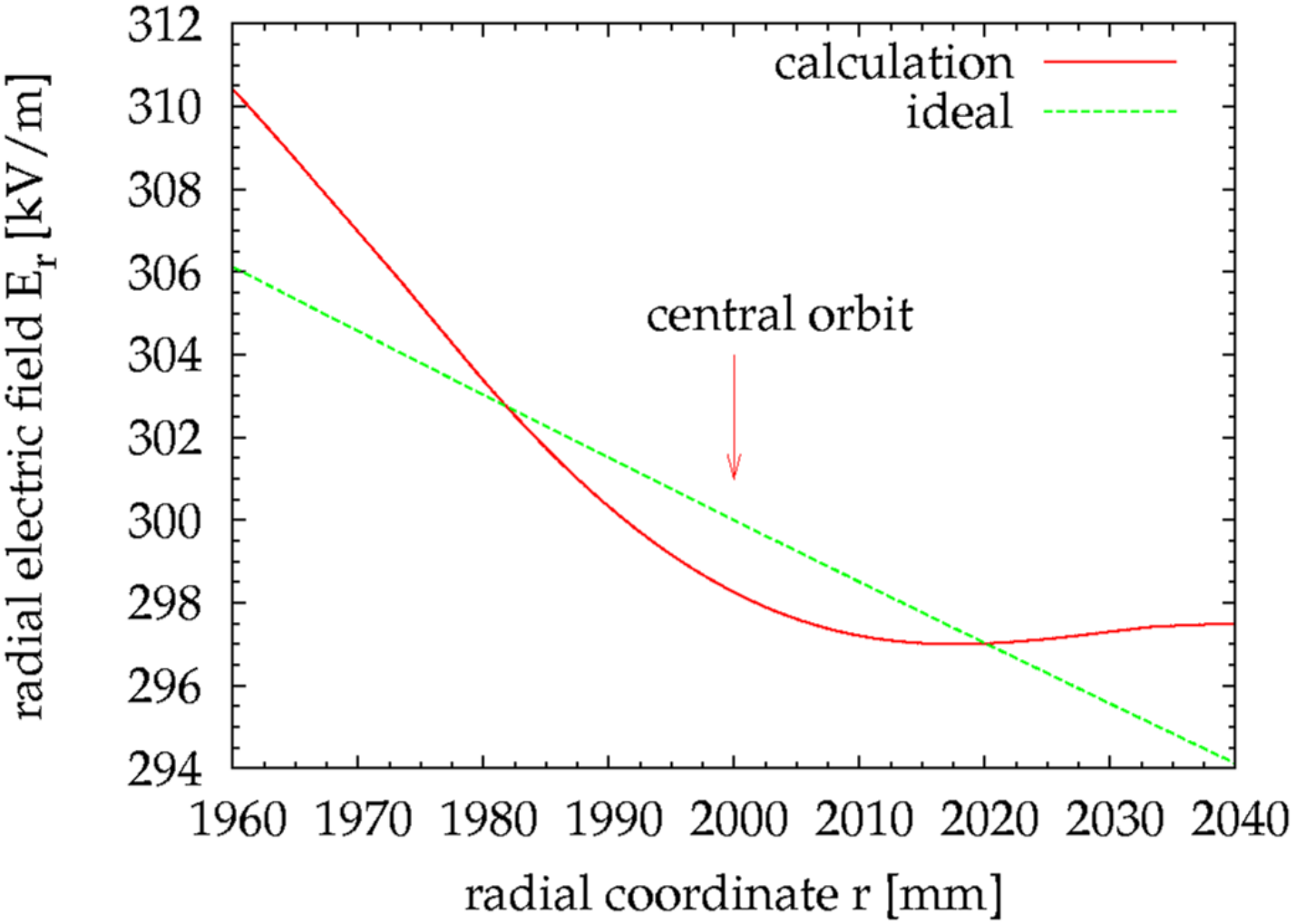

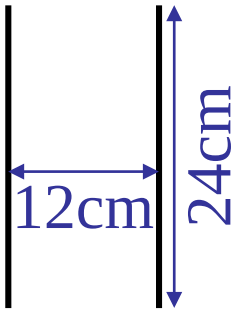

ρ =2 m

Matching

Matching

matched horizontal phase space
at center injection straight section

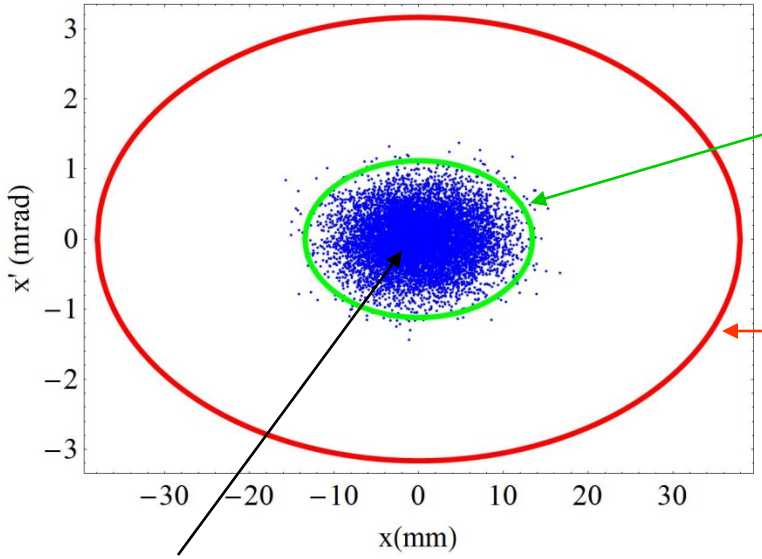

horizontal phase space of injector beam
ε_x=15 mm·mrad

"closed orbit"
in transverse
phase space

horizontal
acceptance
$A_x(\varepsilon_y \to 0)$

vertical
acceptance
$A_y(\varepsilon_x \to 0)$

matched vertical phase space
at center injection straight section

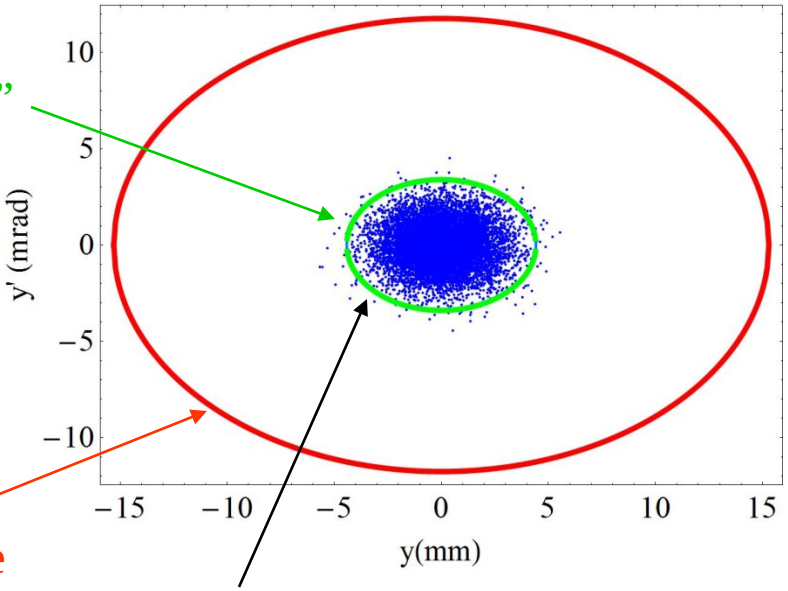

vertical phase space of injector beam
ε_y=15 mm·mrad

matching condition:

$$\alpha_{x,i} = \alpha_{x,CSR}$$

$$\alpha_{y,i} = \alpha_{y,CSR}$$

$$\beta_{x,i} = \beta_{x,CSR}$$

$$\beta_{y,i} = \beta_{y,CSR}$$

injector beam →

← CSR TWISS parameter
at the center of straight section
for injection

remark: no dispersion matching is done

Mismatching

horizontal phase space direct after injection at center of injection straight section

phase space of the injected particle starts to rotate with double betatron frequency

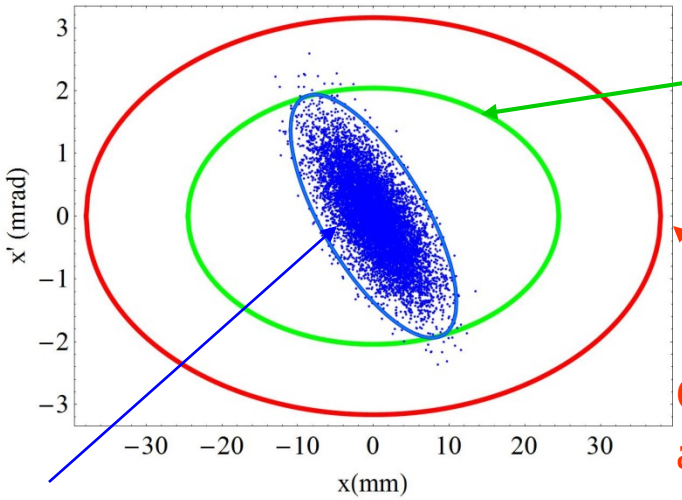

"closed orbit" in transverse phase space

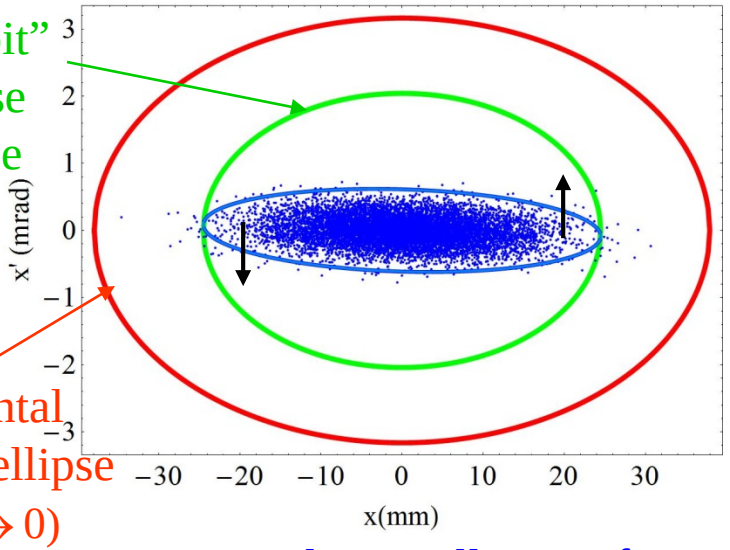

phase space injector beam
ε_x=15 mm·mrad

CSR horizontal acceptance ellipse
$A_x(\varepsilon_y \to 0)$

envelop oscillation of injected ion beam

due to non linearity's horizontal phase space blow up

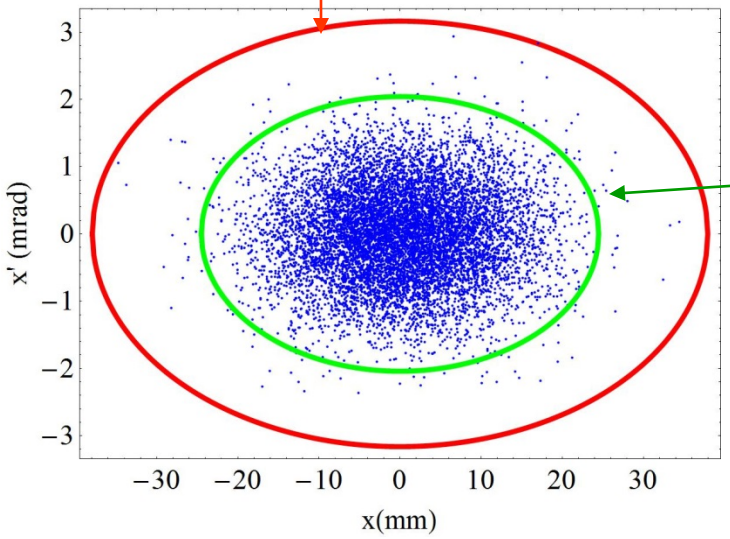

"closed orbit" in transverse phase space
ε_x=50 mm·mrad

First turn diagnose

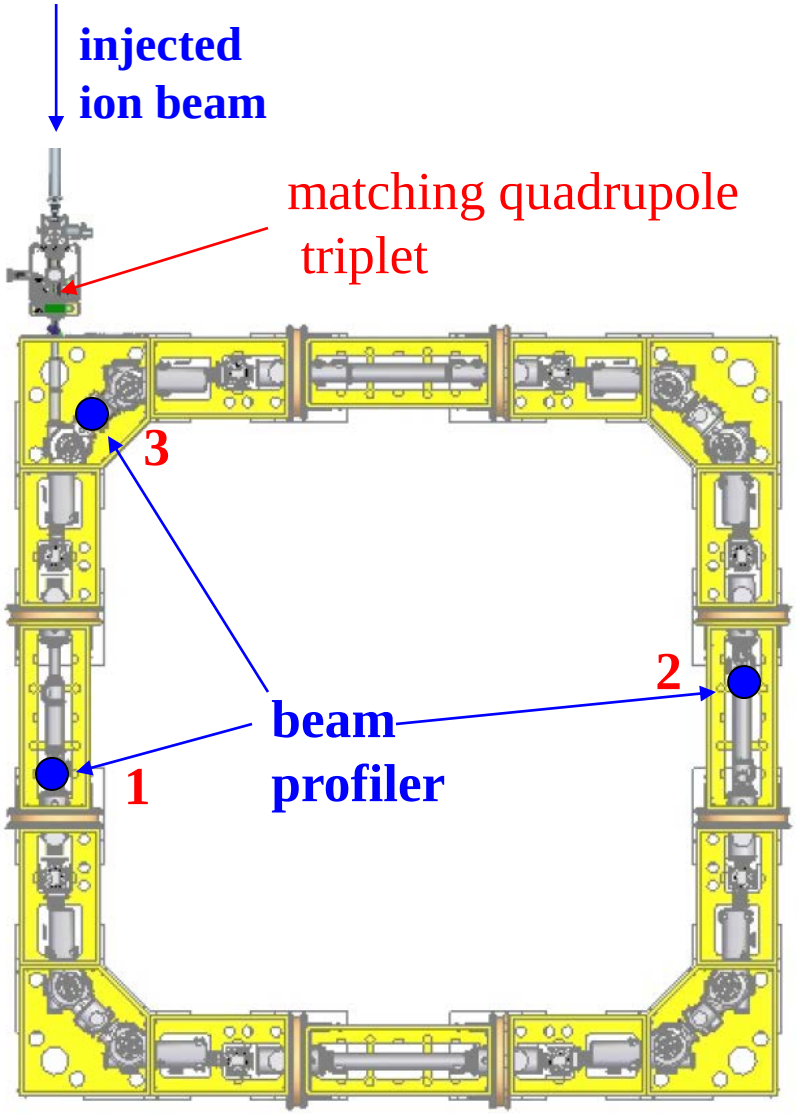

beam profile

-used to detect the beam on its first turn

-used to check the matching condition with profiler 1 and 2:

horizontal and vertical beam width at position 1 and 2 should be equal.

ß function of CSR

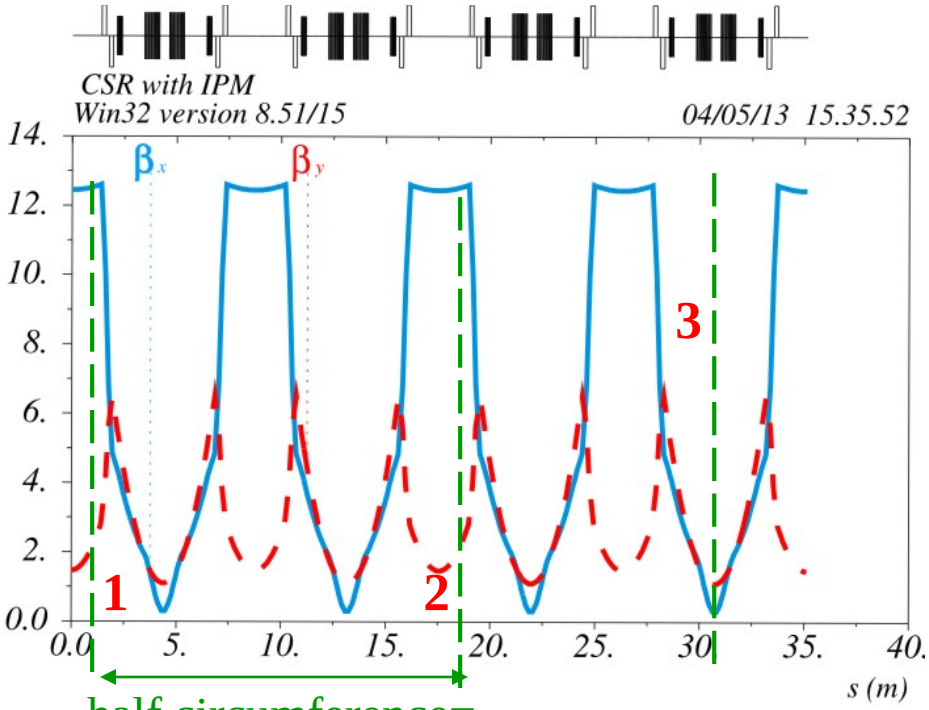

half circumference=
distance between profiler 1 and 2

Slip factor η and momentum compaction α_p

Slip factor η of an momentum compaction α_p of an electrostatic storage ring

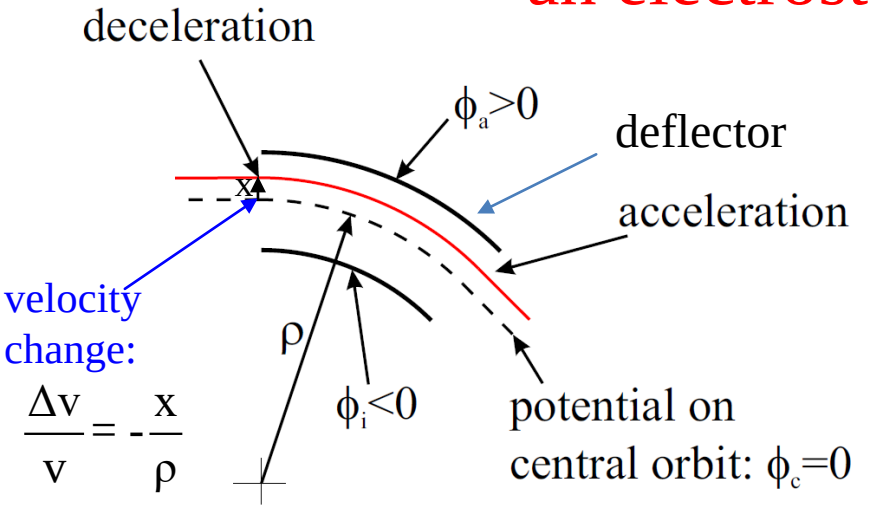

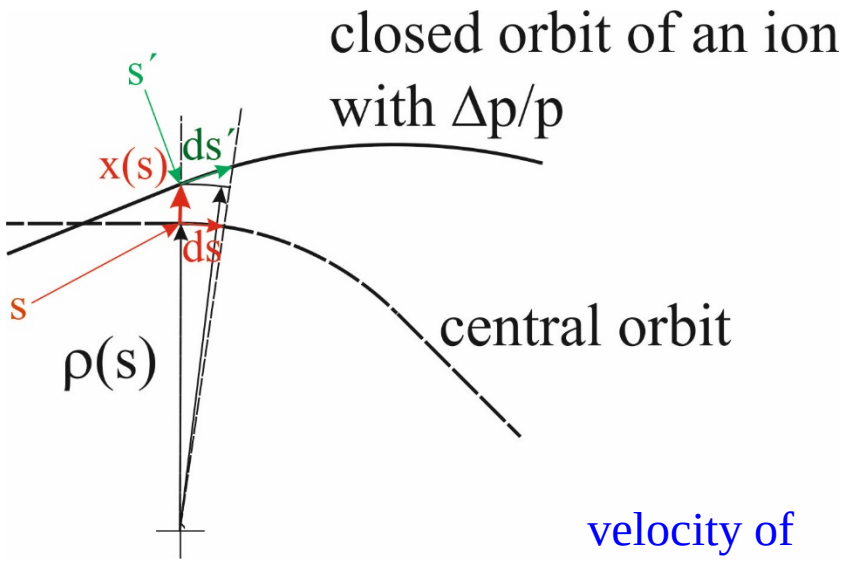

Revolution time T=1/f

$$T = \int_0^{C(E)} \frac{ds'}{v(s')}$$ with $$ds' = \left(1+\frac{x(s)}{\rho(s)}\right)ds$$ and $$v(s') = \left(1-\frac{x(s)}{\rho(s)}\right)v_0$$

position of closed orbit

velocity of central particle

slip factor η non relativistic case (first order):

$$\eta = \frac{\Delta f / f}{\Delta p / p} = 1 - 2\alpha_p$$ with $$\alpha_p = \frac{\Delta C / C}{\Delta p / p}$$

different to a magnetic storage ring

8th International Particle Accelerator Conference
IOP Conf. Series: Journal of Physics: Conf. Series **874** (2017) 012049

Closed orbit shift by electrical potential scaling

equation of motion

$$m\frac{d^2\vec{r}(t)}{dt^2}=Q\vec{E}(\vec{r}(t))$$

With $\vec{E}(\vec{r}(t))=-\nabla\phi(\vec{r}(t))$ and $v(t)=\frac{ds}{dt}$

$$\frac{m}{2}\frac{dv^2(s)}{ds}\frac{d\vec{r}(s)}{ds}+mv^2(s)\frac{d^2\vec{r}(s)}{dt^2}=-Q\nabla\phi(\vec{r}(s))$$

with $v^2(s)=\frac{2}{m}\left(E-Q\phi(\vec{r}(s))\right)$ (non relativistic approach)

$$\frac{d}{ds}\left(E-Q\phi(\vec{r}(s))\right)\frac{d\vec{r}(s)}{ds}+2\left(E-Q\phi(\vec{r}(s))\right)\frac{d^2\vec{r}(s)}{dt^2}=-Q\nabla\phi(\vec{r}(s))$$

equation of motion for changing ion energy: $E\rightarrow\alpha\cdot E$

$\vec{r}(s)\rightarrow\vec{r}'(s')$

(1)

$$\frac{d}{ds}\left(\frac{\alpha E}{Q}-\phi(\vec{r}'(s'))\right)\frac{d\vec{r}'(s')}{ds}+2\left(\frac{\alpha E}{Q}-\phi(\vec{r}'(s'))\right)\frac{d^2\vec{r}'(s')}{dt^2}=-\nabla\phi(\vec{r}'(s'))$$

equation of motion for changing potential: $\phi\rightarrow\beta\cdot\phi$

$\vec{r}(s)\rightarrow\vec{r}'(s')$

(2)

$$\frac{d}{ds}\left(\frac{E}{\beta Q}-\phi(\vec{r}'(s'))\right)\frac{d\vec{r}'(s')}{ds}+2\left(\frac{E}{\beta Q}-\phi(\vec{r}'(s'))\right)\frac{d^2\vec{r}'(s')}{dt^2}=-\nabla\phi(\vec{r}'(s'))$$

The two differential equations (1) and (2) are identical for $\vec{r}'(s')$ if:

$$\left(\frac{\alpha E}{Q}-\phi(\vec{r}'(s'))\right)=\left(\frac{E}{\beta Q}-\phi(\vec{r}'(s'))\right)$$

or

$$\alpha=\frac{1}{\beta}$$

This means:

a change of the ion energy by ΔE/E has the same effect on the ion orbit as a change of all potentials by -Δϕ/ϕ

$$-\frac{\Delta\phi}{\phi}=\frac{\Delta E}{E}$$

for same ion orbit

closed orbit length C:

$$\frac{\Delta C}{C}=\begin{cases}\alpha_p\frac{1}{2}\frac{\Delta E}{E}\\ -\alpha_p\frac{1}{2}\frac{\Delta\phi}{\phi}\end{cases}$$

Measurement of the momentum compaction α_p

if the ion orbit will change by a potential change $\Delta\phi$ the new revolution time will be:

$$T = \int_0^{C(E)} \frac{ds'}{v(s')} \qquad ds' = \left(1 + \frac{x(s)}{\rho(s)}\right) ds$$

where x(s) is new closed orbit with respect to the central orbit, with:

$$v(s') = \left(1 - \frac{x(s)}{\rho(s)}\right) v_0$$

it follows

$$T = \frac{1}{v_0} \int_0^{C_0} \left(1 + 2\frac{x(s)}{\rho(s)}\right) ds = T_0 \left(1 + 2\frac{\Delta C}{C}\right)$$

because a change of potential by $\Delta\phi/\phi$ has the same effect on the close orbit as an energy change $-\Delta E/E$:

$$\frac{\Delta C}{C} = -\alpha_p \frac{1}{2}\frac{\Delta\phi}{\phi} \quad \Rightarrow \quad T = T_0\left(1 - \alpha_p \frac{\Delta\phi}{\phi}\right)$$

$\Rightarrow$ change of the revolution frequency: $\boxed{\frac{\Delta f}{f_0} = \alpha_p \frac{\Delta\phi}{\phi}}$

<u>experiment:</u>
revolution frequency f is measured as a function of ϕ

$$\Rightarrow \quad \alpha_p = \frac{\Delta f / f}{\Delta\phi / \phi}$$

Measurement of the momentum compaction factor α_p

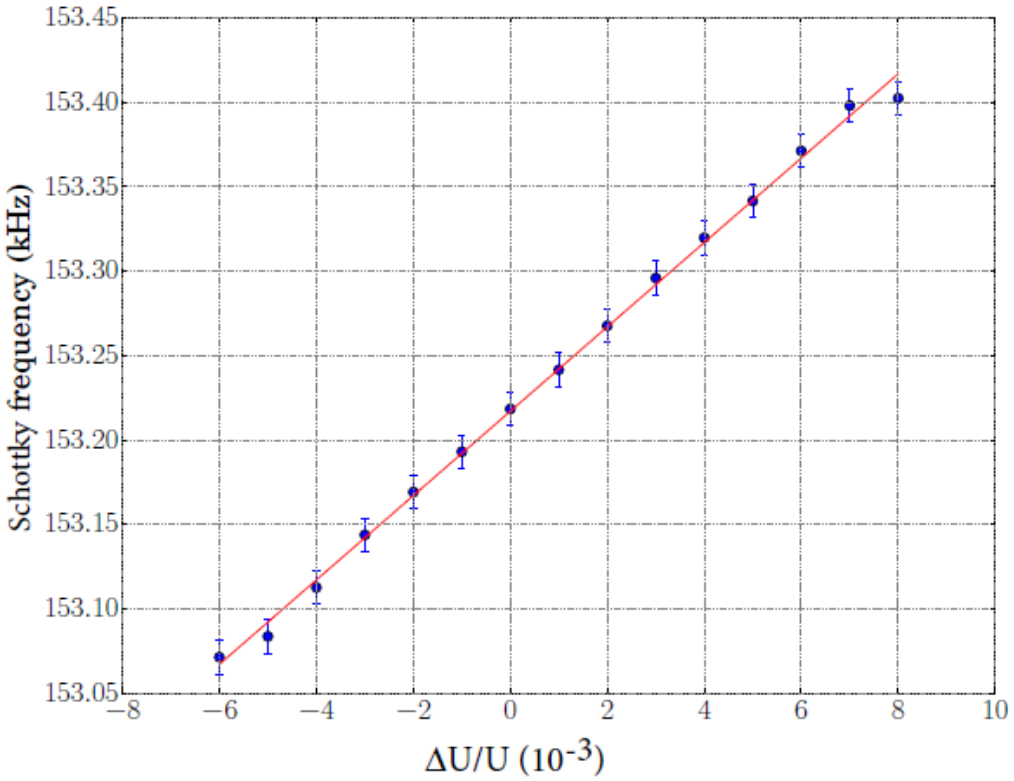

Figure 2. Schottky frequency measured at 10^{th} harmonic of the revolution frequency as a function of the variation of the voltages of all CSR deflectors and quadrupoles expressed by $\Delta U/U_0$.

beam: $^{40}Ar^{+}$ E=60 keV

$$\frac{\Delta f}{f_0} = \alpha_p \frac{\Delta \phi}{\phi}$$

revolution frequency

potential

result:

α_p=0.163

with

$\eta = 1 - 2 \cdot \alpha_p$

η=0.674

$$\frac{\Delta U}{U} = \frac{\Delta \phi}{\phi} \qquad \frac{\Delta f_{Schottky}}{f_{Schottky}} = \frac{\Delta f}{f} \qquad f_{Schottky} = 10 \cdot f$$

All kinds of subjects

Quadrupole strength in MAD8

electrostatic quadrupole

$$k_{mad} = \frac{U}{R_0^2}\frac{Q}{E_0}\frac{L_{eff}}{L_{MAD}}$$

quadrupole strength in MAD8

$$[k_{mad}] = \frac{1}{m^2}$$

U- electrode voltage
E_0-kinetic energy
Q- ion charge
R_0-aperture radius
L_{eff}-effective length ← determined with TOSCA and tune measurement

in first order transport matrix of an electrostatic quadrupole is the transport matrix of an magnetic quadrupole

Space charge limit of a stored ion beam

incoherent tune shift: $N = \frac{A}{q^2}\frac{2\pi}{r_p}\cdot B\cdot\beta^2\cdot\gamma^3\cdot\varepsilon_{2\sigma}\cdot(-\Delta Q)$

maximum possible emittance

$$\varepsilon_{2\sigma} \approx \left(\frac{2}{3}\right)^2 A_c(\varepsilon_x=\varepsilon_y)$$

pessimistic

$$A_c(\varepsilon_x=\varepsilon_y) \approx A_x(\varepsilon_y\to 0)/2$$
$$A_x(\varepsilon_x=\varepsilon_y) \le A_x(\varepsilon_y\to 0)$$

2σ emittance

ΔQ- maximum possible tune shift

acceptance with:

working diagram (S=1)

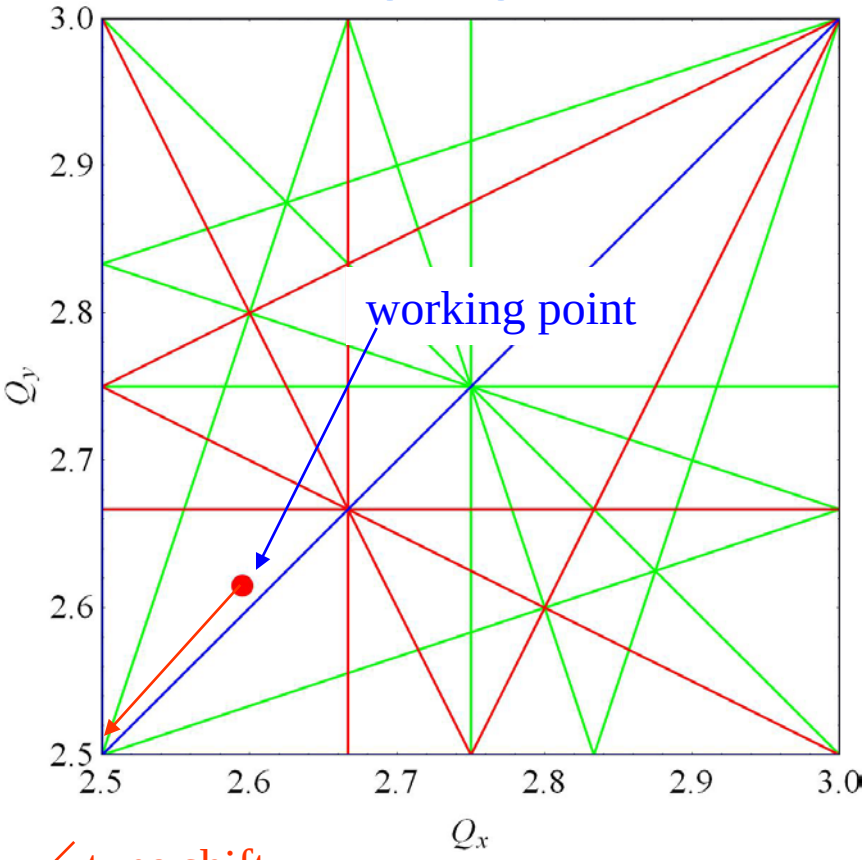

tune shift

calculated for q=1, B=1 and **ΔQ= -0.1**

maximum possible particle number N

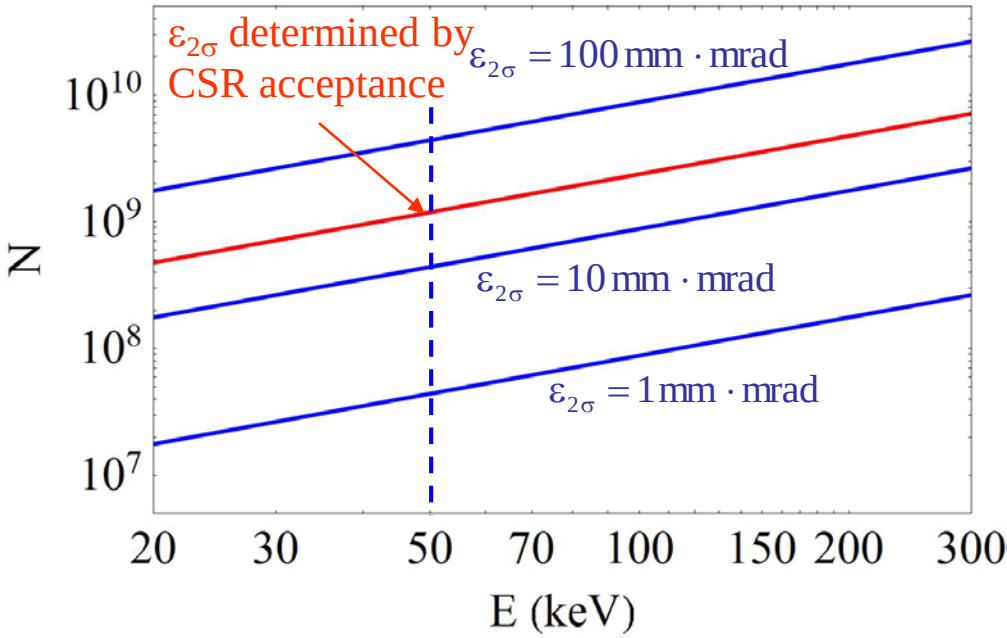

remark: $N\sim A\cdot\beta^2\sim E$ (γ=1) particle number N valid for all single charged ions !

Space charge limit of a cooled stored proton beam

incoherent tune shift: $N = \frac{2\pi}{r_p} \cdot B \cdot \beta^2 \cdot \gamma^3 \cdot \varepsilon \cdot (-\Delta Q)$

TSR: $N=5.3\cdot10^9$ $E=23$ MeV $\varepsilon=0.4$ mm·mrad $B=1$ $\Rightarrow$ **$-\Delta Q=0.065$**

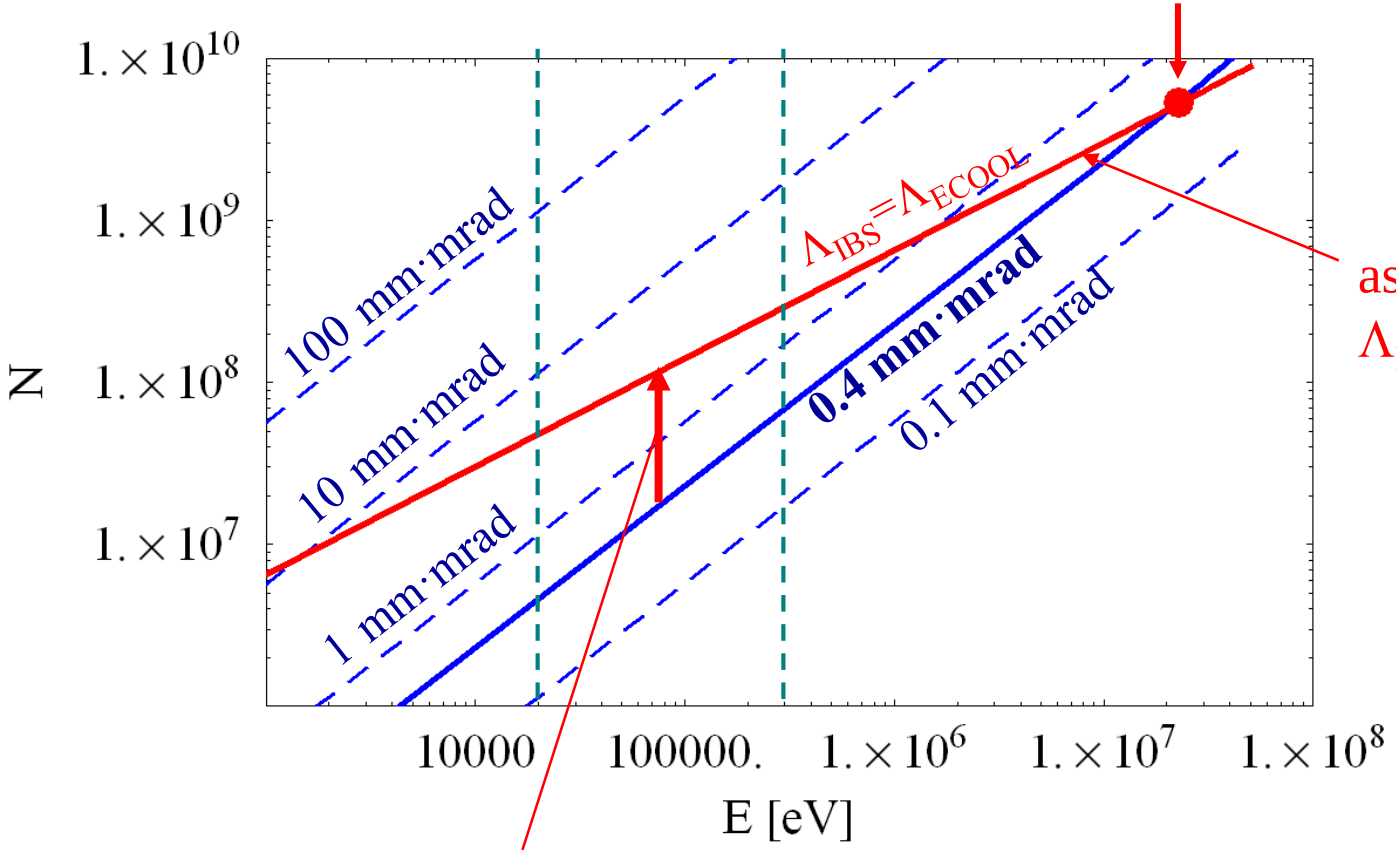

assumption: Λ_{ECOOL}=const

due to large intra beam scattering rates
ε is increased

IBS rate $\Lambda_{IBS} \sim \frac{N}{\beta^3 \cdot \varepsilon^2 \cdot \Delta p/p \cdot L_B}$

Tune as function of the quadrupole strength at working point II

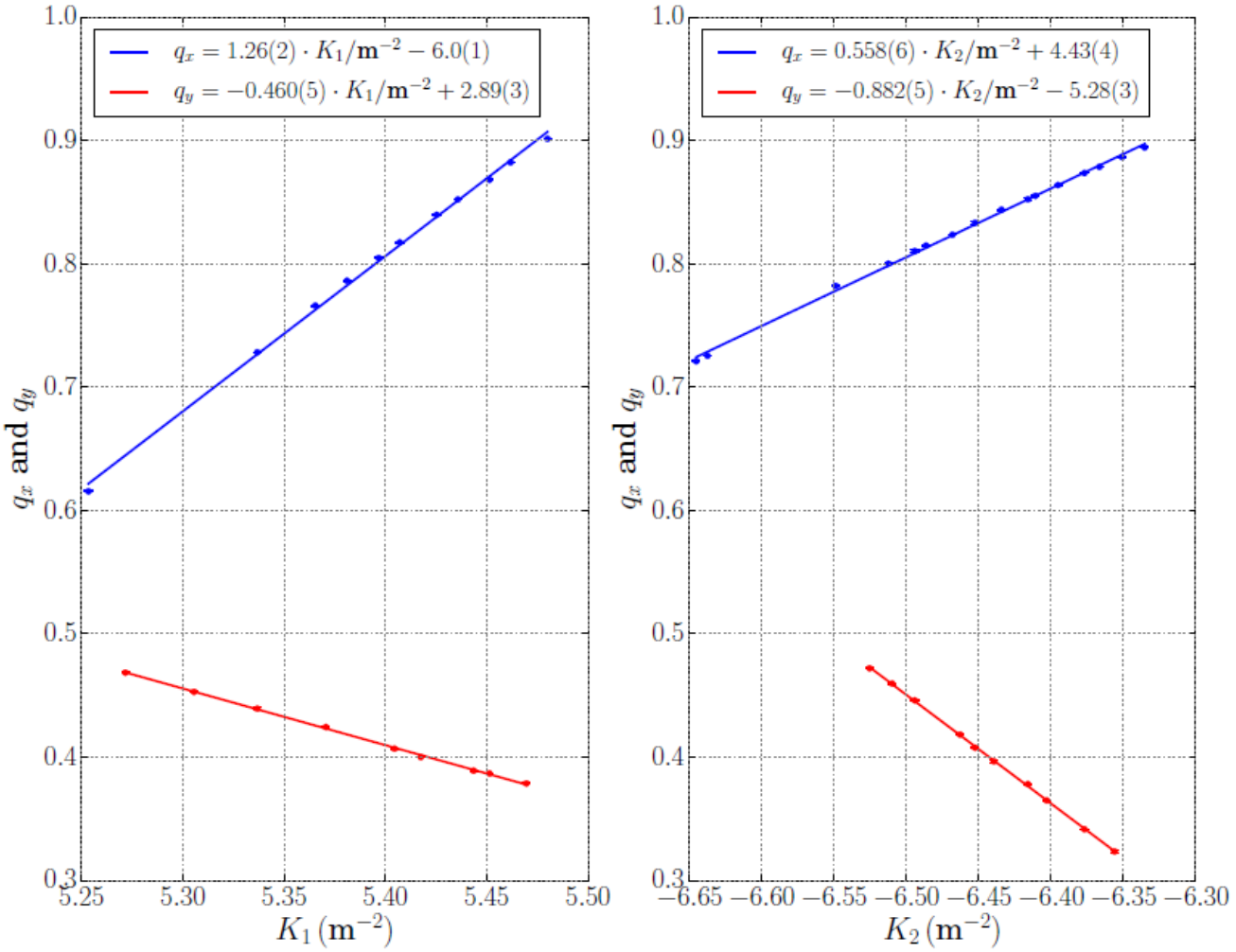

Figure 5.19: Measured fractional tune values q_x (blue) and q_y (red) as functions of the quadrupole strengths of family 1 (left column) with $K_2 = -6.44(9)\,\mathrm{m}^{-2}$ and 2 (right column) with $K_1 = 5.43(8)\,\mathrm{m}^{-2}$ at the first working point.

CSR as a mass spectrometer for charge molecular fragments

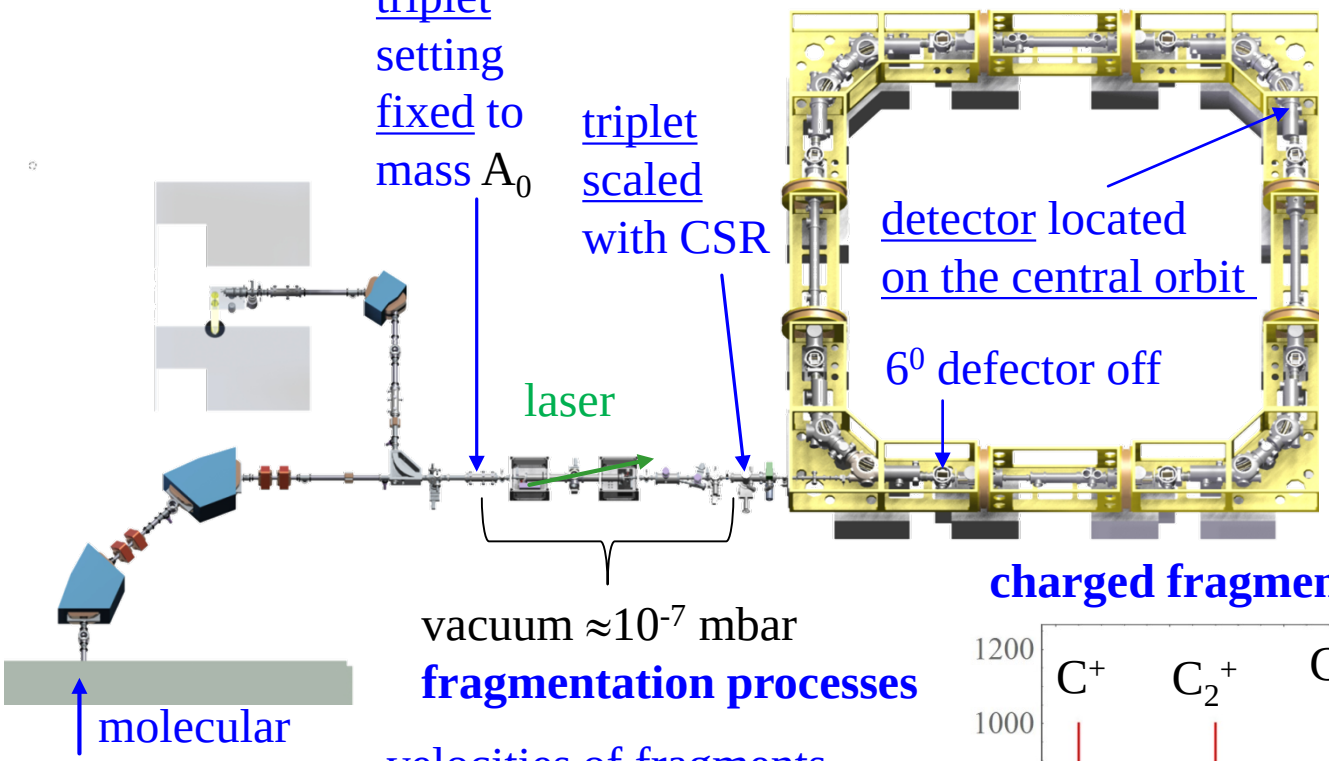

A- atomic mass number of fragments

A_0-atomic mass number of stored molecules

E_0- energy of stored ion beam with mass A_0

velocities of fragments conserved:

$\Rightarrow$ energy of the fragments

$$E_f = \frac{A}{A_0} E_0$$

$$\Rightarrow A = A_0 \frac{U}{U_0}$$

scaling factor of all voltages

charged fragment spectrum of C_7^+ cluster

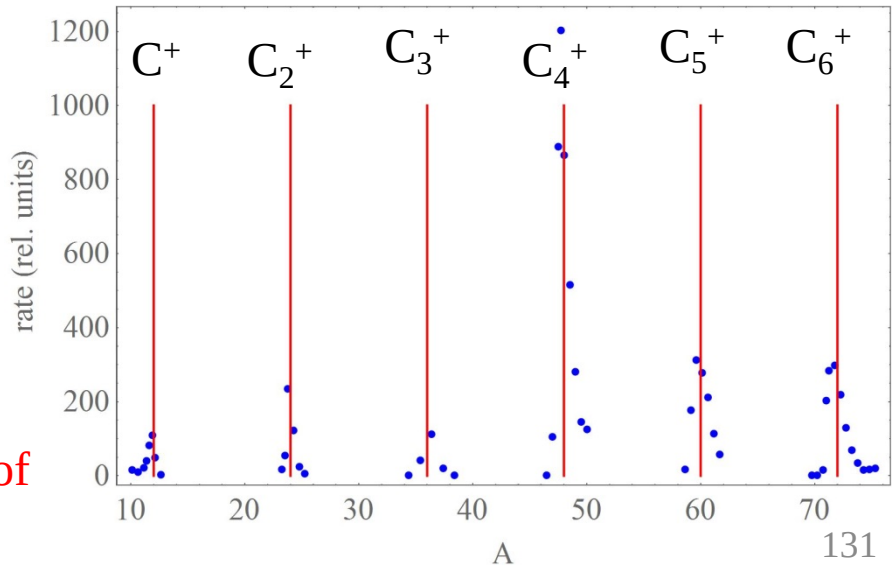

Laser tracker measurements to measure the position of the elements at warm and cold conditions

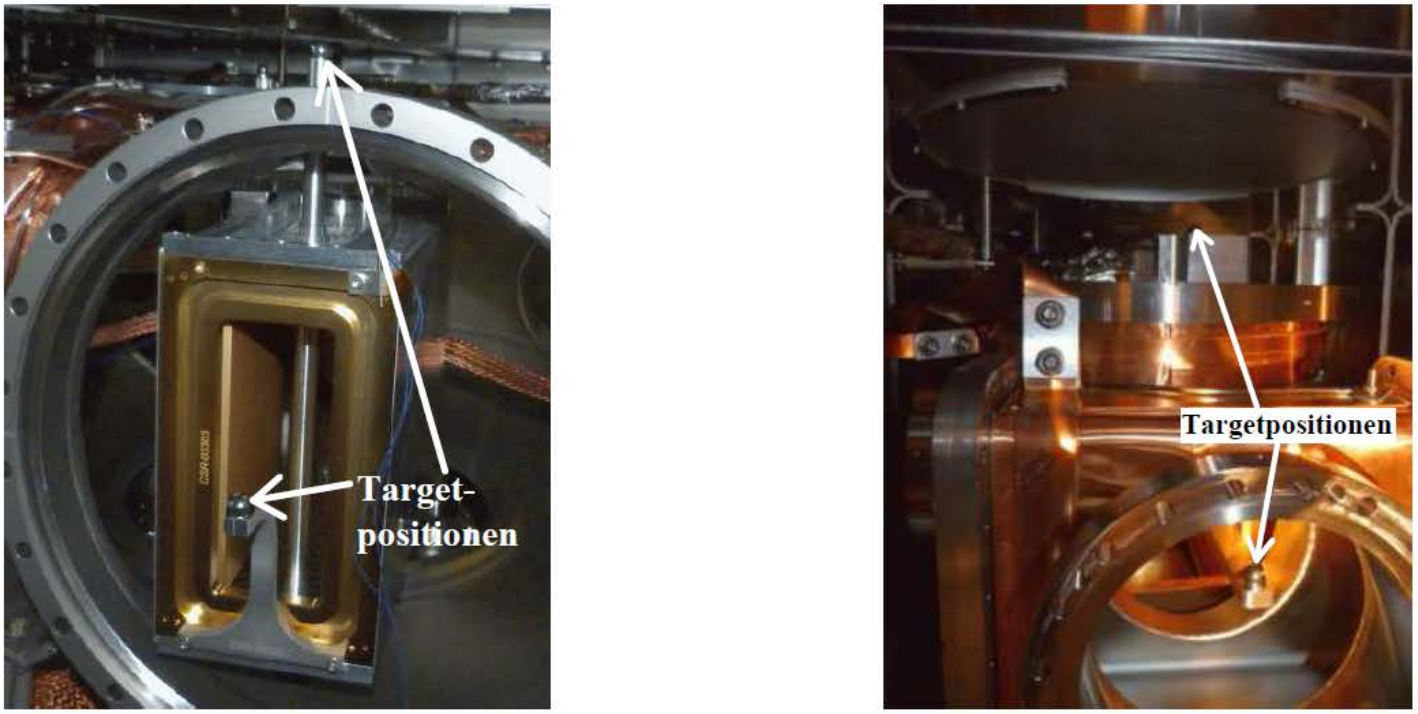

(a) (b)

Abbildung 4.13: Targethalterung zur Vermessung von 39°- a) und 6°-Deflektoren b) im warmen und kalten Zustand.